The roles of the potassium-uptake systems, Trk and Kdp, in the extracellular and intracellular growth of *Mycobacterium tuberculosis*

By

Ayman Gassim Elamin Osman

Submitted in partial fulfilment of the requirements for the degree

PhD (Medical Immunology)

Department of Medical Immunology
Faculty of Health Sciences
University of Pretoria

January 2020

PUBLICATION AND PRESENTATION

Publication

- Cholo M.C., van Rensburg E.J., Osman A.G. and Anderson R. (2015). Expression of the genes encoding the Trk and Kdp potassium transport systems of *Mycobacterium tuberculosis* during Growth *In Vitro*. *BioMed Research International*. vol. 2015 (2015): 608682. doi:10.1155/2015/608682

Presentation

- Osman A., Balhana R., Allam M., Earland C., Fourie P.B., Kana B., Ismail A., Stoker N., Anderson R. and Cholo M.C. The roles of the potassium-uptake systems, Trk and Kdp, in the extracellular and intracellular growth of *Mycobacterium tuberculosis*. Presented as an oral presentation at the University of Pretoria, Faculty of Health Sciences Research Day, 20 August 2019.

DECLARATION

I hereby declare that the work contained in this thesis is my original work and that I strictly followed norms in academia wherever I used other people's work and wherever I was assisted. I further declare that this body of work has not been presented before for and qualification at this or any other institution. This work is submitted in fulfilment of the requirements for Doctor Philosophy in Science degree at the University of Pretoria.

Student Name: Ayman Osman Date: 17 Feb 2020

Signature: …….

ACKNOWLEDGMENTS

First and foremost, my sincere thanks and gratitude to the Almighty Allah for directing me towards my goal and providing me strength and patience to continue my academic pursuit.

I would also like to sincerely thank the following persons:

Dr Moloko Cholo, my supervisor, for providing invaluable academic support during the entire project, especially so during experimental design, data collection (including assistance with phenotypic analysis), data analysis and writing of the thesis. She was prompt in her responses and accommodating at all times. What an accessible, knowledgeable, strong and selfless personality! Thank you so much for your tremendous support.

Prof Ronald Anderson, for his invaluable contributions, providing me with insightful guidance, tremendous mentorship, support and encouragements throughout the entire journey of my project.

Profs Riana Cockeran and Pieter Meyer, former and current Heads of Department of Immunology, for their encouragements and relevant administrative support.

Prof Bernard Fourie, my co-supervisor, Department of Medical Microbiology, University of Pretoria for scientific advices, encouragements and academic support.

All staff members of Department of Medical Immunology, for their invaluable assistance, encouragements and support throughout my studies. Special thanks to Prof Annette Theron and Dr Helen Steel for laboratory and technical support in immunological experiments.

My study mates in the TB research, Mrs Tebogo Matjokotja, Mr Sam Rasehlo, Mr Oupa Modiba and Mr Sizeka Mashele, for their support, encouragements and invaluable team spirit.

The Department of Immunology, National Health Laboratory Service (NHLS), and the TB Platform at Medical Research Council (MRC), for provision of research facilities.

To the following collaborators:

- Prof R. Balhana and Prof N. Stoker, The Royal Veterinary College, United Kingdom, for provision of plasmid molecules and technical advice throughout the mutagenesis procedures.
- Dr C. Earland and Prof B. Kana, Centre of Excellence for Biomedical TB Research, Wits University, for training and technical advices during the mutant construction.
- Dr M. Allam and Dr A. Ismail, Sequencing Core Facility, National Institute for Communicable Diseases (NICD), for their undeniably excellent support in genotypic analysis, providing of the whole genome sequencing and bioinformatics data analysis.

The National Research Foundation, MRC and the NHLS for financial support for this research project.

Finally, and not least, but most importantly, my great father, Gassim Osman and mother, Suad Nasr, and my supportive siblings, my loving wife, Mrs Fatima Osman, and our wonderful children: son Fady, and daughters, Reela and Reema as well as other family members and friends for every measure of support I have received. I say a big thank you!

SUMMARY

Background: Tuberculosis (TB), a disease caused by *Mycobacterium tuberculosis* (*Mtb*) bacterium, is responsible for high mortality rates globally. The disease control measures are hindered by the incomplete understanding of bacterial pathogenicity. Potassium (K^+) has been shown to be an essential component of *Mtb* virulence mechanisms. However, the roles of the K^+ transport systems in the bacteria have not been completely characterised. In *Mtb*, two active K^+-uptake systems, Trk and Kdp have been identified. Previous studies conducted using mutants of single operons, which included the *ceoBC* and *kdpDE* genes, resulted in mutant strains with different growth rates, suggesting the existence of mutual compensatory activity of these systems during bacterial growth.

Objectives: The aim of the current study was to determine the roles of the *Mtb* Trk and Kdp, during bacterial growth by generating K^+-uptake-deletion mutant strains of *Mtb*, in which both the *trk (ceoBC)* and *kdp* (*kdpDE* and *kdpFABC*) genes are inactivated, (triple-gene knockout) and investigating the functional roles of these transporters by evaluating the phenotypic characteristics of the mutant in relation to the wild-type (WT) strain.

Methodology: The *Mtb* triple-gene knockout was constructed by allelic replacement using homologous recombination (HR), following electroporation of mutated *kdpFABC (i.e kdpDFC)* allele-carrying pNILRB5-derived suicide delivery vector (SDV) into a TK-double knockout mutant, characterised by mutation of the *ceoBC* and *kdpDE* operons, which resulted in sequential formation of single-crossover (SCO) and double-crossover (DCO) (triple-gene knockout). This represented a significant accomplishment. The mutant was then used for phenotypic characterisation of the K^+-uptake transporters by comparing its growth kinetics with those of the WT strain extracellularly in planktonic and biofilm assays and intracellularly in human monocyte-derived macrophages.

Results: The SDV construction was confirmed by PCR and whole genome sequencing (WGS), illustrated by amplification of the 868-bp *kdpDFC* mutated fragment and absence of genomic reads at the *kdpFABC* region respectively, confirming mutation of the *kdpFABC* operon. Following electroporation with SDV, at least more than 20 SCO and two DCO clones were isolated, which were also confirmed genotypically by PCR and WGS. Gene knock-outs including *ceoBC* and *kdpDE* operons, were also confirmed by WGS. Phenotypic characterisation demonstrated that bacterial growth was affected by deletion of the two K^+-uptake transporters in all three growth environments i.e. plantonic, biofilm and intracellular enviroments. In this context, the TKkdpDFC mutant demonstrated an increase in growth in the

planktonic assay, attenuation of biofilm formation and decreased intracellular survival in macrophages.

Conclusion: The use of mutagenesis tools using the pNILRB5-generated SDV for homologous recombination is effective in generation of mutants revealing that the two K^+-uptake transporters are essential for various stages of bacterial growth, underscoring the potential of these systems as novel drug and vaccine targets.

Keywords: Tuberculosis; *Mycobacterium tuberculosis*; potassium, K^+-uptake system; Trk and Kdp; pNILRB5; suicide-delivery vector; single-crossover; double-crossover; bacterial growth.

TABLE OF CONTENTS

PUBLICATION AND PRESENTATION i

DECLARATION ii

ACKNOWLEDGMENTS iii

SUMMARY v

TABLE OF CONTENTS vii

LIST OF FIGURES xiii

LIST OF TABLES xiv

ABBREVIATIONS xv

INTRODUCTION 1

CHAPTER ONE: LITERATURE REVIEW 2

1.1. BACKGROUND OF TUBERCULOSIS DISEASE 2

1.1.1. History 2

1.1.2 *Mycobacterium tuberculosis* complex 3

1.1.3. Burden of tuberculosis 4

1.1.4. Factors affecting burden of tuberculosis 4

1.1.5. Control measures in tuberculosis 5

1.1.5.1. Diagnosis 6

1.1.5.2. Treatment 7

1.1.5.2.1. Drug-sensitive tuberculosis treatment 7

1.1.5.2.2. Drug-resistant tuberculosis treatment 7

1.1.5.3. Prevention 8

1.2 *MYCOBACTERIUM TUBERCULOSIS* BACTERIA 8

1.2.1. Characteristics of *Mycobacterium tuberculosis* bacterium 8

1.2.2. Structure of *Mycobacterium tuberculosis* cell wall 9

1.3. PATHOGENESIS OF TUBERCULOSIS 9

1.4. HOST DEFENCE MECHANISMS 10

1.4.1. Macrophage-associated defence mechanisms 10

1.4.1.1. Intracellular killing 10

1.4.1.2. Apoptosis 10

1.4.1.3. Autophagy 10
1.4.2. Granuloma 11
1.4.3. Cytokines 12
1.5. MYCOBACTERIAL SURVIVAL MECHANISMS 12
1.5.1. Surface receptors 13
1.5.2. Inhibition of phagosomal maturation 13
1.5.3. Inhibition of phagolysosomal fusion 13
1.5.4. Inhibition of oxidative stress 14
1.5.5. Inhibition of apoptosis and autophagy 14
1.5.6. Granuloma formation 14
1.5.7. Mycobacterial biofilm formation in the host 14
1.5.8 Mycobacterial ion-transporters 15
1.6. REFERENCES 16
CHAPTER TWO: POTASSIUM TRANSPORT SYSTEMS OF *MYCOBACTERIUM TUBERCULOSIS* 27
2.1. CELLULAR POTASSIUM CONCENTRATIONS 27
2.2. BACTERIAL POTASSIUM INFLUX SYSTEMS 27
2.2.1. Bacterial Trk transporters 27
2.2.2. Ktr transporters 28
2.2.3. Bacterial Kdp transporters 29
2.2.4. Role of potassium-influx systems in virulence of bacteria 29
2.3. BACTERIAL POTASSIUM EFFLUX SYSTEMS 30
2.4. POTASSIUM TRANSPORTERS IN *MYCOBACTERIUM TUBERCULOSIS* 31
2.4.1. Potassium-uptake systems of *Mycobacterium tuberculosis* 31
2.4.1.1. The Trk system 31
2.4.1.2. The Kdp system 32
2.4.2. Role of the potassium-uptake systems in bacterial virulence 33
2.5 REFERENCES 34
CHAPTER THREE: RATIONALE, HYPOTHESIS, AIM AND OBJECTIVES, AND SIGNIFICANCE OF THE STUDY 43

3.1. Rationale of the study 43
3.2 Study hypothesis 43
3.3. Aim of the study 43
3.4. Objectives of the study 43
3.5 Significance of the study 44
4. CHAPTER FOUR: MUTANT CONSTRUCTION 45
4.1. INTRODUCTION 45
4.2. AIM AND OBJECTIVES 47
4.2.1. AIM 47
4.2.2. OBJECTIVES 47
4.3. MATERIALS AND METHODS 48
4.3.1. MATERIALS 48
4.3.1.1. Bacterial and plasmid strains 48
4.3.1.2. Reagents and antimicrobial agents 48
4.3.1.3. Growth media 49
4.3.1.4. Enzymes 49
4.3.1.5. Oligonucleotides 49
4.3.1.6. Solutions and buffers 50
4.3.1. METHODS 50
4.3.2.1. MUTAGENESIS PROCESSES 51
4.3.2.1.1. Suicide-delivery vector construction in *Escherichia coli* 51
A. Construction of the pRB5kdpDF` plasmid 52
B. Construction of the pRB5kdpDFC` plasmid 53
C. Construction of the pRB5kdpDFC17` plasmid: Suicide-delivery vector 53
4.3.2.1.2. Homologous recombination in the *Mycobacterium tuberculosis* TK-deletion mutant strain 55
D. Isolation of single-crossover clones: TKpRB5kdpDFC17` 55
E. Isolation of double-crossover clones: TKkdpDFC 56
4.3.2.2. STANDARD OPERATING PROCEDURES FOR CONSTRUCTION OF THE MUTANT STRAIN 56
4.3.2.2.1. Cloning procedures in *Escherichia coli* 57
F. Plasmids 57
F.1 Plasmid growth in *Escherichia coli* bacteria 57
F.2. Plasmid DNA extraction 57
F.3. Plasmid DNA digestion with restriction enzymes 57
F.4. Purification of the digested vector 58
F.5 Gel electrophoresis 58
F.6. T4 polymerase treatment of plasmid DNA 58

G. Chromosomal DNA 58
G.1. *Mycobacterium tuberculosis* bacterial growth 58
G.2. *Mycobacterium tuberculosis* chromosomal DNA extraction 59
G.3. Polymerase chain reaction of the insert fragments 59
G.4. Purification of polymerase chain reaction-synthesized insert fragments 60
G.5. T4 polymerase treatment of polymerase chain reaction-synthesized insert fragments 60
H. Ligation 60
H.1. Ligase-independent ligation 60
H.2. Ligase-dependent ligation 60
4.3.2.2.2. Homologous recombination procedures in *Mycobacterium tuberculosis* 61
J. Electroporation of *Mycobacterium tuberculosis* TK-deletion mutant strain with the suicide delivery vector 61
J.1. Preparation of competent cells 61
J.2. Electroporation of competent cells with the suicide-delivery vector 62
K. Isolation of single-crossover clones 62
L. Isolation of double-crossover clones 62
4.3.2.2.3. Characterisation of double-crossover clones 63
M. Phenotypic characterisation 63
M.1. Sucrose sensitivity testing 63
M.2. Kanamycin sensitivity testing 63
N. Genotypic characterisation 63
N.1. Polymerase chain reaction 63
N.2. Whole genome sequencing 64

4.4. RESULTS 64

4.4.1. Suicide-delivery vector, pRB5kdpDFC17` construction 64
4.4.1.1 pRB5kdpDF` plasmid constructs 66
4.4.1.2. pRB5kdpDFC` plasmid constructs 66
4.4.1.3. pRB5kdpDFC17` plasmid constructs: Suicide-delivery vector 67
4.4.1.3.1. Polymerase chain reaction analysis of the suicide-delivery vector 67
4.4.1.3.2. Whole genome sequencing of suicide-delivery vector 68

4.4.2. *Mycobacterium tuberculosis* TKkdpDFC mutant construction 69
4.4.2.1. Isolation of single-crossover clones 70
4.4.2.2. Isolation of double-crossover constructs 71

4.4.3 Characterisation of double-crossover constructs 72
4.4.3.1. Phenotypic characterisation 72
4.4.3.1.1. Sucrose sensitivity testing 72
4.4.3.1.2. Kanamycin sensitivity testing 72
4.4.3.2. Genotypic characterisation of DCO for allelic replacement 73
4.4.3.2.1. Polymerase chain reaction 73

4.5. DISCUSSION 75

4.6. CONCLUSION 76
4.7. REFERENCES 77
CHAPTER FIVE: PHENOTYPIC CHARACTERIZATION 79
5.1. INTRODUCTION 79
5.2. AIM AND OBJECTIVES 80
5.2.1. AIM 80
5.2.2. OBJECTIVES 80
5.3. MATERIALS AND METHODS 81
5.3.1. MATERIALS 81
5.3.1.1. Bacterial strains 81
5.3.1.2. Growth media 81
5.3.1.3. Reagents and chemicals 81
5.3.2. METHODS 81
5.3.2.1. Inoculum preparation 82
5.3.2.2 Planktonic culture 82
5.3.2.2.1. Rubidium uptake 82
5.3.2.2.2. Growth rate measurements for WT and TKkdpDFC strains 83
5.3.2.2.3. Measurement of extracellular pH 83
5.3.2.3. Biofilm culture 83
5.3.2.3.1. Biofilm growth rate determination 83
5.3.2.3.2 Biofilm quantification 84
5.3.2.3.3 Measurement of extracellular pH 84
5.3.2.4. Intracellular assay 84
5.3.2.4.1. Macrophage cultures 84
5.3.2.4.1.1. Preparation of macrophages 85
5.3.2.4.1.1.1. Venous blood 85
5.3.2.4.1.1.2. Isolation of mononuclear leucocytes from blood 85
5.3.2.4.1.1.3. Separation and maturation of monocytes 86
5.3.2.4.1.1.4. Harvesting of macrophages 86
5.3.2.4.1.1.5. Preparation of macrophages for infection 86
5.3.2.4.2. Intracellular growth in macrophages 87
5.3.2.5. Statistical analysis and presentation of data 87
5.4. RESULTS 87
5.4.1. Inoculum 87
5.3.2. Extracellular assays 88
5.3.2.1. Planktonic cultures 88
5.3.2.1.1. Rubidium uptake 88

5.3.2.1.2. Rates of growth 88
5.3.2.1.3. Extracellular pH 89
5.3.2.2 Biofilm culture 90
5.3.2.2.1 Biofilm quantification 90
5.3.2.2.2 Biofilm rates of growth 90
5.3.2.2.3 Extracellular pH 90
5.3.2.3.1. Bacterial uptake by macrophages 92
5.3.2.3.2. Intracellular growth in macrophages 92

5.5. DISCUSSION 93

5.6. CONCLUSION 94

5.7. REFERENCES 95

CHAPTER SIX: GENERAL DISCUSSION AND CONCLUSION 97

APPENDICES 100

LIST OF FIGURES

Chapter One

Figure 1.1: Estimated tuberculosis incidence rate worldwide 4
Figure 1.2: Schematic representation of the *Mycobacterium tuberculosis* cell wall. 9
Figure 1.3: The infection process of *Mycobacterium tuberculosis* and the formation of a caseating granuloma.....12

Chapter Two

Figure 2.1: Transcription of the *trk* genes of *Mycobacterium tuberculosis* and other mycobacteria. 32

Chapter Four

Figure 4.1: Homologous recombination based on the two-step strategy. 51
Figure 4.2: Structure of pNILRB5. 52
Figure 4.3: Schematic illustration of the construction of the suicide delivery vector. 55
Figure 4.4: Homologous recombination in TK-deletion mutant of *Mycobacterium tuberculosis.* 56
Figure 4.5: Construction of the suicide-delivery vector, pRB5kdpDFC17`. 65
Figure 4.6: PCR synthesis of upstream *kdpDF* of white kanamycin-resistant colonies. 66
Figure 4.7: PCR synthesis of downstream *kdpC* of white kanamycin-, sucrose-resistant colonies. 67
Figure 4.8: PCR synthesis of upstream *kdpDF* (A) and downstream *kdpC* (B) fragments in the suicide-delivery vector.. 68
Figure 4.9: Whole genome sequencing of the suicide-delivery vector aligned with that of the H_{37}RV strain.....69
Figure 4.10: Homologous recombination between the TK mutant strain and the pRB5kdpDFC17`SDV vector. 70
Figure 4.11: Characterisation of the single crossover clones.....71
Figure 4.12: Development of double-crossover colonies on 7H10 containing X-gal and hygromycin 72
Figure 4.13: Kanamycin-sensitivity testing of white sucrose-resistant colonies 73
Figure 4.14: PCR confirmation of the *kdpDFC* mutation.....74

Figure 4.15: Whole genome sequencing of *Mycobacterium tuberculosis* strains 75

Chapter Five

Figure 5.1: The inoculum sizes of the wild-type and mutant strain of *Mycobacterium tuberculosis* 88

Figure 5.2: Planktonic cultures of the wild-type and TKkdpDFC mutant strains of *Mycobacterium tuberculosis* 89

Figure 5.3: Biofilm cultures of the wild-type and the mutant strains of *Mycobacterium tuberculosis*. 91

Figure 5.4: Macrophage cultures comparing the wild-type and mutant strains of *Mycobacterium tuberculosis*. 92

LIST OF TABLES

Table 1: Bacterial and plasmid strains 48

Table 2: Enzymes used during the cloning procedure 49

Table 3: Oligonucleotides used for PCR amplification of the inserts.....50

Table 4: Oligonucleotides used for screening for the mutation 50

Table 5: PCR conditions 59

ABBREVIATIONS

AFB:	Acid fast bacilli
AMs:	Alveolar macrophages
ART:	Antiretroviral therapy
ATP:	Adenosine triphosphate
BSA:	Bovine serum albumin
BCG:	Bacillus Calmette-Guérin
Ca^{2+}:	Calcium
$CaCl_2$:	Calcium chloride
CFU:	Colony-forming unit
CO_2:	Carbon dioxide
DCO:	Double-crossover
dCTP:	Deoxycytidine triphosphate
DCs:	Dendritic cells
dGTP:	Deoxyguanosine triphosphate
DMSO:	Dimethyl sulfoxide
DNA:	Deoxy-ribo nucleic acid
dH_2O:	Distilled water
DOTS:	Directly observed treatment short course strategy
EGTA:	Ethylene glycol-bis (2-aminoethylene)-N,N,N,N-tetraceticacid
EMB:	Ethambutol
EPS:	Extracellular polymeric substances
ESAT:	Early secretory antigenic target
FcR:	Fragment crystallizable region
GSX:	Glutathione-S-conjugates
H^+:	Hydrogen Ion
H_2O_2:	Hydrogen peroxide
HBSS:	Hanks' balanced salt solution
HIV:	Human immunodeficiency virus
HR:	Homologous recombination
ICF:	Intensified case finding
IFN-γ:	Interferon gamma
Ig:	Immunoglobulin
IGRAs:	Interferon-gamma release assays

IL:	Interleukin
INH:	Isoniazid
IPT:	Isoniazid preventive therapy
K^+:	Potassium ion
KCl:	Potassium chloride
KH_2PO_4:	Potassium dihydrogen phosphate
KUP:	Potassium uptake permease
LA:	Luria-Bertani agar
LAM:	Lipoarabinomannan
LB:	Luria-Bertani broth
LIC:	Ligation-independent cloning
LJ media:	Lowenstein-Jensen media
LLO:	Listeriolysin O
MCS:	Multi-cloning sites
MDR:	Multi-drug resistance
MGIT:	Mycobacterial growth indicator tube
Mg^{2+}:	Magnesium ion
$MgSO_4$:	Magnesium sulphate
MNL:	Mononuclear leucocytes
MOI:	Multiplicity of infection
Mtb:	*Mycobacterium tuberculosis*
Na^+:	Sodium ion
NAA:	Nucleic acid amplification
NaCl:	Sodium chloride
NAD^+:	Nicotinamide adenine dinucleotide
NADPH:	Nicotinamide adenine dinucleotide phosphate
NaOH:	Sodium hydroxide
NH_4Br:	Ammonium bromide
NH_4CI:	Ammonium chloride
NHLS:	National Health Laboratory Service
NICD:	National Institute for Communicable Diseases
NK cells:	Natural killer cells
NLRP3:	Nucleotide-binding/leucine-rich repeat pyrin domain containing 3
OADC:	Oleic acid/albumin/dextrose/catalase

OD:	Optical density
PAMPs:	Pathogen-associated molecular patterns
PAS:	Para-aminosalicylic acid
PBS:	Phosphate-buffered saline
PCR:	Polymerase chain reaction
PCWDEs	Plant-cell wall degrading enzymes
PIM:	Phosphatidyl inositol mannosides
PMF:	Proton motive force
PMNLs:	Polymorphonuclear leukocytes
PRPs:	Pattern recognition receptors
PZA:	Pyrazinamide
$^{86}Rb^{+}$:	Rubidium
RbCl:	Rubidium chloride
RIF:	Rifampin
ROI:	Reactive oxygen intermediates
ROS:	Reactive oxygen species
rRNA:	ribosomal ribonucleic acid
RT:	Room temperature
SCO:	Single-crossover
SDS:	Sodium dodecyl sulphate
SDV:	Suicide-delivery vector
SOC:	Super optimal broth with catabolite repression
SPI1:	Salmonella Pathogenicity Island 1
STR:	Streptomycin
TAE:	Tris-acetate-EDTA
TB:	Tuberculosis
TCA:	Trichloroacetic acid
TCS:	Two-component system
TDM:	Trehalose 6, 6'- dimycolate
TDR:	Totally drug-resistant
TE:	Tris-EDTA
TGF-β:	Transforming growth factor-beta
TLRs:	Toll-like receptors
TNF:	Tumor necrosis factor

TTSS:	Type III secretion system
TST:	Tuberculin skin test
UV:	Ultra-violet
UVR:	Ultra-violet radiation
WGS:	Whole genome sequencing
WHO:	World Health Organization
WT:	Wild-type
XDR:	Extremely drug-resistant
ZN:	Ziehl-Neelsen

INTRODUCTION

Despite the availability of effective chemotherapy, is it estimated that *Mycobacterium tuberculosis* infects about a third of the world's population and 8 million new cases of tuberculosis and 2 million deaths from this disease occur annually (WHO, 2016). The situation is made worse by the emergence and spread of multi- and extensively drug-resistant strains of *M. tuberculosis* strains that are resistant to first- and second-line drugs. The identification of novel drug or vaccine targets and development of new tuberculosis drugs with new model of action has become crucial. This can be achieved by a complete understanding of the pathogenesis of the mycobacterial pathogen.

The potassium ion (K^+) is the most abundant monovalent cation in all living cells. It is essential for a variety of cellular functions, including maintenance of turgor pressure, osmoregulation, pH homeostasis, membrane potential regulation, enzyme activation and gene expression (Epstein, 2003; Follmann et al., 2009; Ochrombel et al., 2011). Its high intracellular K^+ concentrations, ranging from 300 to 1000 millimolar (mM) (Steyn et al., 2003) is maintained by several influx and efflux K^+ transport systems (Su et al., 2009). As they are essential to many cellular functions, K^+ transport systems have become an attractive target for novel antibacterial drugs or vaccine.

Several genes encoding K^+ transporters in *M. tuberculosis*, including influx and efflux systems, have been identified (Cole et al., 1998). However, these systems have not been well characterised and there is scanty information available on them. The K^+ influx systems consist of two active K^+-uptake transporters, the Trk and Kdp (Cole et al., 1998). The *Mtb* Trk system is made up of two TrkA proteins, CeoB and CeoC, encoded by the *ceoB* (684 base pairs (bp)) and *ceoC* (663 bp) genes, respectively. The *Mtb* Kdp systems are inducible and consist of P-type, ATP-driven K^+ transporters. The P-type ATPase system consists of six proteins, KdpF, KdpA, KdpB, KdpC, KdpD, and KdpE, encoded by separated *kdpDE* and *kdpFABC* operons. It also has a high affinity for K^+ (Cholo et al., 2006). While the roles of the different K^+-uptake systems have been well described in virulence of other bacteria, limited information is available on these systems in *M. tuberculosis.*

CHAPTER ONE: LITERATURE REVIEW

1.1. BACKGROUND OF TUBERCULOSIS DISEASE

1.1.1. History

Tuberculosis (TB) is one of the oldest and deadliest infectious diseases globally, first recorded in India, China and Egypt dating back to 3300, 2300 and 4000 years respectively (Zink et al., 2003; Barberis et al., 2017).

In the past, the disease was known by many names, including 'consumption' due to people losing weight; 'king's evil' because of the old belief that people affected by the disease could be healed after a royal touch; 'lupus vulgaris' due to the development of cutaneous lesions (Ducati et al., 2006; Barberis et al., 2017) and 'phthisis', a Greek term which means wasting away.

In 1882, a breakthrough in the disease was attained when TB was discovered as an infectious disease through the discovery of tubercle bacilli by Robert Koch through his invention of a microscopy staining procedure, which was later modified by Franz Ziehl and Friedrich Neelsen to the Ziehl-Neelsen (ZN) staining method as it is currently known (Koch and Cote, 1965). This finding was followed by the isolation of the bacterium from specimens derived from infected animals and patients using a solidified serum-based medium and the illustration of contagiousness of the disease by reproducing the disease using inocula from infected animals and patients (Cambau and Drancourt, 2014).

Despite Koch's discoveries, the disease epidemic was steadily increasing and was the highest in the 18^{th} and 19^{th} centuries, specifically in Europe, reaching 20 - 30% of TB-associated deaths (Dye and Williams, 2010). The increase in the disease was attributed to overcrowded living conditions (Dye and Williams, 2010), with the number of cases decreasing as the living conditions improved (Snowden, 2008).

In 1921, a preventative mechanism for the disease was established with the discovery of the Bacillus Calmette-Guérin (BCG) vaccine (Calmette, 1922). Currently, BCG is the only vaccine available to prevent TB, with prolonged safety profiles lasting for over 50 years (Aronson et al., 2004). However, the efficacy of the vaccine has been shown to be affected by time and geographical regions (Andersen and Doherty, 2005).

Further improvements in the decline of the disease were attained during the antibiotic era. In 1943, streptomycin (STR) was discovered by Schatz, Bugie, and Waksman (Schatz et a., 1944), leading to TB becoming a treatable disease. This was followed by the discovery of Para-aminosalicylic acid (PAS) synthesised two years prior to STR (Lehmann, 1946), and the

more potent agent, isoniazid (INH) (Robitzek and Selikoff, 1952). Due to monotherapy used in the treatment of TB patients with these antibiotics, complications such as drug resistance, side-effects and relapse in patients developed (Robitzek and Selikoff, 1952; Ahearn and Fearon, 1989). A triple drug-combination therapy, comprising of INH, STR, and PAS, was then developed and was administrered to patients for 18 to 24 months (Iseman, 2002). Subsequently, ethambutol (EMB), which was effective against INH/STR-resistant *Mycobacterium tuberculosis* (*Mtb*), was added to the treatment regimen in 1961 (Thomas et al., 1961) and rifampin (RIF) in 1966 (Sensi, 1983), reducing the treatment schedule to nine months. Later, pyrazinamide (PZA) was discovered and used in the formulation of a four-drug regimen, which consisted of INH, RIF, EMB, and is currently used for treatment of patients for six months (McKenzie et al., 1948).

However, the emergence of multi-drug resistant (MDR), extremely drug-resistant (XDR) and totally drug-resistant (TDR) *Mtb* isolates has complicated the control of the disease (Navin et al., 2002; Dheda et al., 2010), and associated with poor treatment outcomes (Sotgiu et al., 2009).

In addition, the emergence of human immunodeficiency virus (HIV) in the 1980s has further exacerbated the incidence of TB. HIV has contributed to the scourge of the disease by suppressing the immune system, thereby increasing the chances of TB disease reactivation in latent TB-infected people (Winter et al., 2018).

1.1.2 *Mycobacterium tuberculosis* complex

Mtb belongs to the genus Mycobacterium, which includes more than 170 species (Tortoli, 2014). It is a member of the *Mtb* complex, which is made up of genetically-related bacteria with 99.9% similarity at the nucleotide level and identity at 16S rRNA sequences (Sreevatsan et al., 1997). The members of the *Mtb* complex include *Mycobacterium africanum, M. bovis, M. microti, M. canettii, M. caprae, M. pinnipedii, M. suricattae, M. mungi, M. dassie, and M. oryx* (Alexander et al., 2010; van Ingen et al., 2012). These *Mtb* complex organisms differ, however, in their host tropisms, phenotypes, and pathogenicities (Wirth et al., 2008). For instance, *M. canettii* and *M. africanum*, cause tuberculosis in humans in African subjects or those of African ancestry (Forrellad et al., 2013), *M. bovis* in humans, domestic and wild animals (Velayati et al., 2007) *M. microti* in voles and immunocompromised human patients (Brosch et al., 2002) and *M. caprae* in cattle, pigs, red deer, wild boars and humans (Rodríguez et al., 2011), while the remaining complex members such as *M. pinnipedii, M. suricattae, M.*

mungi, M. dassie, and M. oryx cause disease in seals, meerkats, mongooses, dassies, and members of the Bovidae family respectively (Alexander et al., 2010; Van Ingen et al., 2012).

1.1.3. Burden of tuberculosis

TB remains the leading pandemic threatening public health globally, causing more deaths from a single infectious agent than HIV (WHO, 2019). About a third of the world's population is infected with *Mtb* and 10 million people developed the disease, while 1.2 million died of it, in 2018 globally (WHO, 2019) (Figure 1.1).

Approximately two thirds of new TB cases reported in 2018, were in South-East Asia and Africa, with the highest number of cases recorded in India (27%), China (9%), Indonesia (8%), the Philippines (6%), Pakistan (6%), Nigeria (4%), Bangladesh (4%) and South Africa (3%) (WHO, 2019).

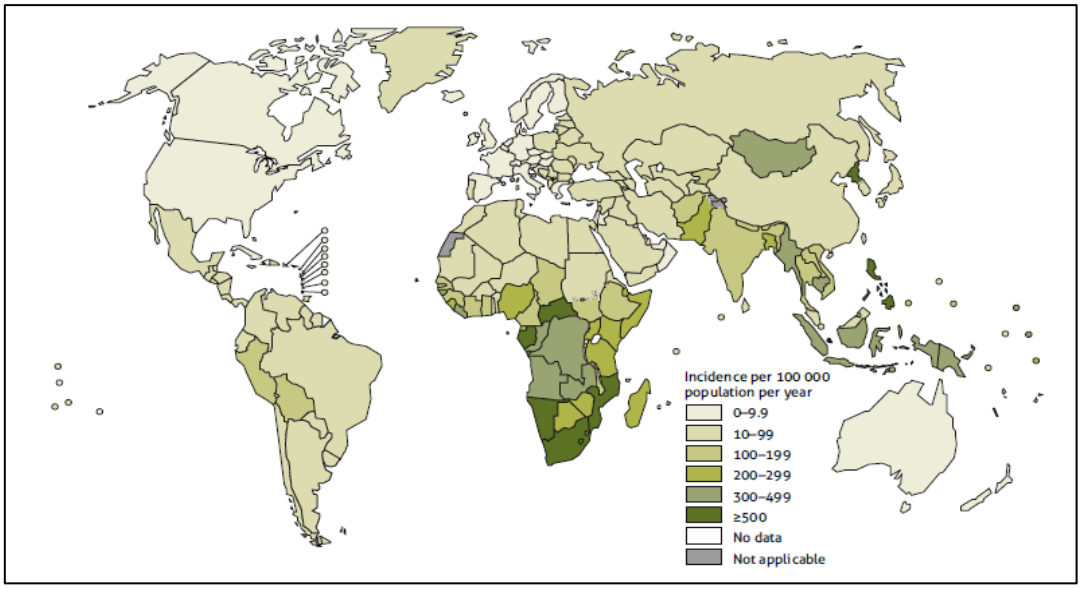

Figure 1.1: Estimated tuberculosis incidence rate worldwide in 2018 (WHO, 2019).

1.1.4. Factors affecting burden of tuberculosis

The global increase in the prevalence of TB is attributed largely to HIV infection, which accounts for approximately 10% of all TB cases (WHO, 2017). TB is also a threat to HIV-infected individuals, being the most common cause of death in these patients, accounting for at least 26% of HIV-related deaths (Corbett et al., 2003). HIV infection leads to weakening of

the host's immune system promoting the development of active TB (Paterson, 2003; Corbett et al., 2003).

Another factor contributing to the TB pandemic is the co-mobidity associated with conditions such as type 2 diabetes mellitus, renal insufficiency, and silicosis due in part to their use of corticosteroids and immunosuppressive agents, as well as to disease-associated immunosuppression in the case of diabetes mellitus (Getahun et al., 2015). Poverty is an additional risk factor for TB, and is associated with poor treatment adherence due to low socio-economic status, leading to poor treatment outcomes in patients (Lönnroth et al., 2010; Tankimovich, 2013; Van Hest et al., 2014).

Another contributing factor to the disease epidemic is the development of drug resistance. The emergence of MDR (resistance to INH and RIF) and XDR (resistance to INH and RIF plus resistance to all fluoroquinolones and to at least one of the three injectable second-line drugs (i.e., amikacin, kanamycin, or capreomycin), has also exacerbated the disease burden (Minion et al., 2013). In 2016, about 4.1% of new TB cases and 19% of previously treated cases were MDR-TB or RIF resistant (WHO, 2017).

1.1.5. Control measures in tuberculosis

The control of TB disease remains a major global challenge. Despite this, the global TB incidence rates have been declining since 2000, with at least 1.5% cases fewer reported per year, reaching a decline in incidence of 18% in 2015 (WHO, 2016). The decline in the number of TB cases has been attributed mainly to improved control measures, which include treatment and diagnostic strategies (WHO, 2017). Other control measures recommended by WHO include early identification of potential TB patients (Chronic coughers) who present as outpatients so that they are given a priority for TB (triage). People attending HIV clinics should be screened for TB regularly. In addition, those showing symptoms consistent with pulmonary TB should be tested promptly. In the wards, pulmonary TB suspects should be placed in one section of the general ward with good ventilation and If possible, these TB suspects should be encouraged to spend daylight hours outside the ward. TB suspects should also be educated on proper cough hygiene. Despite these achievements, improvements in the control mechanisms are still required.

1.1.5.1. Diagnosis

Early diagnosis is crucial in the control of TB as late detection increases the risk of spreading the infection (WHO, 2017). The currently available methods of TB diagnosis include chest X-ray, smear microscopy, culture, molecular (GeneXpert) and interferon-gamma (IFN-γ) release assays. Chest radiography is used for TB screening in individuals with cough symptoms lasting for at least two weeks presenting with chronic fever and/or weight loss. However, radiologic changes are not specific for diagnosing pulmonary TB, as these may overlap with those of community-acquired pneumonia (WHO, 2017). The common radiographic features associated with active TB include consolidations or cavities in the lungs.

Direct sputum smear microscopy (using ZN staining) is the most widely used technique for pulmonary TB diagnosis and is available in most primary health-care laboratories (WHO, 2015). The method results in the acid-fast bacilli (AFB) appearing as bright red rods, while the non-AFB as blue. However, although specific, the technique has low and variable sensitivity (WHO, 2015). Culture is also widely used and considered the 'gold standard' for the diagnosis of TB. It is sensitive and can also be used for drug susceptibility testing (Schön et al., 2017). Growth of TB bacilli on traditional solid medium, such as Lowenstein-Jensen (LJ) requires 2 - 8 weeks, and 10 - 14 days in liquid media such as the BACTEC mycobacterial growth indicator tube (MGIT) 960 system (Kanchana et al., 2000; Chihota et al., 2010).

GeneXpert MTB/RIF is a molecular beacon technology designed to identify sequences amplified in a semi-nested real time- polymerase chain reaction (PCR) to detect the presence of *Mtb* complex directely from samples and concurrently RIF resistance (Helb et al., 2010). It is an automated rapid procedure, with results being obtainable within two hours and is based on nucleic acid amplification (NAA) performed in a cartridge (Helb et al., 2010). The GeneXpert cartridges are pre-loaded with all of the necessary reagents for sample processing, deoxyribonucleic acid (DNA) extraction, amplification, and laser detection of the amplified *rpoB* gene target. Due to the closed cartridge system, the risk of aerosol formation is low (Banada et al., 2010). It is the initial diagnostic test in all TB suspects. The next generation of GeneXpert technology (Xpert MTB/RIF Ultra), which is more sensitive, has been developed and is used in the most challenging settings (Dorman et al., 2018). As opposed to GeneXpert MTB/RIF, the ultra has a larger reaction chamber and incorporates two different multicopy amplification targets (IS6110 and IS1081) intended to reduce the limit of detection of bacterial colony-forming units.

IFN-γ release assays (IGRAs) are conventional immunoassays used for TB diagnosis. They are designed to measure systemic IFN-γ levels as an indicator of *Mtb* infection. IFN-γ is

released by T-cells when stimulated by *Mtb*-specific antigens. These antigens include early secretory antigenic target (ESAT)-6, culture filtrate protein (CFP)-10 and TB7.7 (P4) (Mazurek et al., 2005). Blood is drawn from the TB suspects and mixed with synthetic peptides representing ESAT-6, CFP-10 and TB7.7 within 16 hours. IFN-g concentration is then determined and sample declared positive, negative or indeterminant according to the interpretation criteria for a particular IGRA

A tuberculin skin test (TST) determines if a person is infected with *Mtb* or has been exposed to the tubercle bacilli (Nayak and Acharjya, 2012). The test involves intradermal injection of tubercle antigen followed by development of a delayed hypersensitivity reaction forming an induration within 48 - 72 hours (Nayak and Acharjya, 2012).

1.1.5.2. Treatment

1.1.5.2.1. Drug-sensitive tuberculosis treatment

Antimicrobial therapy of drug-sensitive TB patients involves daily intake of a multi-drug regimen, consisting of four first-line drugs, which includes INH, RIF, PZA, and EMB, for a minimum period of six months. The treatment is given in two sequential stages, which include the initial intensive phase of two months with four drugs and the continuation phase which involves administration of INH and RIF for four to six months (Elkomy et al., 2013). Administration of the treatment is through directly observed, short course (DOTS) therapy programmes (Bishai et al., 2010). DOTS is intended to promote adherence to TB treatment and has so far achieved over 80% cure rate (WHO, 2006).

1.1.5.2.2. Drug-resistant tuberculosis treatment

Treatment of drug-resistant TB patients involves the use of second-line drugs, which are antibiotics other than the first-line agents used in the treatment of drug-sensitive TB (Caminero et al., 2010). Currently, MDR-TB patients are treated with a short-term regimen for 9-12 months, which contains kanamycin, moxifloxacin, prothionamide, clofazimine, bedaquiline, PZA, high-dose INH and EMB (Varaine et al., 2016). Additional second-line drugs that require approval from relevant regulatory authorities include pretomanid and delamanid for the treatment of drug-resistant TB patients (Tiberi et al., 2017).

1.1.5.3. Prevention

The most effective preventative strategy for TB has been through vaccination with BCG, which is the only licensed vaccine against TB. It is, however, only effective against childhood and miliary TB. Additionally, its efficacy varies with different geographical settings and populations. For instance in India, the vaccine is less effective due to high prevalence of environmental mycobacteria (Fine, 1995; Brandt et al., 2002; De Lisle et al., 2005). So too is the vaccine less effective in Malawi where studies showed no protective effect from BCG for TB and more cases of pulmonary TB were observed in the BCG vaccine group (Ponnighans et al., 1992). Studies in America and other western countries indicated that the vaccine is effective against the the disease at least 50% overall and was even more effective against disseminated disease and meningitis with a calculated protective effect as high as 86% (Rodrigues et al., 1963; Colditz et al., 1994).

Currently, several novel vaccine candidates, which represent diverse approaches including recombinant BCG, attenuated *Mtb*, viral-vectored platforms, purified recombinant proteins and novel adjuvants, have been developed and are being evaluated in clinical trials.

Other preventive interventions include intensified case finding (ICF), INH preventive therapy (IPT) and antiretroviral therapy (ART) (Harries et al., 2010). These mechanisms are effective for the control of TB in HIV-infected individuals (WHO, 2017).

1.2 MYCOBACTERIUM TUBERCULOSIS BACTERIA

1.2.1. Characteristics of *Mycobacterium tuberculosis* bacterium

Mtb is a Gram-positive acid-fast bacterium (Ducati et al., 2006). Its acid fastness is mainly due to the high content of cell-wall mycolic acids (Daffe and Draper, 1998; Marrakchi et al., 2014) (Figure 1.2). The bacterium is a rod-shaped bacillus which is 0.5 μm in diameter and 1-4 μm in length (Ducati et al., 2006). Its cell-wall lacks capsules, which allows the bacteria to aggregate resulting in cord formation (Ghosh et al., 2009).

It is a non-sporulating (Ghosh et al., 2009), facultatively intracellular and strictly aerobic, organism growing mostly in highly-oxygenated tissues such as the lungs. It has a long generation time of 12 to 18 hours for replication and requires a temperature of 37°C, Carbon dioxide (CO_2) of 5-10% and pH levels between 6.5 and 6.8 for optimal growth. It forms pale yellow colonies when growing on solid medium (Palange et al., 2016).

1.2.2. Structure of *Mycobacterium tuberculosis* cell wall

Mtb has a high lipid content in its cell-wall. The cell-wall is composed of three major components, which include mycolic acids, cord factor and wax-D as shown in Figure 1.2 (Alderwick et al., 2007; Meena and Rajni, 2010). Mycolic acids are alpha-branched structures and are responsible for permeability of the mycobacterial cell-wall, while cord factors, which include trehalose 6, 6'- dimycolate (TDM), are surface glycolipids, which are responsible for cord formation during growth. The wax-D molecules are involved in phagocytosis of the bacteria (Brennan, 2003).

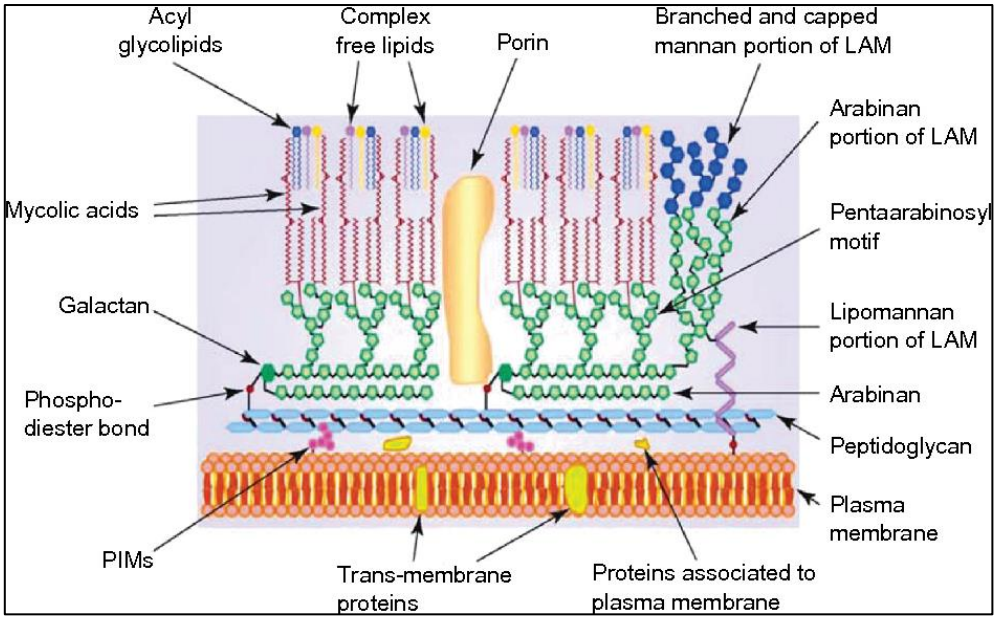

Figure 1.2: Schematic representation of the *Mycobacterium tuberculosis* cell wall (Talip et al., 2013, permission requested).

1.3. PATHOGENESIS OF TUBERCULOSIS

Mtb infection occurs when the tubercle bacilli from aerosols of infected person reach the alveoli of the lungs of the host. In the alveoli, the bacterial pathogen-associated molecular patterns (PAMPs) are recognized by the pattern recognition receptors (PRRs) on surfaces or cytosol of dendritic cells (DCs) and alveolar macrophages (AMs) (Weiss and Schaible, 2015) and are phagocytosed by professional AMs (Urdahl et al., 2011). Following phagocytosis by macrophages, a phagosome is formed in the cytoplasm of these cells (Apt and Kondrat'eva, 2008). The bacteria survive intracellular defence mechanisms and replicate in macrophages. Thereafter they disseminate from the site of infection via the blood or the lymphatic system. The adaptive immune system is then activated, triggering the migration of monocytes,

neutrophils, lymphocytes and other immune cells to the site of infection, resulting in the formation of a granuloma that contains and restricts spreading of the infection (Zumbo et al., 2013) (Figure 1.3).

1.4. HOST DEFENCE MECHANISMS

1.4.1. Macrophage-associated defence mechanisms

1.4.1.1. Intracellular killing

Phagocytes express receptors for complement receptor (CR) and antibodies (fragment crystallizable region (FcR)) that are crucial in complement and antibody-mediated elimination of intracellular *Mtb*. The uptake of immunoglobulin (Ig)G-opsonized *Mtb* induces a respiratory (oxygen) burst, which produces reactive oxygen intermediates (ROIs), permits fusion with lysosomes, and increases production of proinflammatory cytokines, such as tumor necrosis factor-α (TNF-α) (Ismail et al., 2002). Phagocytes and other immune cells express nicotinamide adenine dinucleotide phosphate (NADPH) oxidase, which produces superoxide that spontaneously recombines with other molecules to produce reactive free oxygen radicals and hydrogen peroxide (H_2O_2) (Yang et al., 2012). Neutrophils and monocytes use myeloperoxidase to further combine H_2O_2 with Cl^- to produce hypochlorite, which plays a role in destroying bacteria by damaging *Mtb* DNA and alterating membrane lipids and proteins (Yang et al., 2012).

1.4.1.2. Apoptosis

Apoptosis represents a crucial host defence against pathogens, which involves a complex signaling pathway. It is a highly-regulated process in which the cytoplasm and other cellular organelles of dying cells are enclosed in membrane bound vesicles called apoptotic bodies (Echeverria-Valencia et al., 2017). The apoptotic bodies are taken up by macrophages via receptor-mediated phagocytosis in a process defined as efferocytosis (Martin et al., 2012; Parandhaman and Narayanan, 2014). Upon engulfment, *Mtb* within apoptotic macrophages, together with apoptotic debris, are presented to the lysosomal compartment where *Mtb* bacteria are killed (Kagina et al., 2010).

1.4.1.3. Autophagy

Autophagy is an intracellular process through which cells eliminate damaged organelles, protein aggregates and intracellular pathogens. It involves formation of a double-membrane-

enclosed structure that forms an autophagic vacuole (membrane bound vacuole containing intracellular redundant organelles for digestion) (Kimmey and Stallings, 2016). The process is activated by starvation and other stimuli such as nutrient deficiency, hypothermia and hypoxia (Chu, 2008).

1.4.2. Granuloma

A granuloma is a structured cluster containing *Mtb*-infected macrophages surrounded mainly by uninfected and activated macrophages, T-cells and other immune cells such as polymorphonuclear leukocytes (PMNLs), epithelioid cells and multinucleated giant cells (Buddle et al. 2002; Russell, 2007; Pieters, 2008). Granulomas are characterised by unfavourable growth and survival conditions for the bacterium, which include hypoxia, oxidative and nitrosative stress, altered nutrient availability and limited nutrients (Martin et al., 2016). These conditions allow the bacteria to alter their metabolism, leading to development of slow- and non-replicating organisms (Cardona and Ruiz-Manzano, 2004).

Two kinds of granulomas, caseous and fibrotic, have been demonstrated during *Mtb* infection in cynomolgus macaques, which are high primates evolutionarily close to humans (Lin et al., 2009). The caseous granulomas are characterised by fibroblasts surrounding epitheloid macrophages and neutrophils in the periphery and dead macrophages in the centre, with low oxygen levels, and are commonly associated with active TB (Via et al., 1998). Fibrotic granulomas, on the other hand, are exclusively filled with fibroblasts and infected macrophages and are associated with latent TB infection (Barry et al., 2009). During periods of immunosuppression, granulomas liquefy and the bacteria are released from the degraded granuloma to re-infect lung tissue and spread to new hosts (Kim et al., 2010).

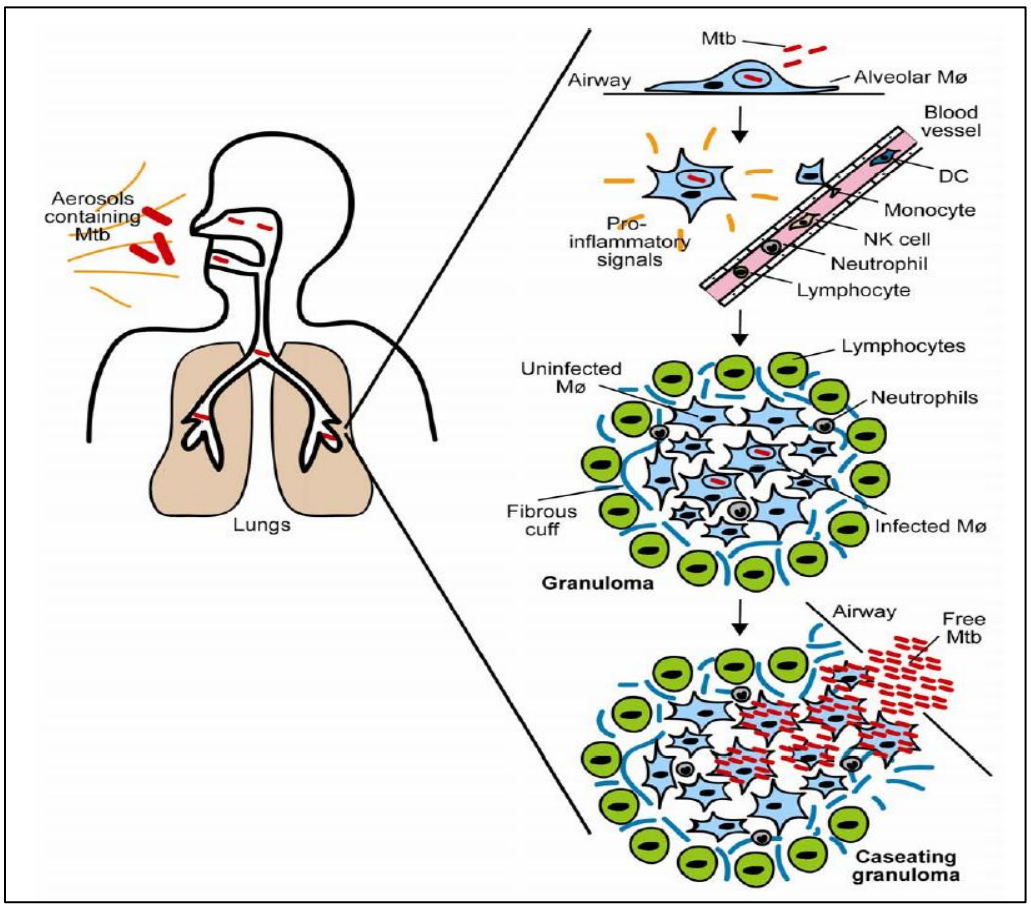

Figure 1.3: The infection process of *Mycobacterium tuberculosis* and the formation of a caseating granuloma (Russell, 2007, permission granted).

1.4.3. Cytokines

Cytokines are small soluble proteins, which include pro-inflammatory and anti-inflammatory cytokines produced by nucleated cells, which influence the activities of the other cells (Domingo-Gonzalez et al., 2016). The interaction of *Mtb* ligands with the PRRs on macrophages, as well as DCs, activates the secretion of cytokines. The pro-inflammatory cytokines produced during *Mtb* infection include, most importantly, Th1 cell- derived IFN-γ, interleukin (IL) 12 and TNF-α (Zuñiga et al., 2012). The anti-inflammatory cytokines counteract the effects of pro-inflammatory cytokines. These include IL-4, IL-10, IL-27 and transforming growth factor (TGF)-β (Villarino et al., 2003).

1.5. MYCOBACTERIAL SURVIVAL MECHANISMS

Bacteria have developed mechanisms for evasion of the host immune system. These mechanisms include the use of alternative surface receptors, inhibition of various macrophage-

associated, including phagosomal maturation, phagolysosomal fusion, oxidative stress, apoptosis and autophagy, and granuloma formation.

1.5.1. Surface receptors

Infection of macrophages by *Mtb* and other pathogenic mycobacteria, involves binding of the microorganisms via opsonisation with complement component C3-derived opsonins deposited on the surface of *Mtb* and internalisation of the bacteria via binding of the opsonised bacteria to CRs, CR1, CR3, as well as mannose receptors, on pulmonary phagocytes (Palucci et al. 2016). These routes of cell entry are different from those of non-pathogenic mycobacteria, which is indicative of their contributions to the survival strategy of the bacteria during intracellular infection (Meena and Rajni, 2010).

Bacterial components, associated with these alternative bacterial routes of infection include the 19-kDa lipoprotein, lipoarabinomannan (LAM) and araLAM, which bind to Toll-like receptors (TLRs) on the surface of host cells, compromisisng the macrophage response to pro-inflammatory cytokines (Means et al., 1999; Fortune et al., 2004).

1.5.2. Inhibition of phagosomal maturation

Mtb inhibits phagosomal maturation, allowing intracellular survival in the vacuole by preventing phagolysosomal fusion. The bacteria secrete various proteins such as ESAT-6, CFP and adenosine triphosphate (ATP) 1/2, which decrease the vacuolar pH, preventing the accumulation of vacuolar ATP and GTP enzymes (Smith et al., 2008). In addition, *Mtb* employs ESAT-6 to lyse the phagosomal membrane, allowing the bacillus to escape into the cytoplasm (Smith et al., 2008; Carlsson et al., 2010).

1.5.3. Inhibition of phagolysosomal fusion

The formation of phagolysosomes exposes the bacteria to antimicrobial, acidic lysosomal enzymes (Kinchen and Ravichandran, 2008). However, *Mtb* is able to evade the activities of these enzymes by budding off from the phagolysosomes and entering the cytoplasm. *Mtb* also uses trehalose glycolipids, which attenuate phagolysosome fusion (Goren, 1977). The pathogen also releases ammonia, which alkalinises the intralysosomal compartment, reducing the potency of intralysosomal enzymes (Hart et al., 1983). Furthermore, *Mtb* interferes with actin

formation required for scaffolding during phagosome-endosome vacuole formation (Guerin and de Chastellier, 2000).

1.5.4. Inhibition of oxidative stress

Mtb utilises ManLAM to suppress the microbicidal activities of macrophages by inhibiting the formation of nitric oxide and reactive oxygen species (ROS) by nitric oxide synthase and NADPH oxidase, respectively (Brandt et al., 2002). *Mtb* also employs the asparagine transporter, AnsP2, and the secreted asparaginase, AnsA, to assimilate nitrogen and resist acid stress during infection through asparagine hydrolysis and ammonia release (Phelan et al. 2018).

1.5.5. Inhibition of apoptosis and autophagy

The expression of bacterial virulence factors such as miR-30A, cell wall 19-kDa lipoprotein and superoxide dismutase lead to suppression of apoptosis and autophagy (Ciaramella et al., 2000; Hinchey et al., 2007; Gajer et al., 2012; Chen et al., 2015). When overexpressed, Chen et al (2015) showed that miR-30A subdues the eradication of intracellular *Mtb* by regulating the production of NO and pro-inflammatory cytokines to alter the relationship with TLRs. As such *Mtb* virulence factors inhibit TNF-α-induced apoptosis and interferes with the caspase, JAK2/STAT1, TNF-α and Bcl-2 pathways thereby lessening macrophage apoptosis and enhancing the survival rate of pathogens (Clay et al., 2008).

1.5.6. Granuloma formation

Granuloma formation allows the mycobacteria to evade immune responses, leading to development of dormant organisms (Silver et al., 2012). Several granuloma-associated factors that lead to dormancy include hypoxia, acidic pH, nutrient limitation and increased levels of ROS (Cardona and Ruiz-Manzano, 2004). These factors allow mycobacteria to alter their metabolic rates, promoting resistance to the immune system and antimicrobial agents (Peddireddy et al., 2017).

1.5.7. Mycobacterial biofilm formation in the host

Mtb is able to form biofilm *in vitro*. Biofilm development involves formation of sessile bacteria enclosed in an extracellular polymeric substance (EPS) matrix, commonly made up of

glycopeptides, DNA, and other molecules (Esteban and García-Coca, 2018). The role of biofilms in the pathogenesis of *Mtb* is not yet known. However, biofilm is used by bacteria for protection against antibiotics (Fux et al., 2005; Islam et al., 2012; Basaraba and Ojha, 2017; Ciofu et al., 2017). Various mechanisms have been proposed to promote drug resistance, including decreased penetration, alterations in bacterial metabolic status and activation of resistance genes (Lewis, 2008; Kester and Fortune, 2014). Resistance to antibiotics by biofilm-forming mycobacteria may lead to treatment failure (Hall-Stoodley et al., 2012).

1.5.8 Mycobacterial ion-transporters

The above examples clearly indicate that M*tb* is a dangerous and persistent bacterial respiratory pathogen. As such, novel insights into other virulence mechanisms and disease pathogenesis including the role of the various K^+ transporters of the pathogen is required. This information is necessary in the development of novel anti-mycobacterial strategies such as antitubercular compounds and vaccines.

1.6. REFERENCES

Ahearn J.M. and Fearon D.T. (1989). Structure and function of the complement receptors, CR1 (CD35) and CR2 (CD21). *Advances in Immunology*, 46, 183-219.

Alderwick L.J., Birch H.L., Mishra A.K., Eggeling L. and Besra G.S. (2007). Structure, function and biosynthesis of the *Mycobacterium tuberculosis* cell wall: arabinogalactan and lipoarabinomannan assembly with a view to discovering new drug targets. *Biochemical Society Transactions*, 35(Pt 5), 1325-1328.

Alexander K.A., Laver P.N., Michel A.L., Williams M., van Helden P.D., Warren R.M. and Gey van Pittius N.C. (2010). Novel *Mycobacterium tuberculosis* complex pathogen, *M. mungi*. *Emerging Infectious Diseases*, 16(8), 1296-1299.

Andersen P. and Doherty T.M. (2005). The success and failure of BCG - implications for a novel tuberculosis vaccine. *Natural Reviews Microbiolology*, 3(8), 656-662.

Apt A.S. and Kondrat'eva T.K. (2008). Tuberculosis: pathogenesis, immune responses and genetics of the host. *Molekuliarnaia Biologiia*, 42(5), 880-890.

Aronson N.E., Santosham M., Comstock G.W., Howard R.S., Moulton L.H., Rhoades E.R. and Harrison L.H. (2004). Long-term efficacy of BCG vaccine in American Indians and Alaska Natives: A 60-year follow-up study. *The Journal of the American Medical Association*, 291(17), 2086-2091.

Banada P.P., Sivasubramani S.K., Blakemore R., Boehme C., Perkins M.D., Fennelly K. and Alland D. (2010). Containment of bioaerosol infection risk by the Xpert MTB/RIF assay and its applicability to point-of-care settings. *Journal of Clinival Microbiology*, 48(10), 3551-3557.

Barberis I., Bragazzi N.L., Galluzzo L. and Martini M. (2017). The history of tuberculosis: from the first historical records to the isolation of Koch's bacillus. *Journal of Preventative Medicine and Hyg*, 58(1): E9-E12.

Barry C.E., Boshoff H.I., Dartois V., Dick T., Ehrt S., Flynn J., et al. (2009). The spectrum of latent tuberculosis: rethinking the biology and intervention strategies. *Natural Reviews Microbiolology*, 7(12), 845-855.

Basaraba R.J. and Ojha A.K. (2017). Mycobacterial biofilms: revisiting tuberculosis bacilli in extracellular necrotizing lesions. *Microbiology Spectrum*, 5(3).

Bishai J.D., Bishai W.R. and Bishai D.M. (2010). Heightened vulnerability to MDR-TB epidemics after controlling drug-susceptible TB. *PloS One*, 5(9), e12843.

Brandt L., Feino Cunha J., Weinreich Olsen A., Chilima B., Hirsch P., Appelberg R. and Andersen P. (2002). Failure of the *Mycobacterium bovis* BCG vaccine: some species of environmental mycobacteria block multiplication of BCG and induction of protective immunity to tuberculosis. *Infection and Immunity*, 70(2), 672-678.

Brennan P.J. (2003). Structure, function, and biogenesis of the cell wall of *Mycobacterium tuberculosis*. *Tuberculosis (Edinburg, Scotland)*, 83(1-3), 91-97.

Brosch R., Gordon S.V., Marmiesse M., Brodin P., Buchrieser C., Eiglmeier K., et al. (2002). A new evolutionary scenario for the *Mycobacterium tuberculosis* complex. *Proceedings of the National Academy of Sciences of the United States of America*, 99(6), 3684-3689.

Buddle B., Skinner M., Wedlock D., Collins D. and De Lisle G. (2002). New generation vaccines and delivery systems for control of bovine tuberculosis in cattle and wildlife. *Veterinary Immunolology Immunopathology*, 87(3), 177-185.

Calmette A. (1922). L'ninfection bacillaire et la tuberculose chez l'homme et chez les animaux (Masson et Cie, Paris, 1936)

Cambau E. and Drancourt M. (2014). Steps towards the discovery of *Mycobacterium tuberculosis* by Robert Koch, 1882. *Clinical Microbiology and Infection*, 20(3), 196-201.

Caminero J.A., Sotgiu G., Zumla A. and Migliori G.B. (2010). Best drug treatment for multidrug-resistant and extensively drug-resistant tuberculosis. *The Lancet Infectious Diseases*, 10(9), 621-629.

Cardona P.J. and Ruiz-Manzano J. (2004). On the nature of *Mycobacterium tuberculosis*-latent bacilli. *The European Respiratory Journal*, 24(6), 1044-1051.

Carlsson F., Kim J., Dumitru C., Barck K.H., Carano R.A., Sun M., et al. (2010). Host-detrimental role of Esx-1-mediated inflammasome activation in mycobacterial infection. *PLoS Pathogens*, 6(5), e1000895.

Chen Z., Wang T., Liu Z., Zhang G., Wang J., Feng S. and Liang J. (2015). Inhibition of autophagy by MiR-30A induced by *Mycobacterium tuberculosis* as a possible mechanism of immune escape in human macrophages. *Japanese Journal of Infectious Diseases*, 68, 420-424.

Chihota V.N., Grant A.D., Fielding K., Ndibongo B., van Zyl A., Muirhead D. and Churchyard G.J. (2010). Liquid vs. solid culture for tuberculosis: performance and cost in a resource-constrained setting. *International Journal of Tuberculosis and Lung Diseases*, 14(8), 1024-1031.

Chu C.T. (2008). Eaten alive: autophagy and neuronal cell death after hypoxia-ischemia. *The American Journal of Patholology,* 172(2), 284-287.

Ciaramella A., Martino A., Cicconi R., Colizzi V. and Fraziano M. (2000). Mycobacterial 19-kDa lipoprotein mediates *Mycobacterium tuberculosis*-induced apoptosis in monocytes/macrophages at early stages of infection. *Cell Death Differentiation,* 7(12), 1270-1272.

Ciofu O., Rojo-Molinero E., Macià M.D. and Oliver A. (2017). Antibiotic treatment of biofilm infections. *Acta Pathologica, Microbiologica et Immunologica Scandinavica,* 125(4), 304-319.

Clay H., Volkman H.E. and Ramakrishnan L. (2008). Tumor necrosis factor signaling mediates resistance to mycobacteria by inhibiting bacterial growth and macrophage death. *Immunity,* 29(2), 283-294.

Colditz G.A., Brewer T.F., Berkey C.S., Wilson M.E., Burdic, E. and Fineberg H.V. (1994). Efficacy of BCG vaccine in the prevention of tuberculosis: meta-analysis of the published literature. *JAMA,* 271(9), 698-702.

Corbett E.L., Watt C.J., Walker N., Maher D., Williams B.G., Raviglione M.C. and Dye C. (2003). The growing burden of tuberculosis: global trends and interactions with the HIV epidemic. *Archives of Internal Medicine,* 163(9), 1009-1021.

Daffe M. and Draper P. (1998). The envelope layers of mycobacteria with reference to their pathogenicity. *Advances in Microbial Physiolology,* 39, 131-203.

De Lisle G., Wards B., Buddle B. and Collins D. (2005). The efficacy of live tuberculosis vaccines after presensitization with *Mycobacterium avium*. *Tuberculosis,* 85(1), 3-79.

Dheda K., Schwander S.K., Zhu B., van Zyl-Smit R.N. and Zhang, Y. (2010). The immunology of tuberculosis: from bench to bedside. *Respirology (Carlton, Vic.),* 15(3), 433-450.

Domingo-Gonzalez R., Prince O., Cooper A. and Khader S. (2016). Cytokines and Chemokines in *Mycobacterium tuberculosis* infection. *Microbiolology Spectrum,* 4(5), 1-35.

Dorman S.E., Schumacher S.G., Alland D., Nabeta P., Armstrong D.T. and King B. (2018). Xpert MTB/RIF Ultra for detection of *Mycobacterium tuberculosis* and rifampicin resistance: a prospective multicentre diagnostic accuracy study. *The Lancet Infectious Disease,* 18(1), 76-84.

Ducati R.G., Ruffino-Netto A., Basso L.A. and Santos D.S. (2006). The resumption of consumption - a review on tuberculosis. *Memorias do Instituto Oswaldo Cruz,* 101(7), 697-714.

Dye C. and Williams B.G. (2010). The population dynamics and control of Tuberculosis. *Science*, 328(5980), 856-861.

Echeverria-Valencia, Gabriela, Flores-Villalva S. and Espitia C.I. (2017). Virulence factors and pathogenicity of Mycobacterium. *Mycobacterium Research and Development. Wellman Ribón, IntechOpen*: 231-255.

Elkomy H., Awad M., El-Shora A. and Elsherbeni B. (2013). Assessment of the efficacy of Directly Observed Treatment with short course (DOTS) for pulmonary tuberculosis in Sharkia governorate. *Egyptian Journal of Chest Diseases and Tuberculosis*, 62(2), 257-261.

Esteban J. and García-Coca M. (2018). Mycobacterium biofilms. *Frontiers in Microbiology*, 8, 2651.

Fine P.E. (1995). Variation in protection by BCG: implications of and for heterologous immunity. *Lancet*, 346 (8986), 1339-1345.

Forrellad M.A., Klepp L.I., Gioffré A., Sabio y García J., Morbidoni H.R., Santangelo M., et al. (2013). Virulence factors of the *Mycobacterium tuberculosis* complex. *Virulence*, 4(1), 3-66.

Fortune S.M., Solache A., Jaeger A., Hill P.J., Belisle J.T., Bloom B.R. et al. (2004). *Mycobacterium tuberculosis* inhibits macrophage responses to IFN-gamma through myeloid differentiation factor 88-dependent and -independent mechanisms. *Journal of Immunolology*, 172(10), 6272-6280.

Fux C.A., Costerton J.W., Stewart P.S. and Stoodley P. (2005). Survival strategies of infectious biofilms, *Trends in Microbiology*. 13(1), 34-40.

Gajer P., Brotman R.M., Bai G., Sakamoto J., Schutte U.M., Zhong X. et al. (2012). Temporal dynamics of the human vaginal microbiota. *Science Translational Medicine*, 4(132), 132ra52.

Getahun H., Matteelli A., Chaisson R.E. and Raviglione M. (2015). Latent *Mycobacterium tuberculosis* infection. *The New England Journal of Medicine*, 372(22), 2127-2135.

Ghosh J., Larsson P., Singh B., Pettersson B.M.F., Islam N.M., Sarkar S.N. et al. (2009). Sporulation in mycobacteria. *Proceedings of the National Academy of Sciences of the United States of America, 106(26), 10781-10786.*

Goren M.B. (1977). Phagocyte lysosomes: interactions with infectious agents, phagosomes, and experimental perturbations in function. *Annual Review of Microbiololgy*, 31, 507-533.

Guerin I. and de Chastellier C. (2000). Pathogenic mycobacteria disrupt the macrophage actin filament network. *Infection and Immunity*, 68(5), 2655-2662.

Hall-Stoodley L., Stoodley P., Kathju S., Hoiby N., Moser C., Costerton J. W. et al. (2012). Towards diagnostic guidelines for biofilm-associated infections. *FEMS Immunolology and Medical Microbiology*, 65, 127-145.

Harries A.D., Zachariah R., Corbett E.L., Lawn S.D., Santos-Filho E.T., Chimzizi R. et al. (2010). The HIV-associated tuberculosis epidemic-when will we act? *Lancet*, 375(9729), 1906-1919.

Hart P.D., Young M.R., Jordan M.M., Perkins W.J. and Geisow M.J. (1983). Chemical inhibitors of phagosome-lysosome fusion in cultured macrophages also inhibit saltatory lysosomal movements. A combined microscopic and computer study. *The Journal of Experimental Medicine*, 158(2), 477-492.

Helb D., Jones M., Story E., Boehme C., Wallace E., Ho K. et al. (2010). Rapid detection of *Mycobacterium tuberculosis* and rifampin resistance by use of on-demand, near-patient technology. *Journal of Clinical Microbiology*, 48(1), 229-237.

Hinchey J., Lee S., Jeon B.Y., Basaraba R.J., Venkataswamy M.M., Chen B. et al. (2007). Enhanced priming of adaptive immunity by a proapoptotic mutant of *Mycobacterium tuberculosis*. *The Journal of Clinical Investigation*, 117(8), 2279-2288.

Iseman M.D. (2002). Tuberculosis therapy: past, present and future. *The European Respirotory Journal Supplment*, 36, 87s-94s.

Islam M.S., Richards J.P. and Ojha A.K. (2012). Targeting drug tolerance in mycobacteria: a perspective from mycobacterial biofilms. *Expert Review of Anti-infective Therapy*, 10(9), 1055-1066.

Ismail N., Olano J.P., Feng H.M. and Walker D.H. (2002). Current status of immune mechanisms of killing of intracellular microorganisms. *FEMS Microbiolology Letters*, 207(2), 111-120.

Kagina B.M., Abel B., Scriba T.J., Hughes E.J., Keyser A. Soares, A. et al. (2010). Specific T cell frequency and cytokine expression profile do not correlate with protection against tuberculosis after bacillus Calmette-Guerin vaccination of newborns. *The American Journal of Respiratory and Critical Care Medicine*, 182(8), 1073-1079.

Kanchana M.V., Cheke D., Natyshak I., Connor B., Warner A. and Martin T. (2000). Evaluation of the BACTEC MGIT 960 system for the recovery of mycobacteria. *Diagnostic Microbiolology and Infectious Disease*, 37(1), 31-36.

Kester J.C. and Fortune S.M. (2014) Persisters and beyond: Mechanisms of phenotypic drug resistance and drug tolerance in bacteria. *Critical Reviews in Biochemistry and Molecular Biolology,* 49:2, 91-101.

Kim M.J., Wainwright H.C., Locketz M., Bekker L.G., Walther G.B., Dittrich C. and Visser A. (2010). Caseation of human tuberculosis granulomas correlates with elevated host lipid metabolism. *EMBO Molecular Medicine,* 2(7), 258-274.

Kimmey J.M. and Stallings C.L. (2016). Bacterial pathogens versus autophagy: implications for therapeutic interventions. *Trends Molecular Medicine,* 22(12), 1060-1076.

Kinchen J.M. and Ravichandran K.S. (2008). Review Phagosome maturation: going through the acid test. *Nature Reviews. Molecular Cell Biolology,* 9(10), 781-795.

Koch M.L., Cote R.A. (1965). Comparison of fluorescence microscopy with Ziehl-Neelsen stain for demonstration of acid-fast bacilli in smear preparations and tissue sections. *American Reviews of Respirpiratory Diseases*. 91:283–28

Lehmann J. (1946). Para-aminosalicylic acid in the treatment of tuberculosis. *Lancet,* 247(6384), 15-16.

Lewis H.C., Mølbak K., Reese C., Aarestrup F.M., Selchau M., Sørum M. and Skov R.L. (2008). Pigs as source of methicillin-resistant *Staphylococcus aureus* CC398 infections in humans, Denmark. *Emerging Infectious Diseases,* 14(9), 1383-1389.

Lin P.L., Rodgers M., Smith L., Bigbee M., Myers A., Bigbee C. et al. (2009). Quantitative comparison of active and latent tuberculosis in the cynomolgus macaque model. *Infection and Immunity*. 77, 4631-4642.

Lönnroth K., Castro K.G., Chakaya J.M., Chauhan L.S., Floyd K., Glaziou P. and Raviglione, M.C. (2010). Tuberculosis control and elimination 2010-50: cure, care, and social development. *Lancet,* 375(9728), 1814-1829.

Marrakchi H., Lanéelle M.A. and Daffé M. (2014). Mycolic acids: structures, biosynthesis, and beyond. *Chemistry and Biolology,* 21(1): 67-85.

Martin C.J., Booty M.G., Rosebrock T.R., Nunes-Alves C., Desjardins D.M., Keren I., et al. (2012). Efferocytosis is an innate antibacterial mechanism. *Cell Host and Microbe,* 12(3), 289-300.

Martin C.J., Carey A.F. and Fortune S.M. (2016). A bug's life in the granuloma. Seminars in Immunopathology. *Springer,* 213.

Mazurek G.H., Jereb J., Lobue P., Iademarco M.F., Metchock B. and Vernon A. (2005). Guidelines for using the QuantiFERON-TB Gold test for detecting *Mycobacterium*

tuberculosis infection, United States. *Morbidity and Mortality Weekly Report. Recommendations and Reports*, 54, 49-55.

McKenzie D., Malone L., Kushner S., Oleson J. and Subbarow Y. (1948). The effect of nicotinic acid amide on experimental tuberculosis of white mice. *The Journal of Laboratory and Clinical Medicine*, 33(10), 1249-1253.

Means T.K., Wang S., Lien E., Yoshimura A., Golenbock D.T. and Fenton M.J. (1999). Human toll-like receptors mediate cellular activation by *Mycobacterium tuberculosis*. *Journal of Immunolology*, 163(7), 3920-3927.

Meena L.S. and Rajni (2010). Survival mechanisms of pathogenic *Mycobacterium tuberculosis* H_{37}Rv. *The FEBS Journal*, 277(11), 2416-2427.

Minion J., Gallant V., Wolfe J., Jamieson F. and Long R. (2013). Multidrug and extensively drug-resistant tuberculosis in Canada 1997-2008: demographic and disease characteristics. *PloS One*, 8(1), e53466.

Navin T.R., McNabb S.J. and Crawford J.T. (2002). The continued threat of tuberculosis. *Emerging Infectious Diseases*, 8(11), 1187.

Nayak S. and Acharjya B. (2012). Mantoux test and its interpretation. *Indian Dermatolology Online Journal*, 3(1), 2-6.

Palange P., Narang R., and Kandi V. (2016). Evaluation of culture media for isolation of *Mycobacterium* species from human clinical specimens. *Cureus*, 8(8), e757.

Palucci I., Camassa S., and Cascioferro A. Sali M., Anoosheh S., Zumbo A., et al. (2016). PE_PGRS33 contributes to *Mycobacterium tuberculosis* in macrophages through interaction with TLR2. *PLoS One*, 0150800

Parandhaman D.K. and Narayanan S. (2014). Cell death paradigms in the pathogenesis of *Mycobacterium tuberculosis* infection. *Frontiers Cell and Infection Microbiology*, 4, 31.

Paterson R. (2003). Initiative to unify control of HIV/AIDS and tuberculosis. *The Lancet Infectious Diseases*, 3(3), 119.

Peddireddy V., Doddam S.N. and Ahmed N. (2017). Mycobacterial dormancy systems and host responses in tuberculosis. *Frontiers in Immunolology*, 8, 84.

Phelan J., Basdeo S., Tazoll S. McGivern S., Saborido J.R. and Keane J. (2018). Modulating iron for metabolic support of TB host defense. *Frontiers in Immunolology*, 9, 2296. = Pieters J. (2008). *Mycobacterium tuberculosis* and the macrophage: maintaining a balance. *Cell Host and Microbe*, 3(6), 399-407.

Robitzek E.H. and Selikoff I.J. (1952). Hydrazine derivatives of isonicotinic acid (rimifon marsilid) in the treatment of active progressive caseous-pneumonic tuberculosis; a preliminary report. *American Review of Tuberculosis*, 65(4), 402-428.

Rodrigues L.C., Diwan V.K. and Wheeler, J.G. (1993). Protective effect of BCG against tuberculous meningitis and miliary tuberculosis: a meta-analysis. *International journal of epidemiology*, 22(6), 1154-1158.

Rodríguez S., Bezos J., Romero B., de Juan L., Álvarez J., Castellanos E., et al. (2011). *Mycobacterium caprae* infection in livestock and wildlife, Spain. *Emerging Infectious Diseases*, 17(3), 532-535.

Ponnighaus J. M., Msosa E., Gruer P. J. K., Liomba N. G., Fine P. E. M., and Sterne J. A. C. (1992). Efficacy of BCG vaccine against leprosy and tuberculosis in northern Malawi. *The Lancet*, 339(8794), 636-639.

Russell D.G. (2007). Who puts the tubercle in tuberculosis? *Natural Reviews Microbiolology*, 5(1), 39-47.

Schatz A., Bugle E. and Waksman, S.A. (1944). Streptomycin, a substance exhibiting antibiotic activity against gram-positive and gram-negative bacteria. *Society for Experimental Biology and Medicine*, 55(1), 66-69.

Schön T., Miotto P., Köser C.U., Viveiros M., Böttger E. and Cambau E. (2017). *Mycobacterium tuberculosis* drug-resistance testing: challenges, recent developments and perspectives. *Clinical Microbiolology and Infection*, 23(3), 154-160.

Sensi P. (1983). History of the development of rifampin. *Reviews of Infectious Diseases*, 5(3), s402-s406.

Silver A.C., Arjona A., Walker W.E. and Fikrig E. (2012). The circadian clock controls toll-like receptor 9-mediated innate and adaptive immunity. *Immunity*. 36(2), 251-261.

Smith J., Manoranjan J., Pan M., Bohsali A., Xu J., Liu J., et al. (2008). Evidence for pore formation in host cell membranes by ESX-1-secreted ESAT-6 and its role in *Mycobacterium marinum* escape from the vacuole. *Infection and Immununity*, 76(12), 5478-5487.

Snowden F.M. (2008). Emerging and reemerging diseases: a historical perspective. *Immunological Reviews*, 225, 9-26.

Sotgiu G., Ferrara G., Matteelli A., Richardson M.D., Centis R., Ruesch-Gerdes S., et al. (2009). Epidemiology and clinical management of XDR-TB: a systematic review by TBNET. *The European Respiratory Journal*, 33(4), 871-881.

Urdahl K.B., Shafiani S. and Ernst J.D. (2011). Initiation and regulation of T-cell responses in tuberculosis. *Mucosal Immunolology*. 4(3), 288-293.

Sreevatsan S., Pan X., Stockbauer K.E., Connell N.D., Kreiswirth B.N., Whittam T.S. and Musser J.M. (1997). Restricted structural gene polymorphism in the *Mycobacterium tuberculosis* complex indicates evolutionarily recent global dissemination. *Proceedings of the National Academy of Sciences of the United States of America*, 94(18), 9869-9874.

Talip B.A., Sleator R.D., Lowery C.J., Dooley J.S.G and Snelling W.J. (2013). An update on global tuberculosis (TB). *Infectious Diseases*, 6, 39-50.

Tankimovich M. (2013). Barriers to and interventions for improved tuberculosis detection and treatment among homeless and immigrant populations: a literature review. *Journal of Community Health Nursing*, 30(2), 83-95.

Thomas J., Baughn C., Wilkinson R. and Shepherd R. (1961). A new synthetic compound with antituberculous activity in mice: Ethambutol (Dextro-2, 2′-(ethylenediimino)-di-1-butanol). *The American Review of Respiratory Disease*, 83(6), 891-893.

Tiberi S., Carvalho A.C., Sulis G., Vaghela D., Rendon A., Mello F.C., et al. (2017). The cursed duet today: Tuberculosis and HIV-coinfection. *Presse Medicale*, 46(2 Pt 2), e23-e39.

Tortoli E. (2014). Microbiological features and clinical relevance of new species of the genus Mycobacterium. *Clinical Microbiology Reviews*, 27(4), 727-752.

Van Hest N., Aldridge R., De Vries G., Sandgren A., Hauer B., Hayward A. et al., (2014). Tuberculosis control in big cities and urban risk groups in the European Union: a consensus statement. *Euro Surveillance*, 6, 19(9). pii: 20728.

Van Ingen J., Rahim Z., Mulder A., Boeree M.J., Simeone R., Brosch R. and van Soolingen, D. (2012). Characterization of *Mycobacterium orygis* as *M. tuberculosis* complex subspecies. *Emerging Infectious Diseases*, 18(4), 653-655.

Varaine F., Guglielmetti L., Huerga H., Bonnet M., Kiria N., Sitienei J.K., et al. (2017). Eligibility for the shorter multidrug-resistant tuberculosis regimen: Ambiguities in the World Health Organization recommendations. *The American Journal of Respiratory and Critical Care Medicine*, 194 (8), 1028-1029.

Velayati A.A., Farnia P., Boloorsaze M.R., Sheikholslami M.F., Khalilzadeh S. and Hakeeme S.S., Masjedi M.R. (2007). *Mycobacterium bovis* infection in children in the same family: transmission through inhalation. *Monaldi Archives for Chest Disease*, 67(3), 169-72.

Via L.E., Fratti R.A., McFalone M., Pagan-Ramos E., Deretic D. and Deretic V. (1998). Effects of cytokines on mycobacterial phagosome maturation. *Journal of Cell Science*, 111 (Pt 7), 897-905.

Villarino A., Hibbert L., Lieberman L., Wilson E., Mak T., Yoshida H., et al. (2003). The IL-27R (WSX-1) is required to suppress T cell hyperactivity during infection. *Immunity*, 19(5), 645-655.

Weiss G. and Schaible U.E. (2015). Macrophage defense mechanisms against intracellular bacteria. *Immunological Reviews*, 264(1), 182-203.

Wirth T., Hildebrand F., Allix-Béguec C., Wölbeling F, Kubica T., Kremer K., et al. (2008). Origin, spread and demography of the *Mycobacterium tuberculosis* complex. *PLoS Pathogens*, 4(9), e1000160.

Winter J., Stagg H., Smith C. Lalor M.K., Davidson J.A., Brown A.E. et al. (2018). Trends in, and factors associated with, HIV infection amongst tuberculosis patients in the era of anti-retroviral therapy: a retrospective study in England, Wales, and Northern Ireland. *BMC Medicie*, 16(1), 85.

World Health Organization. (2015). Global tuberculosis report 2015, 20th ed. *https://apps.who.int/iris/handle/10665/191102*. Accessed Aug 2019.

World Health Organization. (2016). Global tuberculosis report 2016. *https://apps.who.int/medicinedocs/en/d/Js23098en*. Accessed Aug 2019.

World Health Organization. (2017). Global tuberculosis report 2017. *https://www.who.int/tb/publications/global_report/gtbr2017_main_text.pdf*. Accessed Aug 2019.

World Health Organization. (2019). Global tuberculosis report 2019. *https://apps.who.int/iris/bitstream/handle/10665/329368/9789241565714-eng.pdf?ua=1*. Accessed Dec 2019.

Yang C.T., Cambier C.J., Davis J.M., Hall C.J., Crosier P.S. and Ramakrishnan L. (2012). Neutrophils exert protection in the early tuberculous granuloma by oxidative killing of mycobacteria phagocytosed from infected macrophages. *Cell Host and Microbe*, 12(3), 301-312.

Zink A.R., Sola C., Reischl U., Grabner W., Rastogi N., Wolf H. and Nerlich A.G. (2003). Characterization of *Mycobacterium tuberculosis* complex DNAs from Egyptian mummies by spoligotyping. *Journal of Clinical Microbiology*, 41(1), 359-367.

Zumbo A., Palucci I., Cascioferro A., Sali M., Ventura M., D'Alfonso P., et al. (2013). Functional dissection of protein domains involved in the immunomodulatory properties

of PE_PGRS33 of *Mycobacterium tuberculosis*. *Pathogens and Disease*, 69(3), 232-239.

Zuñiga, J., Torres-García D., Santos-Mendoza T., Rodriguez-Reyna T.S., Granados J. and Yunis, E.J. (2012). Cellular and humoral mechanisms involved in the control of tuberculosis. *Clinical and and Development Immunologgy*, ID 193923

CHAPTER TWO: POTASSIUM TRANSPORT SYSTEMS OF *MYCOBACTERIUM TUBERCULOSIS*

2.1. CELLULAR POTASSIUM CONCENTRATIONS

The potassium ion (K^+) is the most abundant monovalent cation in all living cells, being essential for a wide variety of cellular functions, which include maintenance of turgor pressure, osmoregulation, pH homeostasis, membrane potential regulation, enzyme activation and gene expression (Epstein, 2003; Follmann et al., 2009; Ochrombel et al., 2011).

Its role in human pathogens has been reported in several bacterial species. In Salmonella species, K^+ is required for the expression and secretion of the effector proteins of the Salmonella pathogenicity island 1 (SPI1)-encoded type III secretion system (TTSS), which enhances epithelial cell invasion (Su et al., 2009) as well as for the synthesis of virulence factors (Liu et al., 2013). In the plant pathogen, *Pectobacterium wasabiae,* K^+ is involved in synthesis of the virulence factor, RsmB, which is involved in production of the plant-cell wall degrading enzymes (PCWDEs), which include cellulases, proteases, pectate lyases and pectin lyases and polygalacturonases (Valente and Xavier, 2016).

The high intracellular K^+ concentrations range between 300 to 1000 millimolar (mM), even in the setting of low extracellular concentrations (Steyn et al., 2003). Bacteria use several K^+ transporters and channels, which include the influx and efflux systems for maintenance of these high K^+ levels (Su et al., 2009).

2.2. BACTERIAL POTASSIUM INFLUX SYSTEMS

The bacterial K^+ influx systems consist of the active K^+-uptake transporters, which include the three bacterial families, Trk/Ktr/HKT, Kup/HAK/KT, and Kdp as well as K^+ channels (Berry et al., 2003; Ballal et al., 2007; Sato et al., 2014). The bacterial K^+-uptake transporters that have been well characterised are those found in the Gram-negative bacterium, *Escherichia coli* (*E. coli),* which include the Trk, Kup and Kdp systems (Liu et al., 2013). These systems differ in their structures and affinities for the cation, maintaining intracellular K^+ concentrations under diverse environmental conditions (Epstein, 2003; Nanatani et al., 2015).

2.2.1. Bacterial Trk transporters

The Trk systems are found in a wide range of bacteria and differ in different organisms. In *E. coli*, the Trk system is a constitutively expressed, multiunit protein complex formed by the

TrkH, TrkG, TrkA and TrkE subunits. The TrkH and TrkG are highly homologous and both require TrkA for functioning. The TrkH-dependent K^+ transport system requires an additional gene *trkE*, encoding the ATP-binding protein while TrkA is the main K^+ transporter (Dosch et al., 1991; Johnson et al., 2009).

The Trk system consists of membrane-spanning and peripheral membrane-associated nucleotide-binding proteins and possesses the nicotinamide adenine dinucleotide (NAD^+)-binding domain of dehydrogenases, operating as a K^+/hydrogen (H^+) symporter (Epstein et al., 1990; Walderhaug et al., 1992; Sharma et al. 2016). It has a low affinity to the cation and transports K^+ at neutral to alkaline pH (Liu et al., 2013).

The K^+-uptake permease (Kup), also known as the TrkD, is also constitutively expressed and has similar affinity for K^+ as the Trk. However, it is the main K^+ transport system under acidic conditions and transports K^+ at lower rates than the Trk (Trchounian and Kobayashi, 1999; Zakharyan and Trchounian, 2001).

2.2.2. Ktr transporters

The Ktr system is found commonly in several Gram-positive bacteria, which include Streptococcal and Staphylococcal species, as well as some Gram-negative enterobactericeae (Gries et al., 2013). Similar to the Trk, it is constitutively expressed and has low-to-moderate affinity for K^+. However, differently from the Trk, it requires sodium ions (Na^+) instead of H^+ for K^+ transportation, functioning as a Na^+/K^+ symporter (Tholema et al., 1999; Matsuda et al., 2004; Gries et al., 2013).

The properties of the Ktr system vary in different bacteria. In most bacteria, it consists of two components, the KtrA and KtrB proteins (Nakamura et al., 1998), which are functionally related to the TrkA and TrkH systems of *E. coli*. However, bacteria such as *Bacillus subtilis* and *Vibrio alginolyticus* have additional systems, known as KtrC and KtrD (Holtmann et al., 2003). Similar to the TrkA, the KtrA possesses the NAD^+-binding domain.

2.2.3. Bacterial Kdp transporters

The Kdp systems are widely distributed in microorganisms and are found in both Gram-positive and Gram-negative bacteria. The Kdp transporters are inducible exhibiting high affinity for the cation (Su et al., 2009; Liu et al., 2013). They operate in low K^+ concentrations (< 5 mM) when other K^+-uptake systems such as the Trk and Kup fail to function (Epstein, 1992; Diskowski et al., 2015).

The Kdp transporters consist of two systems which include the two-component system (TCS) KdpDE and the Kdp-ATPase complex, KdpFABC, encoded by the *kdpDE* and *kdpFABC* operons respectively. Transcription of these operons varies in different organisms. In *E. coli* both operons are transcribed in a similar direction, with *kdpDE* adjoining the *kdpFABC* at the end of kdpC.

The KdpFABC consists of four subunits, KdpF, KdpA, KdpB and KdpC, which play different roles in the transportation of K^+. The KdpF is used for stabilising the complex *in vitro* (Gassel et al., 1999), KdpA is involved in binding and translocation of the cation (Greie, 2011), while the KdpB operates in association with KdpC for ATP hydrolysis (Haupt et al., 2005; Greie and Altendorf, 2007).

The inducible Kdp-ATPase complex is regulated by the TCS histidine kinase, KdpD, and the response regulator, KdpE (Walderhaug et al., 1992). The KdpD responds to a variety of signals, which include low K^+ concentrations, osmotic pressure, intracellular ATP levels and extracellular pH levels (Hamann et al., 2008; Epstein, 2016).

2.2.4. Role of potassium-influx systems in virulence of bacteria

The various K^+-uptake transporters exhibit different roles in the virulence of different bacteria. In *Salmonella enterica*, a major food-borne bacterial pathogen, the Trk transporter is involved in virulence, leading to the expression and secretion of the TTSS protein, required for bacterial invasion of epithelial cells (Su et al., 2009) and intracellular growth (Liu et al. 2013). Additionally, in Salmonella species and also in *Vibrio vulnificus*, the TrkA is required for resistance to antimicrobial peptides (AMPs) and also serum, protamine, and polymyxin B (Chen et al., 2004; Su et al., 2009). It is required for gastric colonisation by *Helicobacter pylori* and production of PCWDEs through induction of the RsmB system in Gram-negative *Pectobacterium wasabiae* bacteria (Valente and Xavier, 2016). In *Francsella tularensis*, in the absence of TrkA protein, the bacterium uses THE TrkH system for its virulence in murine

models of infection (Alkhuder et al., 2010) while in *Streptococcus mutans*, an opportunistic oral pathogen that causes dental caries, Trk2 is used for bacterial growth, survival in acidic conditions and biofilm formation (Binepal et al, 2016).

The Ktr systems have been shown to be essential for adaptation in high osmolarity environments (Holtmann et al., 2003) with KtrC being required for growth in high saline conditions (Price-Whelan et al., 2013).

In the case of the Kdp systems, the KdpFABC is expressed during bacterial growth in low K^+ conditions (Malli and Epstein, 1998; Price-Whelan et al., 2013). In *Photorhabdus asymbiotica*, the KdpDE system is responsible for bacterial resistance to intracellular killing, as well as persistence within insect hemocytes (Vlisidou et al., 2010), as well as for survival of *Yersinia pestis* inside human neutrophils (O'Loughlin et al., 2010) and regulation of a series of virulence factors in *Staphylococcus aureus* (Xue et al., 2011).

2.3. BACTERIAL POTASSIUM EFFLUX SYSTEMS

Most bacteria possess the Kef systems as the major K^+ efflux transporters (Healy et al., 2014; 2016). The Kef system plays an important role in maintenance of intracellular pH and K^+ homeostasis, protecting bacteria against the detrimental effects of electrophilic compounds via acidification of the cytoplasm (Healy et al., 2016).

In *E. coli*, the system is a ligand-gated transporter consisting of the KefGB and KefFC proteins (Ferguson, 1999), with both systems containing a large protein with 12 membrane-spanning (N-terminal) and nucleotide-binding regions (C-terminal) (Munro et al., 1991) and similar ancillary soluble proteins, YheR, and YabF, respectively. The two Kef proteins have amino acid sequences similar to the dehydrogenases (Miller et al., 2000), with the KefFC sharing sequence homology to the TrkA/KtrA (Roosild et al., 2002).

The Kef system operates as a H^+/K^+ antiporter, extruding K^+ in exchange for H^+ (Bakker and Mangerich, 1982) and operates as an emergency system, which is activated by the presence of glutathione-S-conjugates (GSX) formed in the presence of electrophiles, resulting in release of K^+ and acidification of the cytoplasm, preventing cell death (Bakker et al., 1987; Ferguson and Booth, 1998; Ferguson, 1999; Ferguson et al., 2000; Healy et al., 2014). It is however, inhibited by glutathione (GSH) (Healy et al., 2014; Pliotas et al., 2017).

Additionally, *E. coli* possesses the ChaA K^+/H^+ antiporter, which is used for bacterial adaptation in alkaline conditions in elevated K^+ and CI^- concentrations (Radchenko et al., 2006). Its various roles during bacterial virulence have been shown in various bacteria and include facilitation of virulence activities of the pore-forming toxin listeriolysin O (LLO) in *Listeria monocytogenes* (Li et al., 2017), activation of the nucleotide-binding/leucine-rich repeat pyrin domain containing 3 (NLRP3) inflammasome by gut commensal bacteria, causing inflammatory bowel disease (Franchi et al., 2014; Chen et al., 2016), as well as biofilm detachment of bacteria such as *Pseudomonas aeruginosa*, promoting their infectivity (Zhang et al., 2014).

2.4. POTASSIUM TRANSPORTERS IN *MYCOBACTERIUM TUBERCULOSIS*

Similar to other bacteria, several genes encoding K^+ transporters in *Mtb*, including influx and efflux systems, have been identified (Cole et al., 1998). However, in *Mtb* these systems have not been well characterised and limited information is available on them.

2.4.1. Potassium-uptake systems of *Mycobacterium tuberculosis*

The K^+ influx systems consist of two active K^+-uptake transporters, the Trk and Kdp, and the K^+ channels, L-lysine 6-monooxygenase MbtG, a possible transmembrane cation transporte,r Rv3200c, and a conserved hypothetical protein, Rv3237c (Cole et al., 1998).

2.4.1.1. The Trk system

The *Mtb* Trk system consists of two TrkA proteins, CeoB and CeoC, encoded by the *ceoB* (684 base pairs (bp)) and *ceoC* (663 bp) genes, respectively. The systems are constitutively expressed and have a low affinity for the cation. Both CeoB and CeoC proteins have a degree of sequence homology similar to that of the TrkA proteins of *Streptomyces coelicolor* and *E. coli* with CeoB sharing 52% and 25% respectively and the CeoC exhibiting 24% amino acid identity to the TrkA proteins of the two bacterial species. Both proteins possess the NAD^+-binding motif similar to those of other bacteria (Chen and Bishai, 1998; Cole et al., 1998; Agranoff and Krishna, 2004).

The *Mtb* Trk systems also share a high degree of sequence similarity with those of other mycobacteria, exhibiting 99% similarity to those of *M. bovis*/BCG and more than 50% with those of other mycobacteria, and the lowest similarity (31%) with the *M. leprae* pseudogenes.

The two *trk* genes of *Mtb* are tandemly arranged and are similarly transcribed (Figure 2.1) (Cholo et al., 2008).

The Trk systems are used by bacteria during growth in high K^+ concentrations (>15 mM) and at neutral pH (pH 6.8) (Cholo et al., 2006; 2015).

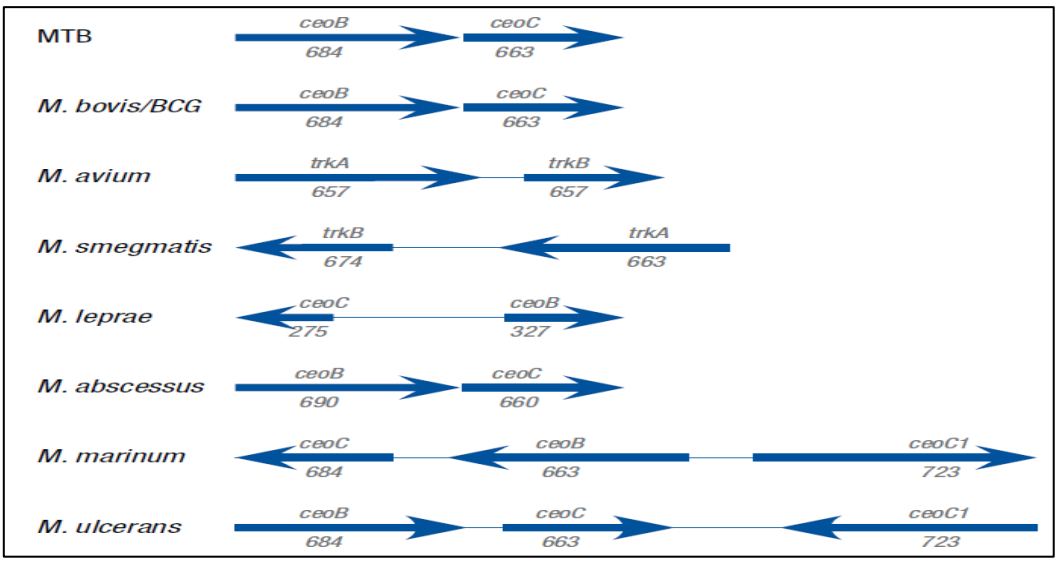

Figure 2.1: Transcription of the *trk genes* of *Mycobacterium tuberculosis* and other mycobacteria (Cholo et al. 2008).

2.4.1.2. The Kdp system

The Kdp systems have also been described in some species of Mycobacteria, including *Mtb*, *M. avium*, *M. bovis*, *M. smegmatis*, *M. marinum* (Cholo et al., 2008; Bretl et al., 2011). However, in some mycobacterial species such as *M. leprae* and *M. ulcerans* the *kdp* genes are not encoded (Cole et al., 1998; Cholo et al., 2008).

Similar to other bacteria, the *Mtb* Kdp systems are inducible and consist of P-type, ATP-driven K^+ transporters. The P-type ATPase system consists of six proteins, KdpF, KdpA, KdpB, KdpC, KdpD, and KdpE, encoded by separated *kdpDE* and *kdpFABC* operons. It also has a high affinity for K^+ (Cholo et al., 2006).

As in other bacteria, the *Mtb* Kdp P-type ATPase is activated by the TCS *kdpDE* operon (Steyn et al., 2003). However, differently from other bacteria such as *E. coli*, the N-KdpD and C-KdpD domains of *Mtb* form ternary complexes with the membrane lipoproteins, LprF and LprJ. These complexes dephosphorylate the KdpE protein, resulting in the transcription of the *kdpFABC* operon (Steyn et al., 2003).

The Kdp system is activated by several stimuli, which include low K^+ concentrations, osmotic pressure and low extracellular pH (Steyn et al., 2003; Cholo et al., 2015). The system is induced as a back-up during low osmolality when the Trk is inefficient or absent (Cholo et al., 2006; 2015).

2.4.2. Role of the potassium-uptake systems in bacterial virulence

The roles of the different K^+-uptake systems in bacterial virulence have been described. However, limited information is available on these systems in *Mtb*. In the case of the Trk systems, the *ceoBC* operon has been shown to be required for bacterial infection and intracellular survival in macrophages (MacGilvary et al., 2019). Further studies have demonstrated the upregulation of the *ceoB* (Rv2691) gene in this experimental setting (Rengarajan et al., 2005)

With regard to the Kdp transporters, several studies have implicated the involvement of the KdpDE systems during various stages of bacterial growth and infection (Parish et al., 2003; Feinbaum et al., 2012; Freeman et al., 2013). During persistence in a nutrient starvation *in vitro* model, *Mtb* bacteria utilise the KdpE protein as the main TCS of the 11 different TCS systems operative in *Mtb* (Betts et al., 2002). *In vivo*, the KdpDE system is required for virulence in a murine model of experimental TB infection (Parish et al., 2003; Sassetti and Rubin 2003). Furthermore, the *Mtb* KdpE system is involved in the regulation of many genes which are essential for metabolism and stress tolerance (Burda et al., 2014; Samir et al., 2016; Parker et al., 2017).

Additionally, the K^+-uptake transporters have been implicated as possible drug targets. The CeoB protein of the Trk system has a high affinity for INH (Argyrou et al., 2006), while both the Trk and Kdp systems are susceptible to inhibition by clofazimine, serving as potential targets for this antibiotic (Cholo et al., 2006). Although the main mechanism involved in the susceptibility of *Mtb* to this riminophenazine antibiotic remains to be convincingly described, the antibiotic may mediate its antimicrobial activity through membrane disruptive mechanisms (Steel et al., 1999; Matlola et al., 2001; Bopape et al., 2004; Cholo et al., 2006; Cholo et al., 2012).

2.5 REFERENCES

Agranoff D. and Krishna, S. (2004). Metal ion transport and regulation in *Mycobacterium tuberculosis*. *Frontiers in Bioscience*, 9, 2996-3006.

Alkhuder K, Meibom K.L., Dubail I., Dupuis M. and Charbit. A. (2010). Identification of trkH, encoding a potassium uptake protein required for *Francisella tularensis* systemic dissemination in mice. *PloS One*, 5, e8966.

Argyrou A., Jin L., Siconilfi-Baez L., Angeletti R.H. and Blanchard J.S. (2006). Proteome-wide profiling of isoniazid targets in *Mycobacterium tuberculosis*. *Biochemistry*, 45(47), 13947-13953.

Bakker E.P. and Mangerich W.E. (1982). N-ethylmaleimide induces K^+-H^+ antiport activity in *Escherichia coli* K-12. *FEMS Letters*, 140(2), 177-180.

Bakker E.P., Booth I.R., Dinnbier U., Epstein W. and Gajewska, A. (1987). Evidence for multiple K^+ export systems in *Escherichia coli*. *Journal of Bacteriolology*, 169(8), 3743-3749.

Ballal A., Basu B. and Apte S.K. (2007). The Kdp-ATPase system and its regulation. *Journal of Biosciences*, 32, 559-568.

Berry S., Esper B., Karandashova I., Teuber M., Elanskaya I., Rögner M., et al. (2003). Potassium uptake in the unicellular cyanobacterium *Synechocystis* sp strain PCC 6803 mainly depends on a Ktr-like system encoded by slr1509 (ntpJ). *FEBS Letters*, 548, 53-58.

Betts J.C., Lukey P.T., Robb L.C., McAdam R.A. and Duncan K. (2002). Evaluation of a nutrient starvation model of *Mycobacterium tuberculosis* persistence by gene and protein expression profiling. *Molecular Microbiology*, 43(3), 717-731.

Binepal G., Gill K., Crowley P., Cordova M., Brady L.J., Senadheera D.B. and Cvitkovitch D. G. (2016). Trk2 potassium transport system in *Streptococcus mutans* and its role in potassium homeostasis, biofilm formation, and stress tolerance. *Journal of Bacteriology*, 198(7), 1087-1100.

Bopape M.C., Steel H.C., Cockeran R., Matlola N.M., Fourie P.B. and Anderson, R. (2004). Antimicrobial activity of clofazimine is not dependent on mycobacterial C-type phospholipases. *The Journal of Antimicrobial Chemotherapy*, 53(6), 971-974.

Bretl D.J., Demetriadou C. and Zahrt T. C. (2011). Adaptation to environmental stimuli within the host: two-component signal transduction systems of *Mycobacterium tuberculosis*. *Microbiology and Molecular Biology Reviews*, 75, 566-582.

Burda W.N., Miller H.K., Krute C.N., Leighton S.L., Carroll R.K. and Shaw L.N. (2014). Investigating the genetic regulation of the ECF sigma factor σ^S in *Staphylococcus aureus. BMC Microbiology*, 14:280.

Chen P. and Bishai W.R. (1998). Novel selection for isoniazid (INH) resistance genes supports a role for NAD^+-binding proteins in mycobacterial INH resistance. *Infection and Immunity*, 66(11), 5099-5106.

Chen K., Shanmugam N.K., Pazos M.A., Hurley B.P. and Cherayil B.J. (2016). Commensal bacteria-induced inflammasome activation in mouse and human macrophagesn is dependent on potassium efflux but does not require phagocytosis or bacterial viability. *PLoS One*, 11, e0160937.

Chen, Y.C., Chuang, Y.C., Chang, C.C., Jeang, C.L. and Chang, M.C. (2004). A K^+ uptake protein, TrkA, is required for serum, protamine, and polymyxin B resistance in *Vibrio vulnificus*. *Infection and Immununity*, 72(2), 629-636.

Cholo M.C., Boshoff H.I., Steel H.C., Cockeran R., Matlola N.M., Downing K.J. et al. (2006). Effects of clofazimine on potassium uptake by a Trk-deletion mutant of *Mycobacterium tuberculosis*. *The Journal of Antimicrobial Chemotherapy*, 57(1), 79-84.

Cholo M.C., Steel H.C., Fourie P.B., Germishuizen W.A. and Anderson R. (2012). Clofazimine: current status and future prospects. *The Journal of Antimicrobial Chemotherapy*, 67(2), 290-298.

Cholo M.C., Van Rensburg E.J. and Anderson R. (2008). Potassium uptake systems of *Mycobacterium tuberculosis*: genomic and protein organisation and potential roles in microbial pathogenesis and chemotherapy. *South African Journal of Epidemiology and Infection*. 23, 13-16.

Cholo M.C., van Rensburg E.J., Osman A.G. and Anderson R. (2015). Expression of the genes encoding the Trk and Kdp potassium transport systems of *Mycobacterium tuberculosis* during growth *in vitro*. *BioMed Research International*, 608682.

Cole S.T., Brosch R., Parkhill J. et al. (1998). Deciphering the biology of *Mycobacterium tuberculosis* from complete genome sequence. *Nature*, 393, 537-544.

Diskowski M., Mikusevic V., Stock C. and Hänel I. (2015). Functional diversity of the superfamily of K^+ transporters to meet various requirements. *Biological Chemistry,* 396, 1003-1014.

Dosch D.C., Helmer G.L., Sutton S.H., Salvacion F.F. and Epstein W. (1991). Genetic analysis of potassium transport loci in *Escherichia coli*: evidence for three constitutive systems mediating uptake potassium. *Journal of Bacteriololgy*, 173(2), 687-696.

Epstein W. (1992). Kdp, a bacterial P-type ATPase whose expression and activity are regulated by turgor pressure. *Acta Physiologica Scandinavica Supplementum*. 607, 193-199.

Epstein W. (2003). The roles and regulation of potassium in bacteria. *Progress in Nucleic Acid Research and Molecular Biology*, 75, 293-320.

Epstein W. (2016). The KdpD sensor kinase of *Escherichia coli* responds to several distinct signals to turn on expression of the Kdp transport system. *Journal of Bacteriology*, 198, 212-220.

Epstein W., Walderhaug M. O., Polarek J. W., Hesse J. E., Dorus E., Daniel J. M., et al. (1990). The bacterial Kdp K^+-ATPase and its relation to other transport ATPases, such as the Na^+/K^+- and Ca^{2+}-ATPases in higher organisms. *Philosophical Transactions of the Royal Scociety*, 326(1236), 479-486.

Feinbaum R.L., Urbach J.M., Liberati N.T., Djonovic S., Adonizio A., Carvunis A.R. and Ausubel, F.M. (2012). Genome-wide identification of *Pseudomonas aeruginosa* virulence-related genes using a Caenorhabditis elegans infection model. *PLoS Pathogens*, 8(7), e1002813.

Ferguson G.P. (1999). Protective mechanisms against toxic electrophiles in *Escherischia coli*. *Trends in Microbiology*, 7(6), 242-247.

Ferguson G.P. and Booth I.R. (1998). Importance of glutathione for growth and survival of *Escherichia coli* cells: detoxification of methylglyoxal and maintenance of intracellular K^+. *Journal of Bacteriology*, 180(16), 4314-4318.

Ferguson G.P., Battista J.R., Lee A.T. and Booth I.R. (2000). Protection of the DNA during the exposure of *Escherichia coli* cells to a toxic metabolite: the role of the KefB and KefC potassium channels. *Molecular Microbiology*, 35(1), 113-122.

Follmann M., Becker M., Ochrombel I., Ott V., Krämer R. and Marin K. (2009). Potassium transport in *Corynebacterium glutamicum* is facilitated by the putative channel protein CglK, which is essential for pH homeostasis and growth at acidic pH. *Journal of Bacteriology*, 191(9), 2944-2952.

Franchi L., Eigenbrod T., Muñoz-Planillo R., Ozkurede U., Kim Y.G., Arindam C., et al. (2014). Cytosolic double-stranded RNA activates the NLRP3 inflammasome via MAVS-induced membrane permeabilization and K^+ efflux. *Journal of Immunology*, 193(8), 4214-4222.

Freeman Z.N., Dorus S. and Waterfield N.R. (2013). The KdpD/KdpE two-component system: integrating K(+) homeostasis and virulence. *PLoS Pathogens*, 9, e1003201.

Gassel M., Möllenkamp T., Puppe W. and Altendorf K. (1999). The *KdpF* subunit is part of the K^+ translocating Kdp complex of *Escherichia coli* and is responsible for stabilization of the complex *in vitro*. *The Journal of Biological Chemistry*, 274, 37901-37907.

Greie J.C. (2011). The KdpFABC complex from *Escherichia coli*: a chimeric K^+ transporter merging ion pumps with ion channels. *European Journal of Cell Biology* 90, 705-710.

Greie J.C. and Altendorf K. (2007). The K^+-translocating KdpFABC complex from *Escherichia coli*: a p-type ATPase with unique features. *Journal of Bioenergetics and Biomembranes*, 39, 397-402.

Gries C.M., Bose J.L., Nuxoll A.S., Fey P.D. and Bayles K.W. (2013). The Ktr potassium transport system in *Staphylococcus aureus* and its role in cell physiology, antimicrobial resistance and pathogenesis. *Molecular Microbiology*, 89(4), 760-773.

Hamann K., Zimmann P. and Altendorf K. (2008). Reduction of turgor is not the stimulus for the sensor kinase KdpD of *Escherichia coli*. *Journal of Bacteriology*, 190, 2360-2367.

Haupt M., Bramkamp M., Coles M., Kessler H. and Altendorf K. (2005). Prokaryotic Kdp-ATPase: recent insights into the structure and function of KdpB. *Journal of Molecular Microbiololgy and Biotechnology,* 10, 120-131.

Healy J., Ekkerman S., Pliotas C., Richard M., Bartlett W., Grayer S.C., et al. (2014). Understanding the structural requirements for activators of the Kef bacterial potassium efflux system. *Biochemistry,* 53(12), 1982-1992.

Healy J., Rasmussen T., Miller S., Booth I.R. and Conway, S.J. (2016). The photochemical thiol-ene reaction as a versatile method for the synthesis of glutathione S-conjugates targeting the bacterial potassium efflux system Kef. *Organic chemistry Frontiers: an International Journal of Organic Chemistry,* 3(4), 439-446.

Holtmann G., Bakker E.P., Uozumi N. and Bremer E. (2003). KtrAB and KtrCD: two K^+ uptake systems in *Bacillus subtilis* and their role in adaptation to hypertonicity. *Journal of Bacteriology,* 185, 1289-1298.

Johnson H.A., Hampton E. and Lesley S.A. (2009). The *Thermotoga maritima* Trk potassium transporter-from frameshift to function. *Journal of Bacteriology,* 191(7), 2276-2284.

Li J., Lam W.W., Lai T.W. and Au S.W. (2017). Degradation of nuclear Ubc9 induced by listeriolysin O is dependent on K^+-efflux. *Biochemical and Biophysical Research Communications,* 493, 1115-1121.

Liu Y., Ho K.K., Su J., Gong H., Chang A.C. and Lu S. (2013). Potassium transport of Salmonella is important for type III secretion and pathogenesis. *Microbiology,* 159(Pt8), 1705-1719.

MacGilvary N.J, Kevorkian Y.L and Tan S. (2019). Potassium response and homeostasis in *Mycobacterium tuberculosis* modulates environmental adaptation and is important for host colonization. *PLoS Pathogens,* 15(2), e1007591.

Malli R. and Epstein W. (1998). Expression of the Kdp ATPase is consistent with regulation by turgor pressure. *Journal of Bacteriology,* 180(19), 5102-5108.

Matlola N.M., Steel H.C. and Anderson, R. (2001). Antimycobacterial action of B4128, a novel tetramethylpiperidyl-substituted phenazine. *The Journal of Antimcrobial and Chemotherapy,* 47(2), 199-202.

Matsuda N., Kobayashi H., Katoh H., Ogawa T., Futatsugi L., Nakamura T., et al. (2004). Na^+-dependent K^+ uptake Ktr system from the *cyanobacterium Synechocystis* sp. PCC 6803 and its role in the early phases of cell adaptation to hyperosmotic shock. *The Journal of Biological Chemistry*, 279, 54952-54962.

Miller S., Ness, L.S., Wood C.M., Fox B.C. and Booth I.R. (2000). Identification of an ancillary protein, YabF, required for activity of the KefC glutathione-gated potassium efflux system in *Escherichia coli*. *Journal of Bacteriology*, 182(22), 6536-6540.

Munro A.W., Ritchie G.Y., Lamb A.J., Douglas R.M. and Booth, I.R. (1991). The cloning and DNA sequence of the gene for the glutathione-regulated potassium-efflux system KefC of *Escherichia coli*. *Molecular Microbiology*, 5(3), 607-616.

Nakamura T., Yamamuro N., Stumpe S., Unemoto T. and Bakker E.P. (1998). Cloning of the *trkAH* gene cluster and characterization of the Trk K(+)-uptake system of *Vibrio alginolyticus*. *Microbiology*, 144(Pt 8), 2281-2289.

Nanatani K., Shijuku T., Takano Y., Zulkifli L., Yamazaki T., Tominaga A., et al. (2015). Comparative analysis of *kdp* and *ktr* mutants reveals distinct roles of the potassium transporters in the model *Cyanobacterium synechocystis* sp strain PCC 6803. *Journal of Bacteriology*. 197, 676-687.

Ochrombel I., Ott L., Krämer R., Burkovski A. and Marin K. (2011). Impact of improved potassium accumulation on pH homeostasis, membrane potential adjustment and survival of *Corynebacterium glutamicum. Biochimica et Biophysica Acta*, 1807(4), 444-450.

O'Loughlin J.L., Spinner J.L., Minnich S.A. and Kobayashi S.D. (2010). *Yersinia pestis* two-component gene regulatory systems promote survival in human neutrophils. *Infection and Immunity*, 78(2), 773-782.

Parker C.T., Russell R., Njoroge J.W., Jimenez A.G., Taussig R. and Sperandio V. (2017). Genetic and mechanistic analyses of the periplasmic domain of the enterohemorrhagic *E. coli* (EHEC) QseC histidine sensor kinase. *Journal of Bacteriology*, 199, e00861-16.

Parish T., Smith D.A., Kendall S., Casali N., Bancroft G.J. and Stoker N.G. (2003). Deletion of two-component regulatory systems increases the virulence of *Mycobacterium tuberculosis*. *Infection and Immunity*, 71(3), 1134-1140.

Pliotas C., Grayer S. C., Ekkerman S., Chan A., Healy J., Marius P., et al. (2017). Adenosine monophosphate binding stabilizes the KTN domain of the *Shewanella denitrificans* Kef potassium efflux system. *Biochemistry*, 56(32), 4219-4234.

Price-Whelan A., Poon C.K., Benson M.A., Eidem T.T., Roux C.M., Boyd J.M., et al. (2013). Transcriptional profiling of *Staphylococcus aureus* during growth in 2 M sodium chloride (NaCl) leads to clarification of physiological roles for Kdp and Ktr K^+ uptake systems. *M Bio*, 4(4), e00407-e00413.

Radchenko M.V., Tanaka K., Waditee R., Oshimi S., Matsuzaki Y., Fukuhara M., et al. (2006). Potassium/proton antiport system of *Escherichia coli*. *Journal of Biological Chemistry*, 281(29), 19822-19829.

Rengarajan, J., Bloom, B.R. and Rubin, E.J. (2005). Genome-wide requirements for *Mycobacterium tuberculosis* adaptation and survival in macrophages. *Proceedings of the National Academy of Sciences of the United States of America*, 102(23), 8327-8332.

Roosild T.P., Miller S., Booth I.R. and Choe S. (2002). A mechanism of regulating transmembrane potassium flux through a ligand-mediated conformational switch. *Cell*, 109(6), 781-791.

Samir R., Hussein S.H., Elhosseiny N.M., Khattab M.S., Shawky A.E. and Attia A.S. (2016). Adaptation to potassium limitation is essential for *Acinetobacter baumannii* pneumonia pathogenesis. *Journal of Infectious Diseases.* 214, 2006-2013.

Sassetti C.M. and Rubin E.J. (2003). Genetic requirements for mycobacterial survival during infection. *Proceedings of the National Academy of Sciences of the United States of America*, 100(22), 12989-12994.

Sato Y., Nanatani K., Hamamoto S., Shimizu M., Takahashi M., Tabuchi-Kobayashi M., et al. (2014). Defining membrane spanning domains and crucial membrane-localized acidic amino acid residues for K^+ transport of a Kup/HAK/KT-type *Escherichia coli* potassium transporter. *Journal of Biochemistry*, 155, 315-323.

Sharma O., O'Seaghdha M., Velarde J.J. and Wessels M.R. (2016). NAD^+-glycohydrolase promotes intracellular survival of Group A *Streptococcus*. *PLoS Pathogens*, 12(3), e1005468.

Steel H.C., Matlola N.M. and Anderson, R. (1999). Inhibition of potassium transport and growth of mycobacteria exposed to clofazimine and B669 is associated with a calcium-independent increase in microbial phospholipase A2 activity. *The Journal of Antimicrobial Chemotherapy*, 44(2), 209-216.

Steyn A.J.C., Joseph J. and Bloom B.R. (2003). Interaction of the sensor module of *Mycobacterium tuberculosis* H_{37}Rv KdpD with members of the Lpr family. *Molecular Microbiology*, 47(4), 1075-1089.

Su J., Gong H. Lai J., Main A. and Lu S. (2009). The potassium transporter Trk and external potassium modulate *Salmonella enterica* protein secretion and virulence. *Infection Immunity*, 77(2), 667-675.

Tholema N., Bakker E.P., Suzuki A. and Nakamura T. (1999). Change to alanine of one out of four selectivity filter glycines in KtrB causes a two orders of magnitude decrease in the affinities for both K^+ and Na^+ of the Na^+ dependent K^+ uptake system KtrAB from *Vibrio alginolyticus*. *FEBS letters*, 450, 217-220.

Trchounian A. and Kobayashi H. (1999). Kup is the major K^+ uptake system in *Escherichia coli* upon hyper-osmotic stress at a low pH. *FEBS Letters*, 26, 447(2-3), 144-148.

Valente R.S. and Xavier K.B. (2016). The Trk potassium transporter is required for RsmB-mediated activation of virulence in the Phytopathogen *Pectobacterium wasabiae*. *Journal of Bacteriology*, 198(2), 248-255.

Vlisidou I., Eleftherianos I., Dorus S., Yang G., ffrench-Constant R.H., Reynolds S.E. and Waterfield N.R. (2010). The KdpD/KdpE two-component system of *Photorhabdus asymbiotica* promotes bacterial survival within *M. sexta* hemocytes. *Journal of Invertebrate Pathology*, 105(3), 352-362.

Walderhaug M.O., Polarek J.W., Voelkner P., Daniel J.M., Hesse J.E., Altendorf K., et al. (1992). KdpD and KdpE, proteins that control expression of the *kdpABC* operon, are members of the two-component sensor-effector class of regulators. *Journal of Bacteriology*. 174, 2152-2159.

Xue T., You Y.B., Hong D., Sun H.P. and Sun B.L. (2011). The *Staphylococcus aureus* KdpDE two-component system couples extracellular K^+ sensing and Agr signaling to infection programming. *Infection and Immunity.* 79, 2154-2167.

Zakharyan E. and Trchounian A. (2001). K^+ influx by Kup in *Escherichia coli* is accompanied by a decrease in H^+ efflux. *FEMS Microbiology Letters*, 204(1), 61-64.

Zhang W., McLamore E.S., Wu R., Stenberg M., Porterfield D.M. and Banks M.K. (2014). Glutathione-gated potassium efflux as a mechanism of active biofilm detachment. *Water Enviroment Research,* 86, 462-469.

CHAPTER THREE: RATIONALE, HYPOTHESIS, AIM AND OBJECTIVES, AND SIGNIFICANCE OF THE STUDY

3.1. Rationale of the study

The current study was undertaken with the primary objective of investigating the roles of the major K^+-uptake transporters of *Mtb* on bacterial growth and survival. Previous studies have been conducted using mutants of single operons, which included the *ceoBC* and *kdpDE* genes, resulting in mutant strains with different growth rates, these being increased in the Trk-deletion mutant and attenuated in the KdpDE-deletion mutant during *in vitro* growth. Bacterial growth rates of the single-operon mutants suggested the existence of mutual compensatory activity of these systems during bacterial growth. This behaviour necessitated the generation of an *Mtb* mutant strain in which the two K^+-uptake transporters (Trk and Kdp) were simultaneously inactivated. The initial strategy to generate this mutant was based on constructing a double-knockout mutant strain of *Mtb* in which both the Trk and KdpDE were inactivated, based on the assumption that inactivation of the *kdpDE* operon would result in concomitant failure of activation of the *kdpFABC* operon, which is seemingly dependent on the function of KdpDE. Surprisingly, however, inactivation of both the Trk and KdpDE systems failed to prevent bacterial growth, albeit that the growth of the double gene-knockout mutant was more attenuated than that of the single *kdpDE*-deletion mutant. Accordingly, in order to achieve complete inactivation of the active K^+-uptake transporters, the current study was focused on generation of a triple gene-knockout of *Mtb* in which all three operons encoding the K^+-uptake transporters were simultaneously inactivated.

3.2 Study hypothesis

We hypothesise that K^+-upstake systems of *Mtb*, the Trk and Kdp are essential for the survival and growth of *Mtb* and their disruption can affect the virulence of the organism leading to its elimination in the host.

3.3. Aim of the study

To determine the roles of the active K^+-uptake systems of *Mtb*, the Trk and Kdp, in bacterial growth.

3.4. Objectives of the study

The objectives were:

- To generate a K^+-uptake-deletion mutant strain of *Mtb*, in which both the *trk (ceoBC)* and *kdp* (*kdpDE* and *kdpFABC*) genes are inactivated using the homologous recombination (HR) strategy;
- To investigate the functional roles of the active K^+-uptake systems by evaluating the phenotypic characteristics of the triple gene-knockout strain relative to the wild-type (WT) strain of *Mtb*, specifically growth in planktonic, biofilm and intracellular environments *in vitro.*

3.5 Significance of the study

Understanding the function of K^+-uptake systems in the survival of *Mtb* in various growth environment is necessary inorder to devise strategies of eliminating the pathogen in the host. K^+-uptake systems can become a novel drug target against *Mtb*.

4. CHAPTER FOUR: MUTANT CONSTRUCTION

4.1. INTRODUCTION

Mutagenesis tools are used for investigation of the functions of genes (Balhana et al., 2010; Basu et al., 2018). In *Mtb*, mutant construction approaches are achieved by either allelic exchange, which involves replacement of WT with the mutated allele (Parish and Stoker, 2000; Balhana et al., 2010) or by integration of replicating vectors in the chromosomes (Sander et al., 1995; Pelicic et al., 1997).

During the allelic exchange procedures, the mutated allele is transferred into the recipient chromosome using a suicide vector. Following plasmid transfer, the homologous regions between the WT and mutated alleles are recognised by recipient cells during replication, resulting in their recombination and exchange of genetic material. This ultimately leads to replacement of WT with the mutated allele, forming the mutant strain.

An allelic exchange can occur during a one- or two-step HR process. In a one-step method, the suicide vector is pre-treated with a phage vector followed by its transfer into the recipient chromosome for two crossover events to occur, forming double-crossover (DCO) clones (mutants) (Jain et al., 2014). However, in a two-step procedure, the suicide vector is transferred into the recipient chromosome resulting in recombination occurring in one site, forming the single-crossover (SCO) clones. During replication of the SCO, the second crossover event takes place, resulting in formation of the DCO (Parish et al., 1999; Parish and Stoker, 2000).

During mutant construction in *Mtb*, the benefit of using a suicide vector has been its non-expression in the recipient chromosome (Parish et al., 1999). The most widely used suicide vectors in *Mtb* to date are the p1NIL vector series. However, recently, the pG5 and the allelic exchange substrate vectors, have been described (Jain et al., 2014; Basu et al., 2018). The p1NIL vectors are characterised by lack of the *oriM* gene and fail to replicate in mycobacterial cell. However, these vectors encode the *oriE* gene, which allows for plasmid replication in *E. coli*, which is useful during cloning procedures for target gene manipulation in the plasmid, while upon completion, the non-replicating plasmid is transferred into mycobacterial strain for allelic replacement.

The p1NIL vectors are characterised by the incorporation of the multi-cloning sites (MCS), the kan^R gene and one PacI site. The MCS encodes recognition sequences for multiple restriction enzymes and following digestion with these enzymes, the site is used for the insertion of target genes. This is followed by manipulation of the target gene either by deletion or insertion with the antibiotic-resistant gene, forming unmarked or marked mutation.

Currently several marked mutated genes have the insertion of hygromycin-resistant (*hyg*^{R}) or kanamycin-resistant (*kan*^{R}) genes. Annealing between the insert and the p1NIL plasmid fragments is mediated by the activity of the ligase enzyme.

The *kan*^{R} gene, is the only phenotypic marker in these plasmids, and is used for the selection of kanamycin-resistant colonies during plasmid growth. However, other suicide vectors such as the pG5 and allelic exchange substrate, have two phenotypic markers, with both plasmids encoding for the *sacB* counter-selectable gene, for selection of sucrose-sensitive clones, as well as the *kan*^{R}/*hyg*^{R} genes for isolation of kanamycin- and hygromycin-resistant clones, respectively (Jain et al., 2014; Basu et al., 2018).

The one *PacI* site of the p1NIL vector is used for the insertion of additional phenotypic markers, which occur as a *PacI* cassette. To date, two phenotypic marker cassettes, which include the *PacI-sacB,lacZ* and *PacI-sacB,lacZ,hyg*^{R}, found in two pGOAL vectors, pGOAL17 and pGOAL19, have been developed. These markers differ with respect to the presence of the *hyg*^{R} gene and have been used for the isolation of hygromycin-marked or -unmarked mutants of *Mtb* respectively (Parish and Stoker, 2000).

Several *Mtb* mutant strains have been successfully constructed using the p1NIL vector series. These include, among others, based on the focus of the current study, three K^+-uptake mutant strains, which include the Trk- (Cholo et al., 2006), KdpDE- (Parish et al., 2003) and the TK-deletion double knockout (Cholo et al., unpublished) mutant strains.

Currently, the modified version of the p1NIL vector, the pNILRB5, has been constructed, which has additional structural features providing improvement in the cloning procedure in *Mtb* mutagenesis, such as high specificity in clone selection (Balhana et al., 2010). In *Mtb*, cloning procedures are associated with low allelic replacement efficiency, which is affected by slow bacterial growth rates (Balhana et al., 2010; Jain et al., 2014).

As opposed to the p1NIL, the pNILRB5 vector is encoded with two ligase-independent cloning (LIC) sites, which are used for the insertion of the upstream and downstream flanking regions of the target gene. These fragments are separated by a few base pairs following their insertion, resulting in deletion of the target gene, forming an unmarked mutation. Furthermore, annealing of these flanking inserts and the plasmid fragment is independent of the activity of ligase enzyme, but is mediated by the activity of the T4 polymerase, which creates strong H^+ bonds between the fragments, for fusion (Aslanidis and de Jong, 1990; Haun et al., 1992; Yang et al., 1993). Two additional phenotypic markers, the *sacB* and *lacZ* genes, are incorporated into the plasmid and are located at the two LIC sites. These two marker genes are replaced by the insertion of the upstream and downstream fragments and are therefore used for the

phenotypic selection of specific insert-carrying plasmid clones. The *sacB* and *lacZ* genes are also incorporated within restriction sites such as the BsaI, SwaI and BseRI, which are rarely encoded in *Mtb* genome (Balhana et al., 2010).

The benefit of using the pNILRB5 plasmid series has been shown in the construction of *M. smegmatis* mutants, which include MSMEG-2309, MSMEG-4718 and MSMEG-5040, for the inactivation of the genes encoding for the probable transcriptional regulatory protein and two transcriptional regulator TetR family proteins, respectively, as well as in slow growing mycobacteria in a two-step AE strategy (Balhana et al., 2010). In the current study, the pNILRB5 plasmid was used in the construction of the *Mtb* TKkdpDFC-deletion mutant, which is characterised by the inactivation of two K^+-uptake transport systems, the Trk and Kdp, with the Trk encoded by *ceoBC*, while the Kdp is encoded by the *kdpDE* and *kdpFABC* operons, respectively.

Due to the existence of the *Mtb* TK-deletion mutant, which has two of the targeted operons, (*ceoBC* and *kdpDE*) inactivated, the construction of the current triple K^+-uptake-deletion knockout strain was achieved by inactivating only the *kdpFABC* operon in the TK-deletion mutant strain. The suicide-delivery vector (SDV), with deletion mutation of the *kdpFABC* operon, was constructed in *E. coli*, followed by its transfer into the *Mtb* TK double-knockout mutant strain for AE.

4.2. AIM AND OBJECTIVES

4.2.1. AIM

To construct the TKkdpDFC-deletion mutant strain of *Mtb*.

4.2.2. OBJECTIVES

- To construct the *kdpFABC*-mutated allele-carrying pNILRB5-derived SDV using cloning procedures in *E. coli*;
- To generate the *Mtb* TKkdpDFC SCO and DCO by AE based on two- step HR procedures;
- To characterise the mutant phenotypically using sucrose and kanamycin sensitivity testing methods, and genotypically using PCR and whole genome sequencing procedures.

4.3. MATERIALS AND METHODS

4.3.1. MATERIALS

4.3.1.1. Bacterial and plasmid strains

All bacterial and plasmid strains are as shown in Table 1. The DH5α Z-competent™ *E. coli* strain purchased from Inqaba Biotec (Pretoria, South Africa), was used for cloning procedures, while the WT *Mtb* (H_{37}Rv) ATCC 26518 strain and the TK mutant (unpublished, provided by Dr MC Cholo, Department of Immunology, University of Pretoria) were used for AE.

The plasmid strains used in cloning procedures, which include the pNILRB5 and pGOAL17, were provided by Professor N Stoker, Royal Veterinary College, London, UK, while other plasmids were constructed as required for this study.

Table 1: Bacterial and plasmid strains

Bacterial and plasmid strains	**Feature or genotype**	**Source**
pNILRB5	*kan^R, oriE, sacB, lacZ*	Balhana *et al*., 2010
pRB5kdpDF`	*kan^R, oriE, sacB, kdpDF*	This study
pRB5kdpDFC`	*kan^R, oriE, kdpDF, kdpC*	This study
pGOAL17	*PacI* cassette (*P_{Ag85}-lacZ P_{hsp} - sacB*), *amp*	Parish and Stoker, 2000
pRB5kdpDFC17`	pRB5kdpDFC`with *PacI* cassette (*P_{Ag85}-lacZ P_{hsp} - sacB*)	This study
Trk/KdpDE (TK)	TrkΔ (*ceoBΔC: hygR*), kdpDEΔ	Cholo *et al*., (unpublished)
H_{37}Rv-ATCC 26518	All genes encoded	ATCC reference strain
DH5α - *E. coli*	F$^-$φ80dlacZΔM15 Δ(lacZYA-argF)U169 deoR, recA1 endA1 hsdR17 ($r_k^-m_k^+$ phoA supE44 λ$^-$ thi-1 gyrA96 relA1)	Zymo Research

4.3.1.2. Reagents and antimicrobial agents

Unless otherwise stated, all reagents and antimicrobial agents used were purchased from the Sigma-Aldrich Chemicals Co (St Louis, MO, USA), Inqaba biotec™ (Pretoria, South Africa), Roche (Basel, Switzerland) and Lasec® (Cape Town, South Africa). The antibiotics, specifically, kanamycin, hygromycin and ampicillin were used at final concentrations of 10,

50, 100 µg/ millilitre (mL), respectively, while X-gal, and sucrose were used at concentrations of 20 g/L and 5%, respectively for selection of plasmid-expressing *E. coli* and *Mtb* bacterial isolates.

4.3.1.3. Growth media

Preparation of bacterial growth media is shown in Appendix A. Luria-Bertani broth (LB) and agar (LA) were used for growth of the *E. coli* strains, while SOB broth was used for preparation of DH5α Z-competent *E. coli* cells.

Middlebrook 7H9 broth and 7H10 agar supplemented with 10% oleic acid/albumin/dextrose/catalase (OADC), 0.2/0.5 % glycerol with/without 0.05% Tween 80, were used for *Mtb* bacterial culture preparations (Appendix A.4 and A.5), while Middlebrook 7H9 broth containing glycine was used for preparation of *Mtb* competent cells. All media were prepared as shown in Appendix A.

4.3.1.4. Enzymes

All enzymes used for cloning purposes were purchased from Inqaba biotec™ (Pretoria, South Africa) and their activities are as shown in Table 2.

Table 2: Enzymes used during the cloning procedure

Enzyme name	**Manufacturer Name**	**Buffer type**	**Temperature preference**	**Time for activity**
Eco31I (BsaI)	Thermo Fisher Scientific	Buffer G	37° C	1 hour
BseRI	New England BioLabs	CutSmart®	37° C	1 hour
PacI	Thermo Fisher Scientific	FastDigest PacI	37° C	1 hour
T4 DNA polymerase	Thermo Fisher Scientific	Thermo Scientific™	RT	5 minute (min)
T4 DNA ligase	Fermentas Sciences	T4 DNA ligase	22° C	10 min

4.3.1.5. Oligonucleotides

All oligonucleotides used in this study are shown in Table 3 and Table 4. These were used for the construction of upstream *kdpDF* and downstream *kdpC* regions as well as for screening for legitimate mutant clones.

Table 3: Oligonucleotides used for PCR amplification of the inserts

Primers (bp)	Target gene	Fragment size (bp)
Forward - 5`TACTTCCAATCCATGGCCACGGATAACGTGAACC3` (34) Reverse - 5`TATCCACCTTTACTGCGATGTTGTCGACCGTAGT3` (34)	*kdpDF*	1164
Forward - 5`TATCCACCCTTACTGCGTGCTCAGGCTGAACCTC3` (34) Reverse - 5`TACTTCCAATCCATGGCGCCTACCAGGTTGACAG3`(34)	*kdpC-trcS*	1143

Table 4: Oligonucleotides used for screening for the mutated *kdpFABC* region

Primers (bp)	Fragment size (bp) (*Mutant allele)*	Fragment size (bp) *(WT allele)*
Forward - 5`CGGGGAAACAACAGTCGAACT3` (21) Reverse - 5`GCGACTGACATTCCGATC3` (18)	No fragment	1041
Forward - 5`CGGGGAAACAACAGTCGAACT3` (21) Reverse – 5`CCTGGTCATCAACGCGGTG3`(19)	868	5014

4.3.1.6. Solutions and buffers

The buffers and solutions used are as listed in Appendix B.

4.3.1. METHODS

The *Mtb* TKkdpDFC-deletion mutant was constructed using HR based on the two-step strategy, as shown in Figure 4.1 (Parish and Stoker, 2000). The procedure involves the transfer of the mutated gene-carrying SDV into the WT strain, resulting in formation of SCO, which is characterised by incorporation of the SDV, the WT and mutated alleles. The formation of the two different SCO constructs is dependent on the site of recombination occurrence, which can be at either position (I: yellow site) or (II: red site) for SCO1 or SCO2, respectively. Due to lack of the *oriM* on the pNILRB5 plasmid during SCO replication, the plasmid is eliminated, while due to the presence of the homologous region between the WT and mutated alleles, the mutated gene is replicated, resulting in replacement of the WT gene, forming DCO constructs.

In the current study, the SDV used was pRB5kdpDFC17`, which carried the mutated *kdpDFC* allele of the *kdpFABC* WT operon, while the recipient *Mtb* strain with the WT

kdpFABC operon was the TK mutant. The resultant DCO strain was the *Mtb* TKkdpDFC-deletion knockout.

The methodology section has been divided into the mutagenesis processes and the standard operating procedures.

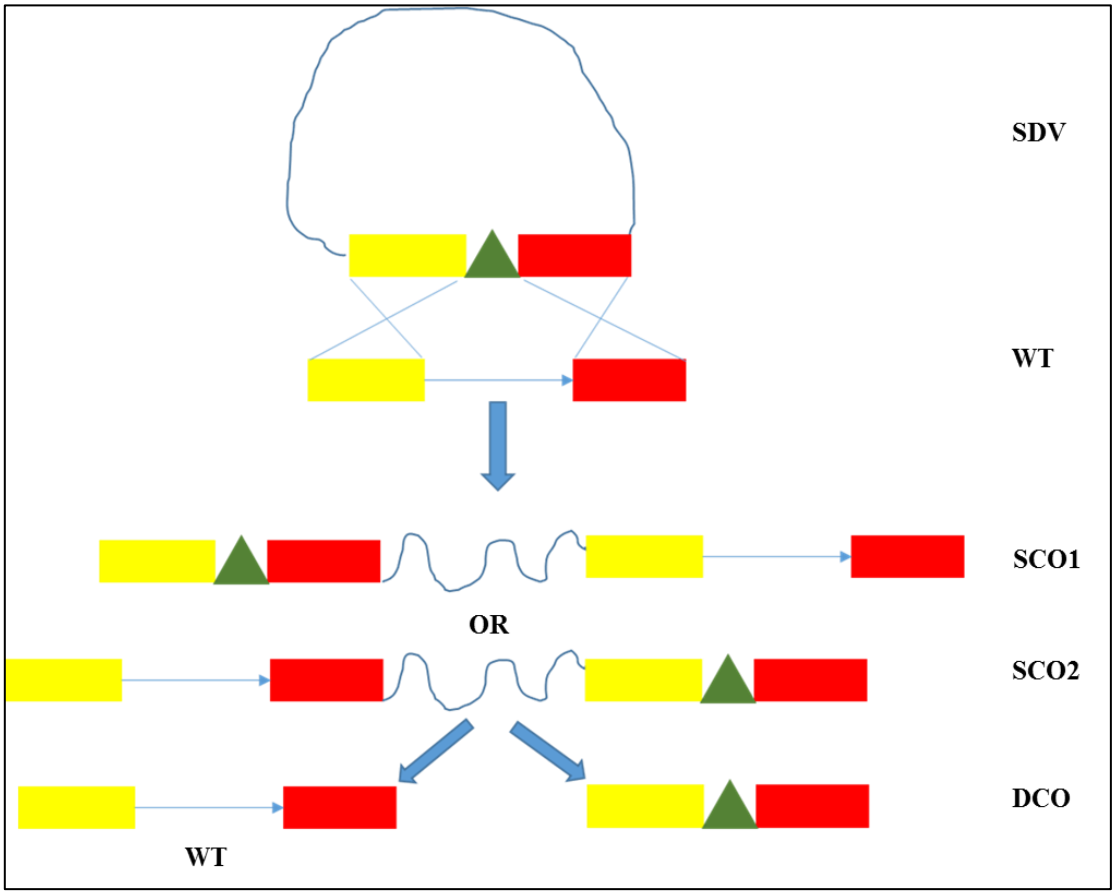

Figure 4.1: Homologous recombination based on the two-step strategy. DCO: double-crossover; SDV: suicide delivery vector; SCO: single-crossover; WT: wild-type.

4.3.2.1. MUTAGENESIS PROCESSES

This section describes the sequence of events involved in the construction of the various plasmids and *Mtb* strains, including the SDV, the SCO and the DCO.

4.3.2.1.1. Suicide-delivery vector construction in *Escherichia coli*

The construction of the SDV was achieved by using the pNILRB5 vector and its structure is shown in Figure 4.2. The pNILRB5 vector is characterised by presence of two LIC sites for the insertion of the upstream and downstream flanking regions of the target gene, the *oriE* for cloning in *E. coli*, the phenotypic marker genes such as kan^R, *lacZ* and *sacB* for selection of

kanamycin-resistant, blue-expressing and sucrose-sensitive colonies, as well as the PacI site for insertion of the *PacI* marker cassettes. The idea behind using SDV was to use a piece of DNA that cannot be recognized in mycobacteria thus cann't replicate.

The construction of the SDV involves sequential insertion of three fragments, which include the flanking upstream region, followed by the downstream and then the marker cassette, resulting in formation of the pRB5kdpDF`, pRB5kdpDFC` and pRB5kdpDFC17` (SDV) plasmids, respectively. The construction of these structures are described below in Sections A, B and C, respectively and are shown in Figure 4.3.

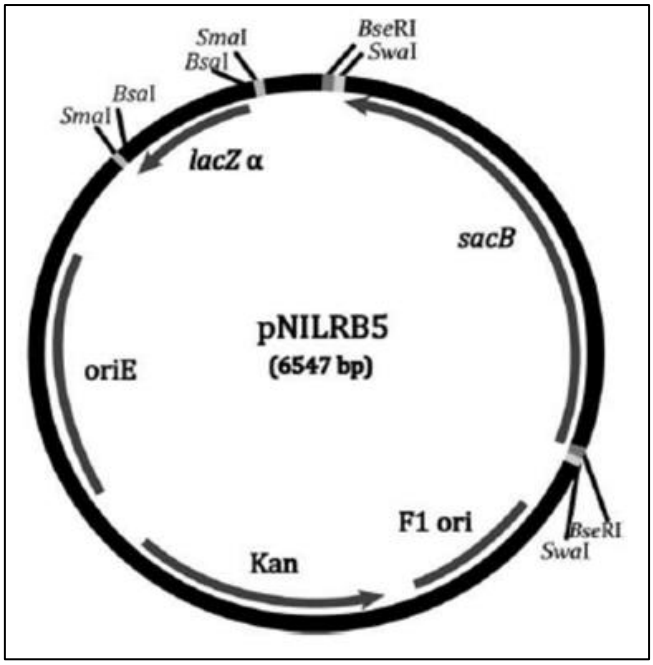

Figure 4.2: Structure of pNILRB5 (Balhana et al., 2010, permission requested).

A. Construction of the pRB5kdpDF` plasmid

The pNILRB5 vector (6547-bp) was digested with BsaI enzyme, resulting in the formation of the 780-bp *BsaI-lacZ* and 5767-bp *BsaI-pNILRB5* fragments. In parallel, 1164-bp-*kdpDF* upstream flanking fragment (primers, Table 3) was synthesised from chromosomal WT *Mtb* H_{37}Rv strain by PCR. The 5767-bp *BsaI-pNILRB5* linear and the PCR-synthesised *kdpDF* fragments were T4 polymerase-treated to create complementary ends with deoxyguanosine triphosphate (dGTP) and deoxycytidine triphosphate (dCTP) as single nucleotides, respectively. The T4 polymerase treatment also resulted in creation of strong H^+ bonds on the fragments. The T4-polymerase-treated fragments were ligated by H^+ bonds using LIC method

(Section H.1), resulting in formation of the pRB5kdpDF` plasmid (6931-bp). The ligates were transformed into DH5α competent *E. coli* cells and the white kanamycin-resistant, sucrose-sensitive transformants were isolated on X-gal, kanamycin-containing LA medium. The development of white colonies was due to the excision of the *lacZ* gene from the plasmid, which is responsible for the blue pigmentation of colonies. The insertion of the *kdpDF'* fragment was confirmed by PCR using sequence-specific primers (Table 3) as described (Section G.3).

B. Construction of the pRB5kdpDFC` plasmid

The pRB5kdpDF` vector (6931-bp) was digested with the BseRI enzyme, resulting in the 1977-bp *BseRI-sacB* and 4954-bp *BseRI-pRB5kdpDF`* linear fragments. Similar to the construction of pRB5kdpDF` in Section A above, the 1143-bp *kdpC* downstream flanking fragment (primers, Table 3), was synthesised by PCR using chromosomal DNA from the $H_{37}$Rv strain. The 4954-bp *BseRI-pRB5kdpDF`* and the PCR synthesized 1143-bp *kdpC* fragments were T4 polymerase-treated (Section G.3) and the fragments ligated following the LIC procedure as described (Section H.1), forming the pRB5kdpDFC` plasmid (6097-bp) (Figure 4.1 (C)). The insertion of the downstream fragment into this plasmid led to separation of both inserts by a few base pairs between each other. Additionally, this construction resulted in deletion of the *kdpFABC* genes. The ligates were transformed into competent *E. coli* cells and the white, kanamycin-, sucrose-resistant transformants were isolated on X-gal, kanamycin, sucrose-containing LA medium. The *sacB* gene is used as a counter-selectable marker and its absence resulted in development of sucrose-resistant clones. The insertion of the downstream *kdpC* fragment was confirmed by PCR using the sequence-specific primers (Table 3) as described (Section G.3).

C. Construction of the pRB5kdpDFC17` plasmid: Suicide-delivery vector

The DNA of the pRB5kdpDFC` and pGOAL17 vectors was digested with the *PacI* enzyme, which linearised the pRB5kdpDFC` plasmid (6097-bp), while digestion of pGOAL17 (8855-bp) resulted in two fragments (2496-bp *PacI-pGOAL17* and 6359-bp *PacI lacZ, sacB* marker cassette). The 6359-bp-*PacI lacZ, sacB* marker cassette and linear 6097-bp *PacI* pRB5kdpDFC` plasmid were ligated to form the pRB5kdpDFC17` plasmid (12456-bp) using the ligase enzyme as described (Section H.2). The ligates were transformed into competent *E. coli* cells and the blue, kanamycin-resistant transformants were isolated on X-gal, kanamycin-

containing LA medium. The presence of the *sacB* gene in the transformants was determined by sucrose-sensitivity testing resulting in the sucrose-sensitive clones. The plasmid was also characterised for the presence of the upstream and downstream inserts by PCR (Section G.3) and WGS (Section N.2). The WGS was performed using the WT $H_{37}Rv$ genomic sequence as reference and the presence of the targeted sequences were shown by the presence of reads aligned to those of the WT, while deletion of the gene was shown by absence of reads.

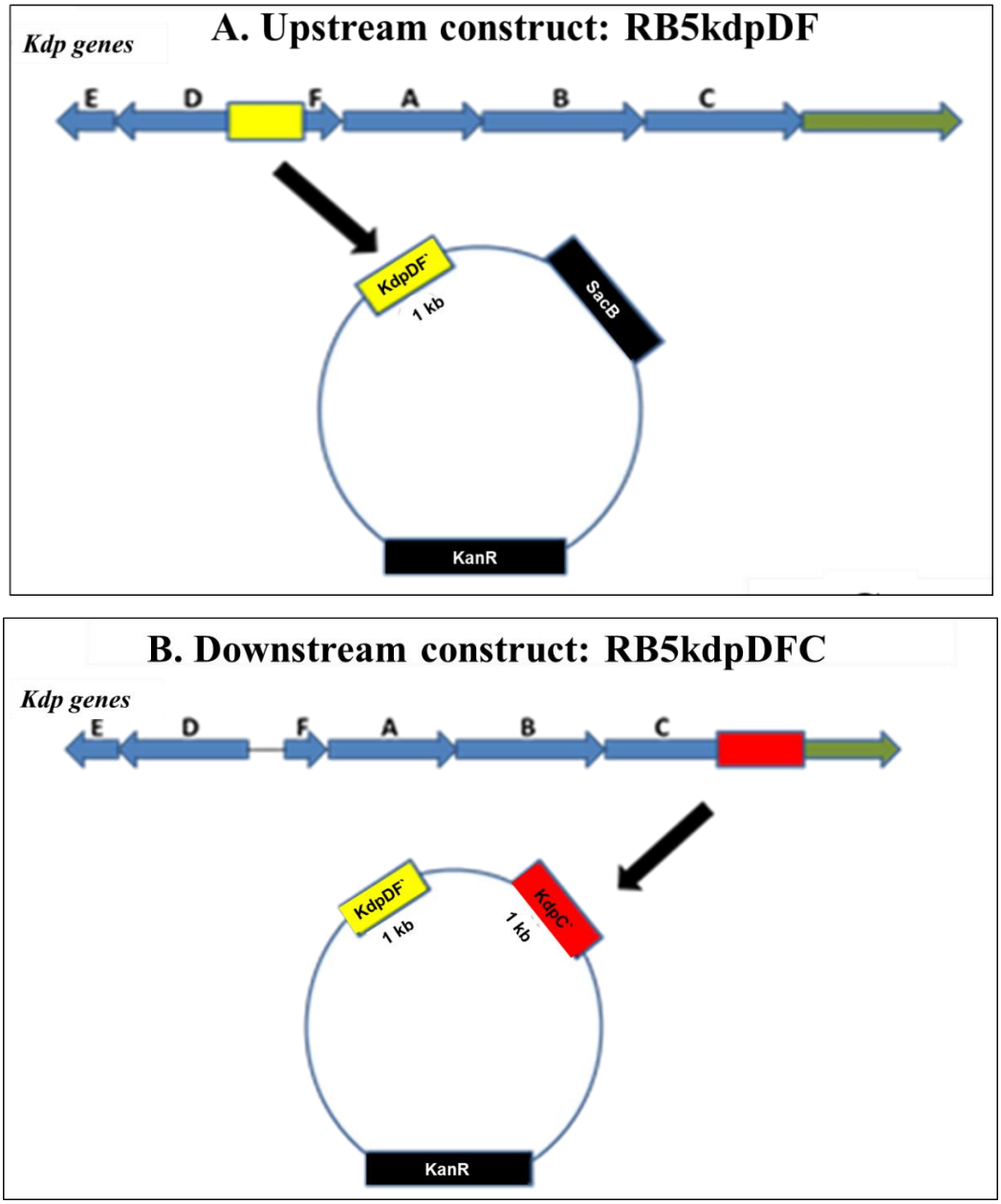

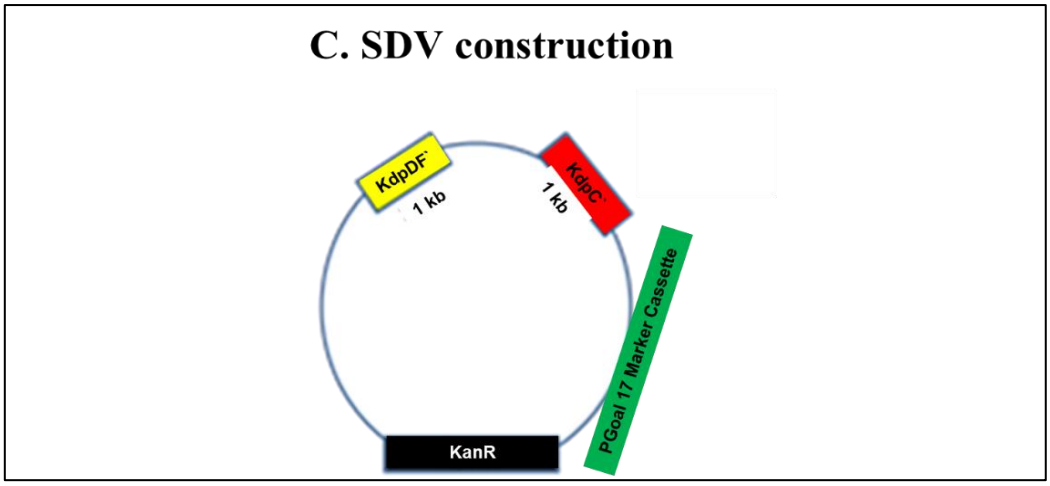

Figure 4.3: Schematic illustration of the construction of the suicide delivery vector. *kdpDF`*: upstream insert; *kdpC`*; downstream insert; *kanR*; kanamycin-resistant gene; *sacB*: sucrose counter-selectable gene.

4.3.2.1.2. Homologous recombination in the *Mycobacterium tuberculosis* TK-deletion mutant strain

Homologous recombination (HR) for *Mtb* mutant construction was conducted by transferring the mutated gene-carrying SDV (Section C), into the recipient TK mutant, resulting in sequential formation of SCO and DCO as described (Section D and E) and the sequences of events are illustrated in Figure 4.4 (red rectangular areas).

D. Isolation of single-crossover clones: TKpRB5kdpDFC17`

The mutated gene-carrying SDV DNA was transferred into the competent *Mtb* TK mutant cells by electroporation (Section J.1 and 2) and the blue, kanamycin-, hygromycin-resistant transformants/ electroporates, which are SCO clones, were isolated on X-gal, kanamycin, hygromycin-containing 7H10 agar medium. The blue, kanamycin-resistant colonies were due to the incorporation of the plasmid into the recipient TK chromosome, while hygromycin resistance of the bacteria was due to the hygromycin-marked mutation of the *ceoBC* operon of the TK mutant (Cholo et al., unpublished). The SCO bacteria are characterised by the incorporation of plasmid, mutated and WT alleles and were confirmed genotypically by PCR for the presence of WT *kdpFABC* and mutated *kdpDFC* alleles (primers, Table 4, Section G.3).

E. Isolation of double-crossover clones: TKkdpDFC

The SCO colonies were grown on plain 7H10 agar medium without the inclusion of selection markers, resulting in the development of white, sucrose-resistant, kanamycin-sensitive colonies, which were confirmed as DCO by PCR using sequence-specific primers (Table 4), showing the presence of the mutated *kdpDFC* fragment, while whole-genome sequencing (Section N.2) for allelic replacement, showed deletion of *kdpFABC* operon.

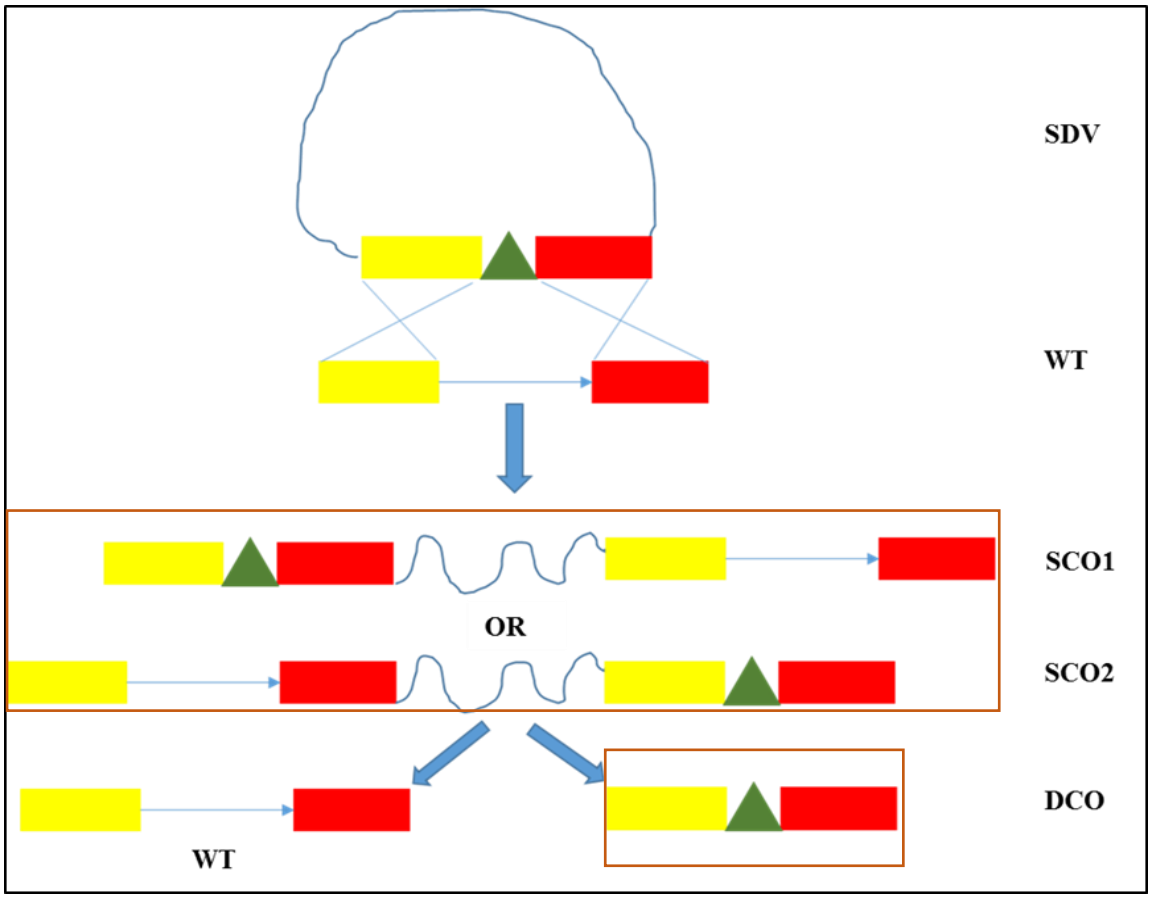

Figure 4.4: Homologous recombination in TK-deletion mutant of *Mycobacterium tuberculosis*. DCO: double-crossover; SDV, suicide delivery vector; single-crossover; WT: wild-type.

4.3.2.2. STANDARD OPERATING PROCEDURES FOR CONSTRUCTION OF THE MUTANT STRAIN

These include cloning procedures in *E. coli* for construction of SDV and HR procedures in *Mtb* for AE.

4.3.2.2.1. Cloning procedures in *Escherichia coli*

The cloning procedures involve treatment of plasmids and chromosomal $H_{37}Rv$ DNA for the construction of SDV.

F. Plasmids

F.1 Plasmid growth in *Escherichia coli* bacteria

A 30 microliter (µL) aliquot of cells containing the plasmid was grown in 30 mL LB broth with selection antibiotics. The pNILRB5, pRB5kdpDF`, pRB5kdpDFC` and pRB5kdpDFC17` plasmids were grown in kanamycin-containing media and the pGOAL17 vector in ampicillin-containing media. The cultures were incubated overnight at 37 °C under shaking conditions (11,000 × g) to mid-log phase (optical density (OD) 1 at 600 nm). The Spectronic Helios UV-Vis spectrophotometer (Merck, USA) was used to measure the OD.

F.2. Plasmid DNA extraction

Plasmid DNA was extracted using Zyppy™ plasmid miniprep kit (Zymo Research, USA: Inqaba biotec, Pretoria, RSA). Briefly, bacterial cells in 600 µL of culture were lysed by adding 100 µL of 7× lysis buffer for 2 min at room temperature (RT), followed by neutralisation of the lysate by addition of 350 µL of cold neutralization buffer. The suspension was centrifuged at 13 500 x g for 2 min and the supernatant (~900 µL) containing the DNA was transferred onto the Zymo-Spin™ IIN column to purify the DNA. The DNA was washed on the spin column with 200 µL Endo-Wash buffer, followed by 400 µL Zyppy wash buffer and centrifuged at 13 500 × g for 15 sec at RT. The plasmid DNA was eluted from the column with 30 µL of Zyppy Elution buffer at 13 500 × g for 30 sec at RT. Two microliters of the eluate were used to measure the concentration of the DNA using the NanoDrop 1000 Spectrophotometer (Thermofisher, USA).

F.3. Plasmid DNA digestion with restriction enzymes

Only the plasmid DNA samples were digested with restriction enzymes in this study. Three restriction enzymes, BsaI, BseRI and PacI, were used and the reaction conditions for each enzyme were as shown in Table 2. The reaction mixtures consisted of 750 - 1000 ng plasmid

DNA added to enzymes and buffers in final volumes of 20 µL. The digests were examined for fragment sizes on 1% gel electrophoresis (Section F.5).

F.4. Purification of the digested vector

The digested DNA samples were purified on spin columns using the QIAamp® DNA Mini kit (Qiagen, RSA). Briefly, the digest DNA mixtures were transferred onto spin columns followed by one wash with 96 - 100% ethanol and two washes with wash buffers. The bound DNA was eluted from the spin column filter with 20 µL of elution buffer.

F.5 Gel electrophoresis

A 1% agarose gel was prepared in 100 mL 1× tris-acetate-EDTA (TAE) buffer incorporating 16% GoodView™ dye II nucleic acid stain (SBS Genetech, China). Three microliters of DNA samples mixed in 5 µL gel-loading tracking dye (0.25% bromophenol blue, 40% (w/v) sucrose) were loaded into wells and separated by electrophoresis at 2V/cm with molecular weight marker III (Roche, Germany) as the reference ladder for determination of DNA fragment sizes. The DNA fragments were viewed using the EL Logic 100 Imaging System (Kodak, USA).

F.6. T4 polymerase treatment of plasmid DNA

T4 polymerase treatment of DNA was performed to generate the 5′ 14-bp nucleotides overhangs on linear DNA for LIC as described (Balhana et al., 2010). The plasmid DNA digests were treated with dGTP as single nucleotide. Approximately 500 - 750 ng digested DNA, in a mixture consisting of 2.5 mM dGTP, 5 mM DTT and 0.1 mg/mL bovine serum albumin (BSA) buffer were polymerised with T4 DNA polymerase in appropriate buffer (New England Biolabs) (Table 2) in a 20 µL final volume, at 22 °C for 30 min followed by inactivation of the enzyme at 75 °C for 20 min.

G. Chromosomal DNA

G.1. *Mycobacterium tuberculosis* bacterial growth

The chromosomal DNA used for preparation of insert fragments for SDV preparation was extracted from the H_{37}Rv strain. A 100 µL aliquot of *Mtb* bacterial cells from frozen stock was grown on Middlebrook 7H10 agar at 37 °C for three weeks to enable the appearance of colonies.

G.2. *Mycobacterium tuberculosis* chromosomal DNA extraction

Chromosomal DNA was extracted using the CTAB method (van Embden et al. 1993). Briefly, bacterial cells from one to two colonies were resuspended in 500 µL tris-EDTA (TE) buffer (Appendix B.1) and heat-killed at 90 ºC for 1h. The bacterial cells were lysed by treating the bacterial suspension with 0.1 mg/mL lysozyme at 37 °C for 1 h, followed by addition of 0.12 mg/mL proteinase K and 1.4% sodium dodecyl sulphate (SDS) at 65 ºC for 20 min. Thereafter, 1 M of NaCl and 6.4 mM CTAB solutions were added and the mixture incubated at 65 ºC for 10 min. The cellular debris was separated from DNA by mixing the suspension with 750 µL of chloroform: isoamyl alcohol (24:1) solution followed by centrifugation at 13 500 × g for 5 min at RT. The upper aqueous phase was isolated and the DNA precipitated by mixing the suspension with 450 µL isopropanol, followed by centrifugation at 13 500 × g, 4 ºC for 20 min. The DNA pellets were washed with 1 mL 70% ethanol by centrifugation as above and air dried at RT. The samples were resuspended in TE buffer and stored at -20 °C for further use.

G.3. Polymerase chain reaction of the insert fragments

PCR was performed for amplification of upstream *kdpDF* and downstream *kdpC* flanking inserts fragments using sequence-specific primers (Table 3). Approximately 10 pg - 200 ng *Mtb* chromosomal DNA was amplified with 0.5 U DNA polymerase in 1× amplification buffer in a reaction mixture consisting of 2% dimethyl sulfoxide (DMSO), 0.8 mM dNTP mixture, and 0.04 µM forward and reverse primers each.

The PCR reaction mixtures were amplified using a Perkin Elmer GeneAmp PCR System 2400 thermal cycler (Perkin Elmer, USA), following conditions described in Table 5.

Table 5: PCR conditions

PCR Step	**Temperature**	**Incubation Time**
Pre-denature	94 °C	5 min
Amplification (35 cycles):		
Denature	94 °C	15 s
Annealing	55 °C	30 s
Extension	68 °C	75 s
Final extension	68 °C	5 min
Hold	4 °C	Indefinite

G.4. Purification of polymerase chain reaction-synthesized insert fragments

The PCR products were purified on the QIAquick spin column using the QIAquick® PCR purification Kit, following the manufacturer's instructions (Qiagen). The PCR products were mixed with PB buffer (5:1 ratio) and transferred to a QIAquick spin column for DNA binding, followed by centrifugation at 13 500 × g for 1 min. The DNA on the spin column was washed with 750 µL PE buffer and eluted with 50 µL distilled water (dH_2O) by centrifugation at 13 500 × g for 1 min.

G.5. T4 polymerase treatment of polymerase chain reaction-synthesized insert fragments

The T4 treatment of insert fragments was performed to create complementary overhangs to the ligating vector. The reaction mixtures were similar to those of plasmid treatment as described (Section F.6.) with dCTP being used instead of dGTP.

H. Ligation

Two types of ligation procedures were performed which included the ligase-independent and -dependent ligations.

H.1. Ligase-independent ligation

The ligase-independent ligation procedure was performed in the absence of the activity of ligase enzyme. The annealing reaction was mediated by H^+ bonds created by T4 polymerase treatment on the termini of the complementary linear plasmid and the insert fragments. The T4 polymerase-treated plasmid and PCR-synthesised fragments in various molarity proportions of the vector: insert mixtures in 10 µL volumes were mixed to anneal at RT for 10 min followed by incubation on ice for 8 min.

H.2. Ligase-dependent ligation

In the ligase-dependent cloning procedure, the annealing reaction was performed in the presence of the ligase enzyme. No T4 polymerase treatment of fragments was performed. However, the reaction mixture took place between vector and insert with complementary ends created by restriction enzyme digestion. The various ratios of vector: insert mixtures were ligated with 0.1 U T4 DNA ligase in 10 µL volume at 22 °C for 10 min.

I. Transformation using the heat-shock method

Transformation involves the transfer of DNA materials into bacterial cells for cloning during bacterial growth. The plasmid used includes *oriE*, which allows for replication in *E. coli*. Transformation was achieved by adding 50 µL of DH5α Z-competent™ *E. coli* cells (Zymo Research) to the ligate mixtures, followed by sequential treatment of the suspension first on ice for 10 min, then at 42 °C for 2 min and on ice again for 1 min. The cells were resuscitated in 200 µL (super optimal broth with catabolite repression) SOC medium (Appendix B.5) at 37 °C for 60 min, followed by centrifugation at 1 500 x g for 3 min. The pellet was resuspended in 100 µL of SOC medium followed by plating on selection LA media.

I.1. Characterisation of transformants

I.1.1. Phenotypic characterisation of transformants

The transformants were plated on LA containing X-gal, sucrose and kanamycin at 37 °C overnight for development of colonies, for selection of *lacZ*-, *sacB*- and kan^R-expressing bacterial clones.

I.1.2. Genotypic characterisation of transformants

The selected colonies were grown in kanamycin-containing LB medium for plasmid DNA extraction (Section F2). The insertions of chromosomal fragments were determined by PCR and WGS (Sections G.3 and N.2).

4.3.2.2.2. Homologous recombination procedures in *Mycobacterium tuberculosis*

J. Electroporation of *Mycobacterium tuberculosis* TK-deletion mutant strain with the suicide delivery vector

J.1. Preparation of competent cells

The *Mtb* competent cells, used for transfer of SDV, were prepared using the TK-deletion mutant strain. The TK bacterial cells were grown in 100 mL 7H9 broth to mid-late logarithmic phase. The cells were treated with pre-warmed, filter-sterilised glycine to a final concentration of 1.5% for approximately 10 - 12 hours at 37 °C prior to harvesting. The cells were pelleted by centrifugation at 1 500 × g for 15 min at 30 °C and washed twice in 1/10 vol of pre-warmed 10% glycerol (37 °C) and resuspended in 400 µL 10 % glycerol (37 °C). The bacterial suspension was then ready for electroporation.

J.2. Electroporation of competent cells with the suicide-delivery vector

Electroporation was performed with the ultra-violet (UV)-treated and -untreated SDV. The UV treatment of the SDV plasmid DNA was performed to create thymidine dimers, which facilitated HR during replication. Approximately 5 µg (10 µL) of SDV plasmid DNA was exposed to ultraviolet radiation (UVR) at 100 mJ/ centimetre $(cm)^2$ for 2 min using Stratalinker® 1800 UV Crosslinker (Bio-Rad, USA).

For electroporation, 400 µL pre-warmed competent TK-deletion mutant cells were added to both UV-untreated and -treated DNA and the mixtures transferred into a MicroPulser™ Cuvette (0.2 cm gab - Bio-Rad, USA) and pulsed at 2.5 kV, 25 µF, 1000 Ω time constant at RT using the MicroPulser™ Electroporator (Bio-Rad, USA). The electroporates were resuscitated with 800 µL 7H9 at 37 °C overnight.

K. Isolation of single-crossover clones

Each electroporate was grown on 7H10 agar incorporated with kanamycin, hygromycin and X-Gal at 37 °C for three weeks for development of SCO colonies. These clones were characterised by blue, kanamycin-, hygromycin-resistant colonies. The DNA of these colonies was extracted and PCR was performed to determine the presence of both the 1041-bp WT *kdpDFA* and 868-bp mutated *kdpDFC* fragments using sequence-specific primer sets (Table 4) and visual detection of PCR products by gel electrophoresis.

L. Isolation of double-crossover clones

The second crossover event was created by growing the SCO clones on a plain Middlebrook 7H10 agar. A 100 µL aliquot of bacterial suspension of one SCO was prepared in phosphate-buffered saline (PBS) and streaked on 7H10 containing X-gal and hygromycin, followed by incubation at 37 °C for three weeks for development of blue and white growth areas. The white growth areas represented elimination of the plasmid from the bacterial genome, while the blue growth areas represented the plasmid-expressing SCO. The white growth areas were selected for phenotypic and genotypic characterisation of the mutants.

4.3.2.2.3. Characterisation of double-crossover clones

M. Phenotypic characterisation

The mutants were characterised phenotypically for the elimination of the plasmid using sucrose and kanamycin sensitivity testing.

M.1. Sucrose sensitivity testing

Sucrose sensitivity was performed for the isolation of the sucrose-resistant clones, following the removal of the counter-selectable marker *sacB* gene in the plasmid. A loopful of cells from the white growth area was resuspended in 100 µL PBS followed by 10-fold serial dilutions (undiluted, 10^{-1} - 10^{-6}). A 100 µL aliquot of the most concentrated cells (undiluted, 10^{-1} and 10^{-2}) was plated on 7H10 medium containing X-gal and sucrose, while aliquots of the less concentrated bacterial suspensions were plated on medium without sucrose. The plates were incubated at 37 °C for three weeks for the development of white sucrose-resistant colonies. These colonies were screened further for kanamycin sensitivity testing.

M.2. Kanamycin sensitivity testing

Kanamycin sensitivity testing was performed for the isolation of kanamycin-sensitive clones, following removal of the kan^R gene in the plasmid. Suspensions of white sucrose-resistant colonies were prepared in 30 - 50 µL PBS and equal volumes of each suspension were spotted on kanamycin-free and -containing 7H10 agar. Due to elimination of the kan^R gene from the plasmid, the mutant clones were sensitive to kanamycin and failed to grow in the presence of kanamycin. DNA was extracted from kanamycin-sensitive colonies for genotypic characterisation.

N. Genotypic characterisation

The mutants were characterised genotypically for allelic replacement using PCR and whole genome sequencing.

N.1. Polymerase chain reaction

PCR was performed using primers described in Table 4 following procedures described in Section G.3, for detection of the presence of the 868-bp mutated *kdpDFC* fragment.

N.2. Whole genome sequencing

DNA sequencing was performed on the positive PCR DCO clones (section above) to confirm mutation of the *kdpFABC* operon. The work was performed in collaboration with the Core Sequencing Facility, NICD, NHLS, South Africa. DNA sequencing was performed using Illumina MiSeq instrument (Illumina, USA).

The extracted DNA was subjected to library preparation with the Nextera XT DNA Sample Preparation Kit (Illumina, San Diego, CA, US) according to the manufacturer's instructions and sequenced using the Illumina MiSeq instrument (Illumina, USA). Briefly, a 1 ng/µL DNA was tagmented (fragmented and tagged) at 55 ^{o}C for 5 min to generate adapter-ligated DNA fragments. Tagmented fragments were amplified by a limited-cycle PCR of 15 cycles to add Illumina sequencing adapters and to create a dual indexed library for each sample. The resulting indexed libraries were purified and size-selected using 100 Agencourt AMPure® XP beads (Beckman Coulter Inc. IN, USA). Purified DNA libraries were quantified and assessed for quality on an Agilent Bioanalyzer (Agilent Technologies, California, US). Libraries were normalised, pooled at equimolar concentrations and denatured using sodium hydroxide (NaOH) prior to loading onto the reagent cartridge. Genome sequencing was carried out on an Illumina MiSeq instrument using a 600-cycle MiSeq Reagent v3 Kit (Illumina) to generate paired-end reads. Sequencing data was retrieved from the genetic analyser as a MiSeq output file and the quality of the reaction was assessed by reviewing the FASTQ report. The adaptor sequences were removed from the sequences and the paired-end sequenced reads were aligned and assembled *de novo* using the Qiagen CLC Genomics Workbench version 11 (Qiagen). Sequencing across the entire target genes was required to verify the exact sequence of the clone as compared to the mother strain and confirm the successful knockout of the target genes. The presence of *kdpFABC* sequence reads were present in the WT and SCO strains, while the TKkdpDFC mutant strains were characterised by the absence of the *kdpFABC* reads.

4.4. RESULTS

4.4.1. Suicide-delivery vector, pRB5kdpDFC17` construction

The SDV was constructed by sequential insertions of 1164-bp *kdpDF'* upstream (B) and 1143-bp *kdpC* downstream flanking regions (D), as well as *PacI-lacZ,sacB* (F) into the pNILRB5 vector (A) resulting in formation of the pRB5kdpDF` (C), pRB5kdpDFC` (E) and

pRB5kdpDFC17` (G) plasmids respectively. The sequences of events in the formation of the SDV are as shown in Figure 4.5.

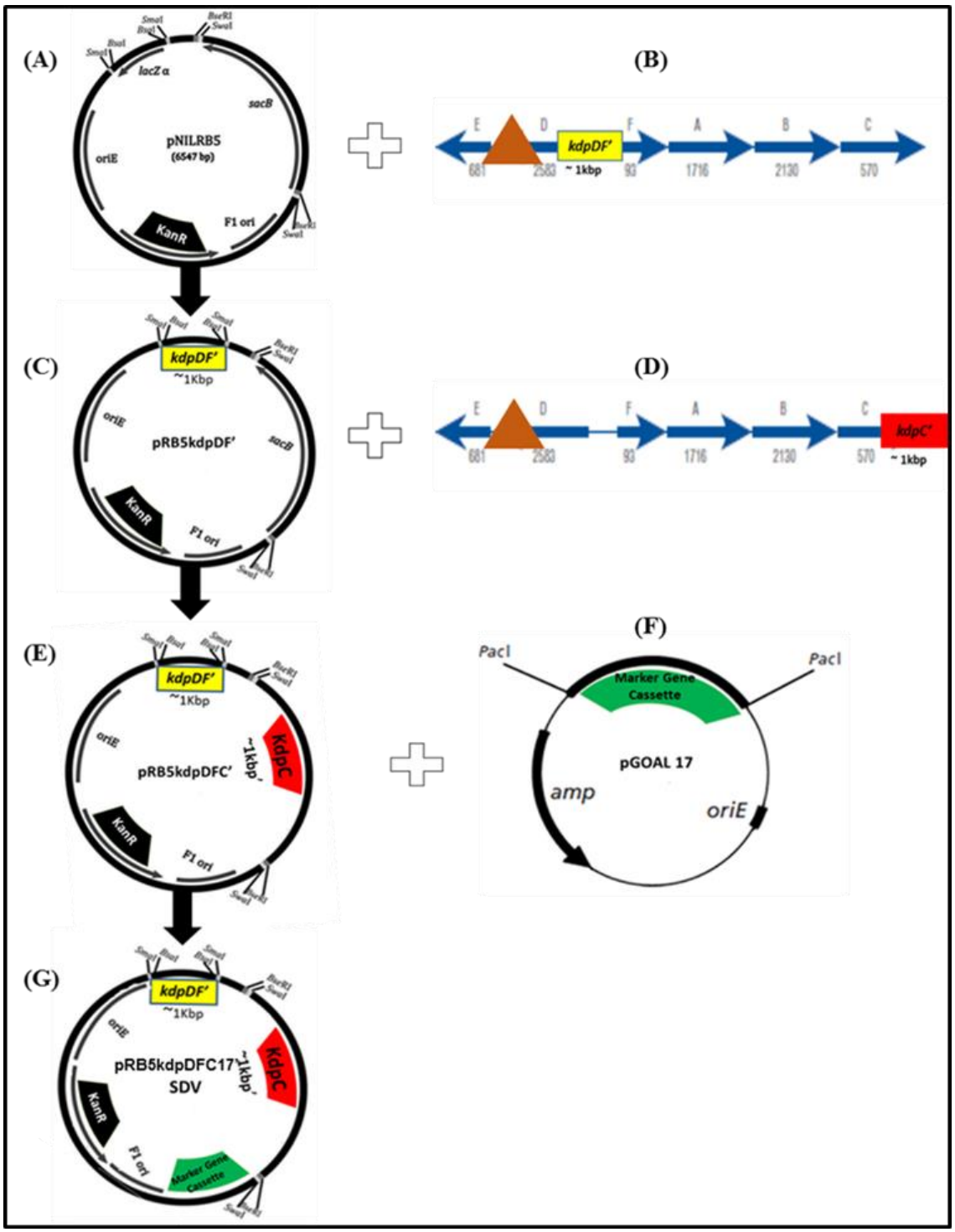

Figure 4.5: Construction of the suicide-delivery vector, pRB5kdpDFC17`. (A) pNILRB5 vector; (B) kdpDF` upstream region; (C) pRB5kdpDF` plasmid; (D) kdpC` downstream region; (E) pRB5kdpDFC`plasmid; (F) pGOAL17 with *PacI-lacZ,sacB* marker cassette.

4.4.1.1 pRB5kdpDF` plasmid constructs

The insertion of 1164-bp *kdpDF'* upstream flanking fragment into the pNILRB5 vector resulted in replacement of the 780-bp *BsaI-lacZ* gene, leading to selection of white kanamycin-resistant colonies. Only two white kanamycin-resistant colonies were isolated (data not shown).

The two colonies were screened for insertion of the 1164-bp *kdpDF* upstream fragment using PCR. The WT DNA and no DNA template samples were included as positive and negative controls respectively. Both colonies showed presence of single 1164-bp fragments corresponding to that of the WT (Figure 4.6).

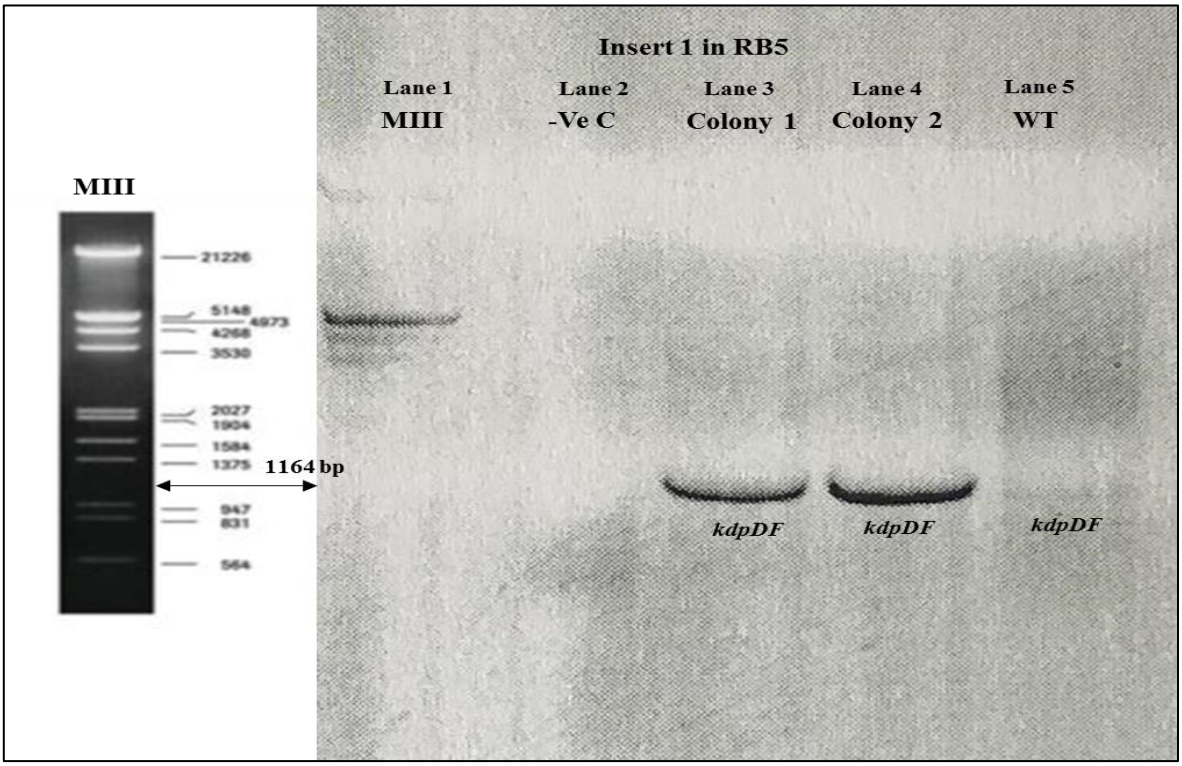

Figure 4.6: PCR synthesis of upstream kdpDF of white kanamycin-resistant colonies. Samples in lanes 1-5 represented molecular weight marker III, no DNA template negative control, colony 1 and colony 2; wild-type $H_{37}Rv$ strain. The arrow indicates the 1164bp kdpDF PCR product.

4.4.1.2. pRB5kdpDFC` plasmid constructs

Insertion of the 1143-bp *kdpC* downstream flanking fragment into the pRB5kdpDF` vector resulted in replacement of the counter-selectable marker *sacB* gene, leading to production of sucrose- resistant clones. Only four white, kanamycin-, sucrose-resistant colonies were isolated from sucrose-containing LA medium (data not shown).

The presence of the 1143-bp *kdpC* downstream insert was confirmed with PCR (primers, Table 4) on all four colonies using WT and no DNA template samples as positive and negative controls respectively (Figure 4.7).

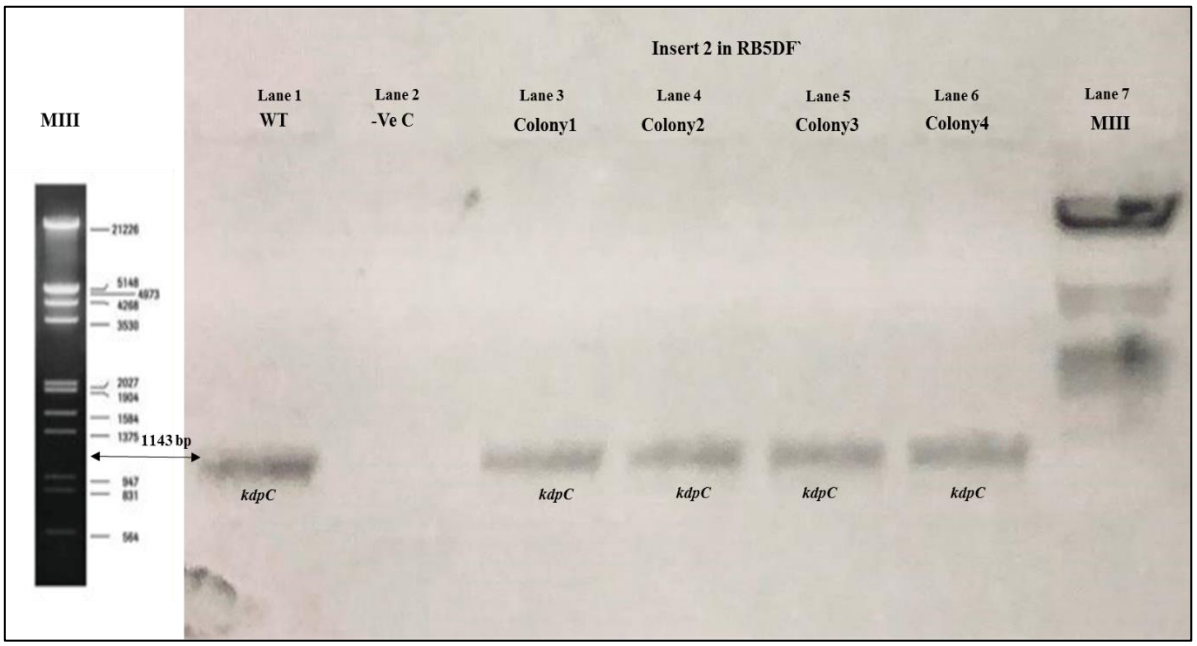

Figure 4.7: PCR synthesis of downstream *kdpC* of white kanamycin-, sucrose-resistant colonies. Samples in lanes 1-7 represent the wild-type H_{37}Rv strain, No DNA template, colonies 1-4 and molecular weight marker III respectively. The arrow indicates the 1143 bp kdpC PCR product.

4.4.1.3. pRB5kdpDFC17` plasmid constructs: Suicide-delivery vector

The insertion of *PacI-lacZ,sacB* from the pGOAL17 vector into the pRB5kdpDFC` resulted in development of blue, kanamycin-resistant, sucrose-sensitive colonies. Only four white kanamycin-resistant colonies were isolated, which were further confirmed to be sucrose-sensitive (data not shown).

4.4.1.3.1. Polymerase chain reaction analysis of the suicide-delivery vector

The presence of the upstream and downstream inserts was confirmed on all four white kanamycin-resistant, sucrose-sensitive colonies using PCR and the results are shown in Figure 4.8.

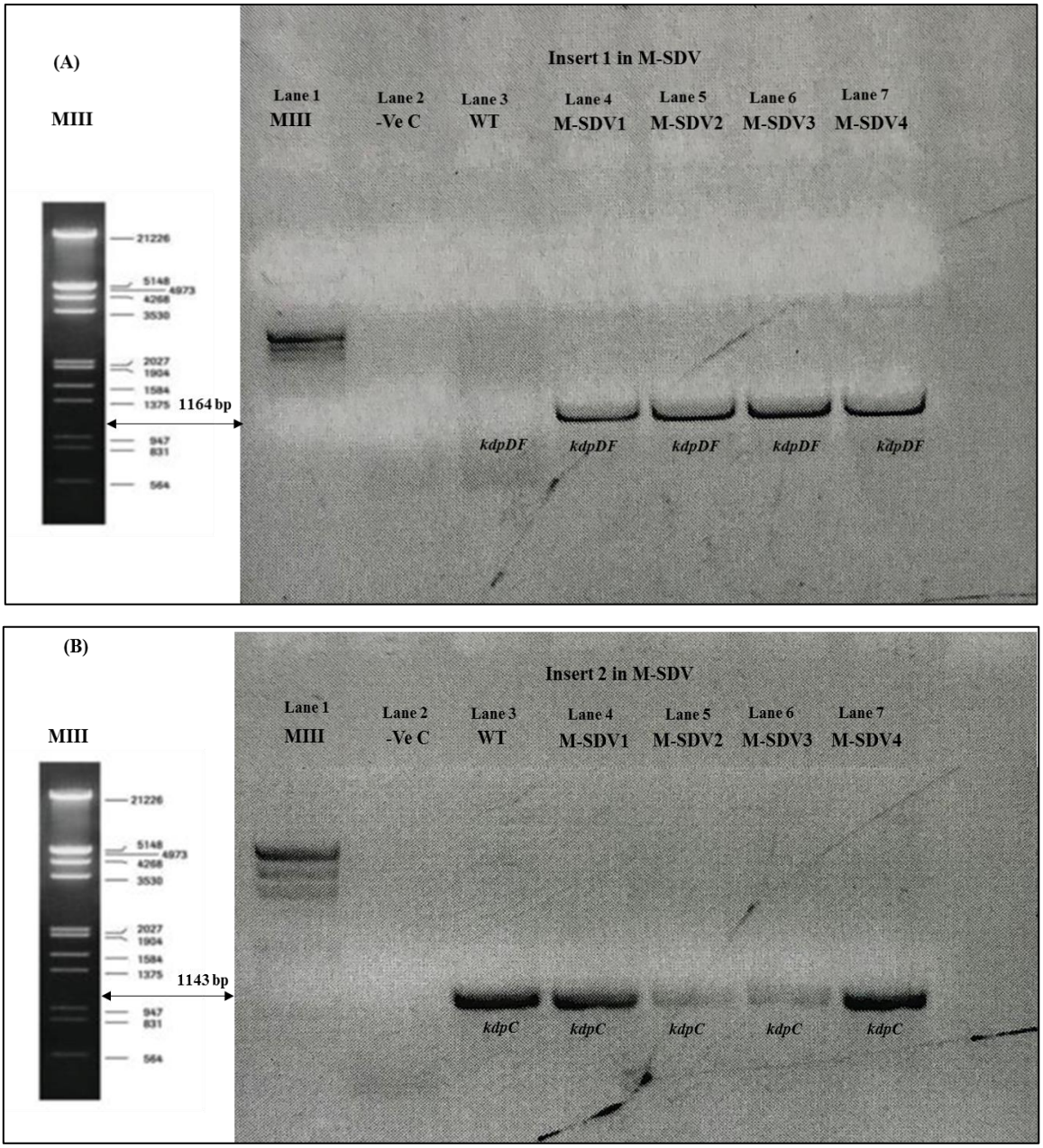

Figure 4.8: PCR synthesis of upstream *kdpDF* (A) and downstream *kdpC* (B) fragments in the suicide-delivery vector. For both gel maps representing the inserts, the samples in lanes 1-7 represent molecular marker III, no DNA template, wild-type H_{37}Rv strain, M-SDV1 - 4 respectively. Arrows indicate the 1164bp kdpDF and 1142bp kdpC PCR products.

4.4.1.3.2. Whole genome sequencing of suicide-delivery vector

Only one SDV, named M-SDV4, was selected for screening using WGS with sequence of the H_{37}Rv strain as reference. Insertion of the upstream *kdpDF* and downstream *kdpC* fragments was shown by the presence of reads at specific targeted positions flanking the *kdpFABC* operon. The *kdpFABC* operon, encoding the four *kdpF*, *kdpA*, *kdpB* and *kdpC* genes, was deleted (Figure 4.9).

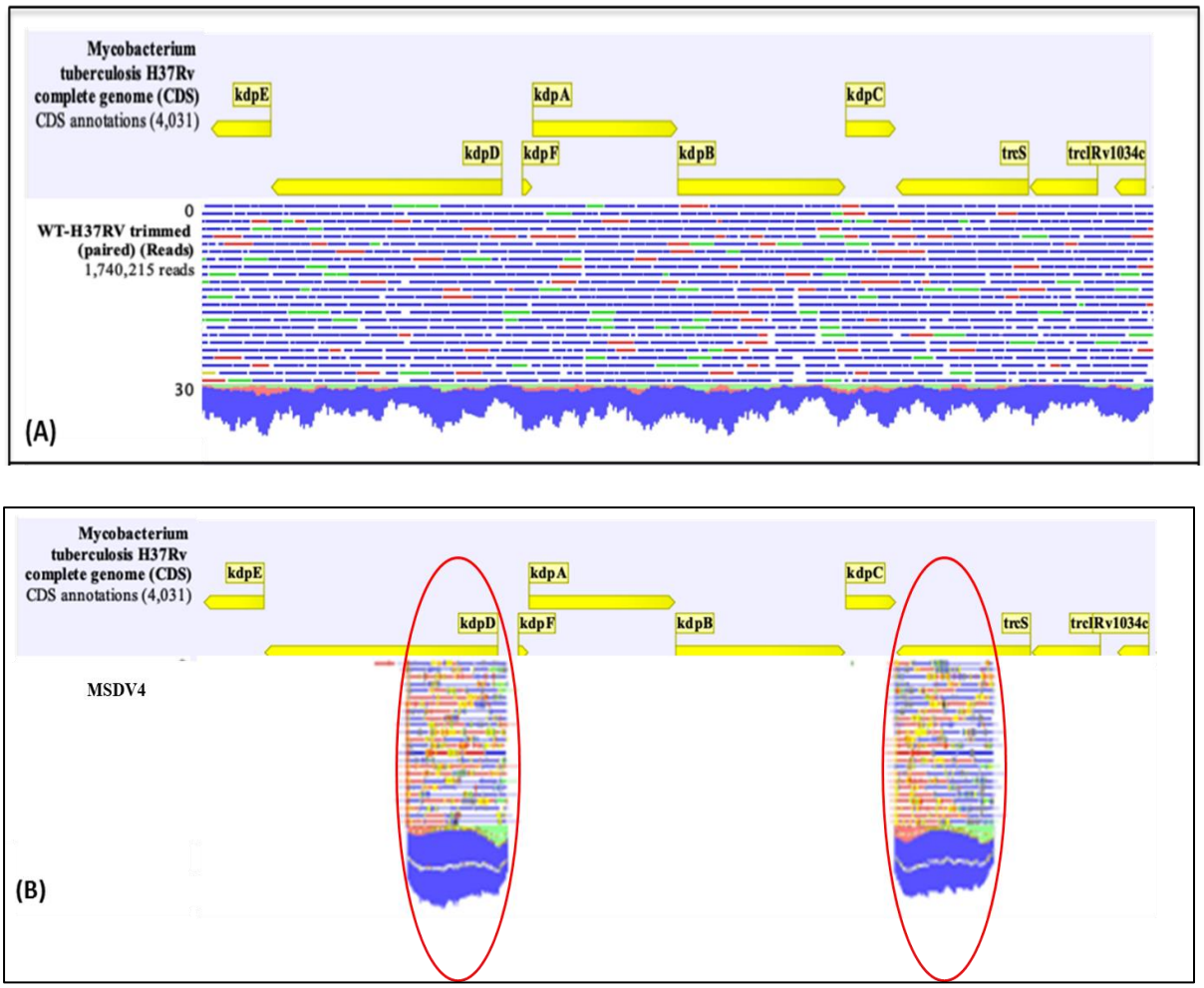

Figure 4.9: Whole genome sequencing of the suicide-delivery vector aligned with that of the H_{37}RV strain. Genomic sequence of the wild-type H_{37}Rv (A) suicide-delivery vector (B) showing upstream *kdpDF* and downstream *kdpC* fragments (areas marked in red).

4.4.2. *Mycobacterium tuberculosis* TKkdpDFC mutant construction

The SDV (Figure 4.10 B) was transferred into the TK mutant through electroporation resulting in development of either SCO1 or SCO2 (Figure 4.10 C and D). Replication of either SCO led to elimination of the plasmid (shown in SCO2) resulting in DCO formation (Figure 4.10 F). Double-crossover homologous-recombination was required to completely eliminate/knockout the target genes. The complete HR process between the SDV and the TK mutant are shown in Figure 4.10.

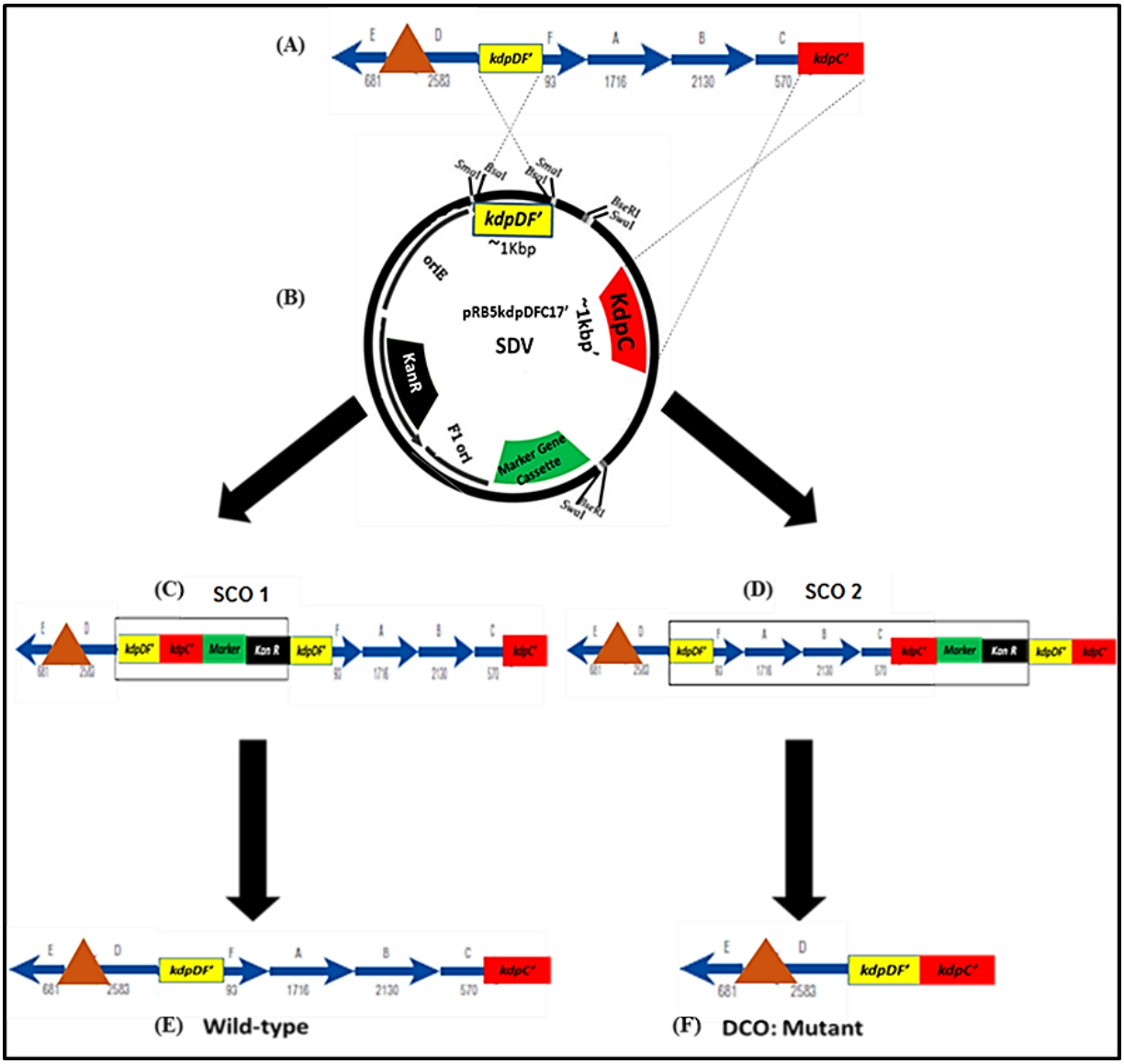

Figure 4.10: Homologous recombination between the TK mutant strain and the pRB5kdpDFC17` SDV vector.

4.4.2.1. Isolation of single-crossover clones

Electroporation of both the UV-untreated and –treated SDV plasmid DNA resulted in formation of blue kanamycin-, hygromycin-resistant *Mtb* colonies, which yielded comparable numbers of SCO colonies. Based on these results, only data representing the UV-untreated plasmid electroporation, is shown in Figure 4.11A.

Five blue kanamycin-resistant colonies were screened by PCR for the presence of both WT and mutated fragments using the PCR method (results are not shown). The WT and SDV were used as positive controls for presence of WT and mutated fragments, respectively. Only the 868-bp mutated allele was amplified in the SCO mutants while the 1041-bp WT allele was

amplified in the WT $H_{37}Rv$ DNA. The presence of the WT allele in the SCO clones was confirmed by PCR for the amplification of the 1041-bp WT allele (Figure 4.11B).

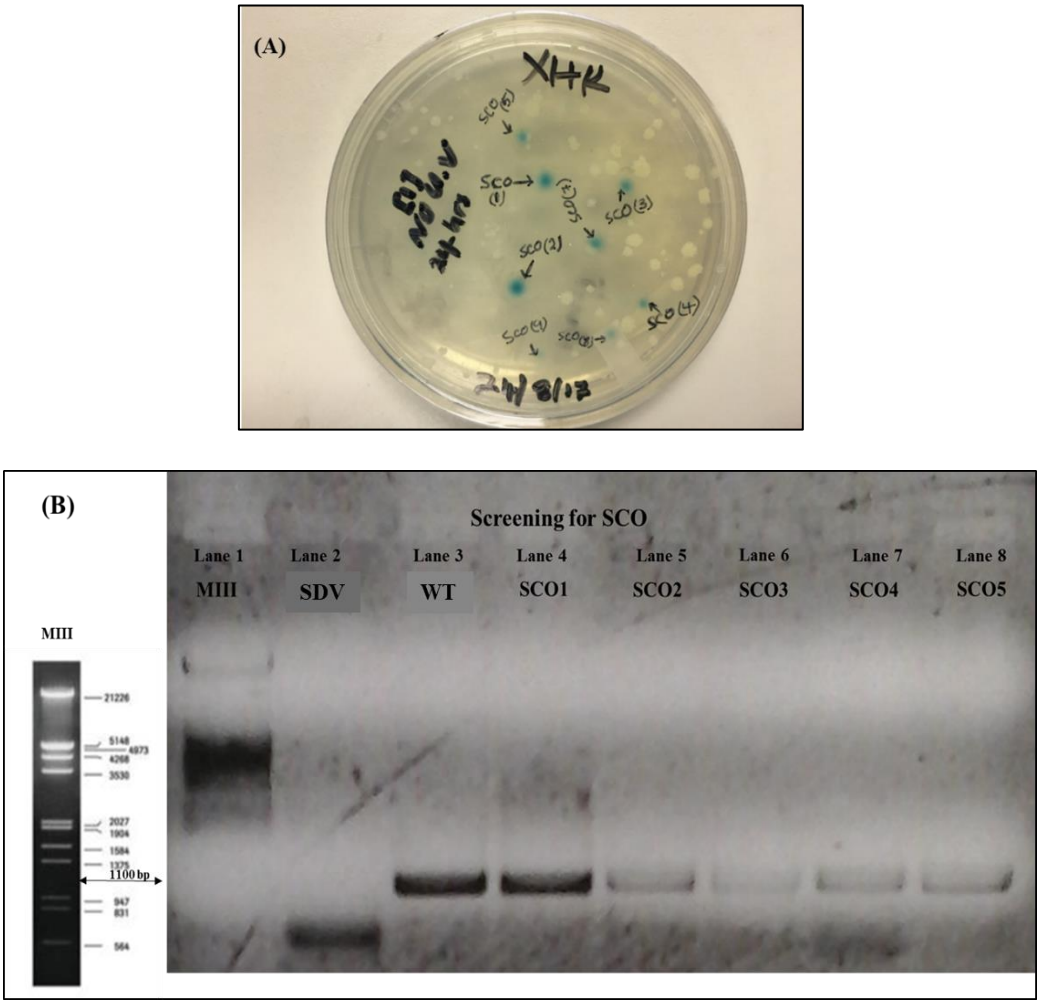

Figure 4.11: Characterisation of the single crossover clones (A) demonstrated phenotypically by blue colonies and (B) genotypically using PCR amplification. Samples in lane 1 - 8 represent molecular weight marker III, SDV, wild-type $H_{37}Rv$, SCO1 - 5 respectively.

4.4.2.2. Isolation of double-crossover constructs

Streaking one SCO colony on 7H10 agar containing X-gal and hygromycin, resulted in confluent white and blue growth areas (Figure 4.12; red circles). The blue and white growth areas indicate the presence and absence of plasmids representing SCO (A) and DCO (B), respectively.

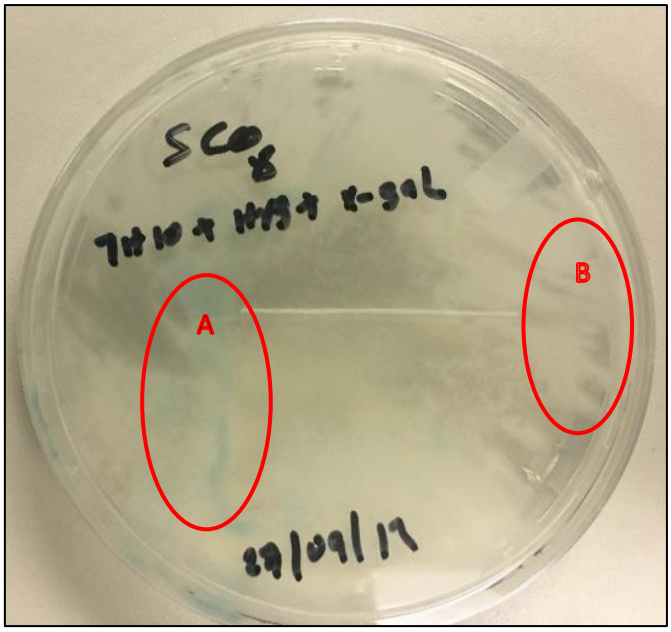

Figure 4.12: Development of double-crossover colonies on 7H10 containing X-gal and hygromycin. The encircled A and B areas represent the single-crossover and double-crossover, respectively.

4.4.3 Characterisation of double-crossover constructs

4.4.3.1. Phenotypic characterisation

The DCO mutants were characterised phenotypically by using sucrose and kanamycin sensitivity testing methods.

4.4.3.1.1. Sucrose sensitivity testing

Sucrose sensitivity testing of white areas resulted in isolation of white sucrose-resistant colonies with different sizes (data not shown).

4.4.3.1.2. Kanamycin sensitivity testing

A set of 20 large and small sucrose-resistant colonies was tested for kanamycin sensitivity and the results are as shown in Figure 4.13 with top and bottom panels representing spotting of big and small colonies, respectively. Two colonies from big and four from small colonies were kanamycin-resistant SCO incorporating the kanamycin-resistant plasmid.

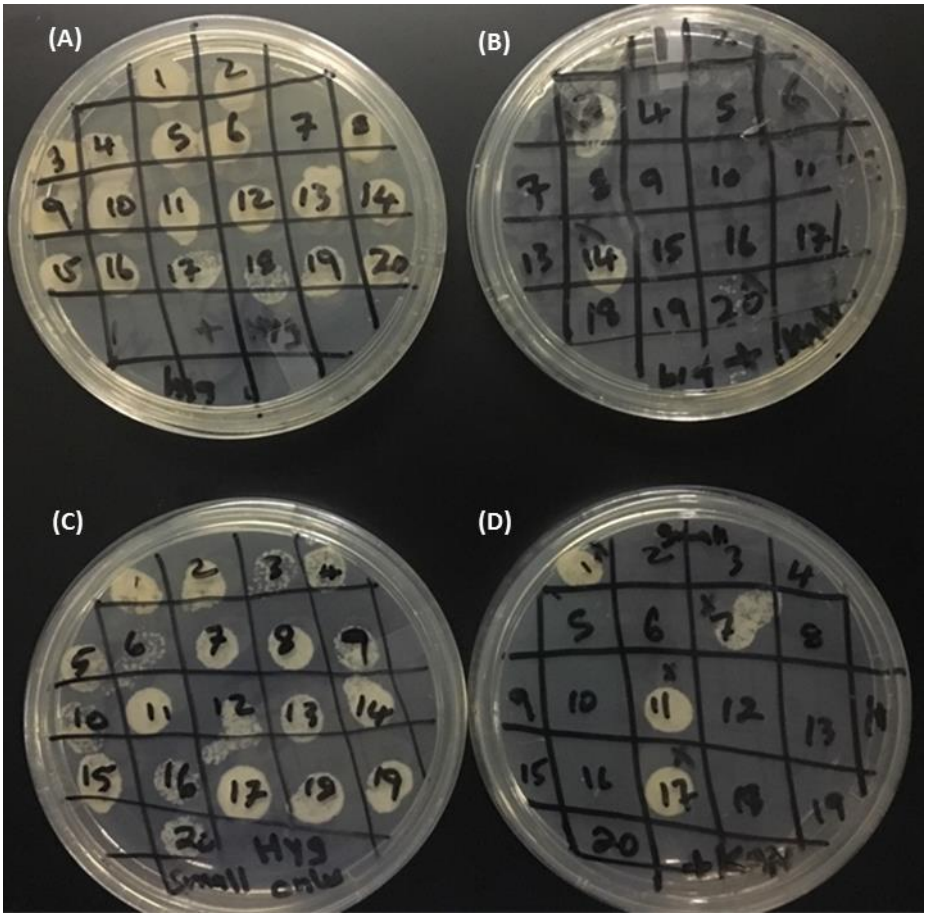

Figure 4.13: Kanamycin-sensitivity testing of white sucrose-resistant colonies. Panel A and B represent the selection of large colonies, while C and D represent the small colonies. In addition, plates A and C and B and D represent the absence and presence of kanamycin in the growth medium, respectively.

4.4.3.2. Genotypic characterisation of DCO for allelic replacement

4.4.3.2.1. Polymerase chain reaction

The white sucrose-resistant, kanamycin-sensitive colonies (Section 4.4.3.1.2) of both large and small sets of colonies were screened for the presence of only the mutated allele using PCR. Screening of all 18 large colonies demonstrated the presence of the WT fragment, while two of the 16 small colonies (colonies 16 and 18, referred to as F16 and F18, respectively) revealed the presence of the mutated band and a faint WT band (Figure 4.14).

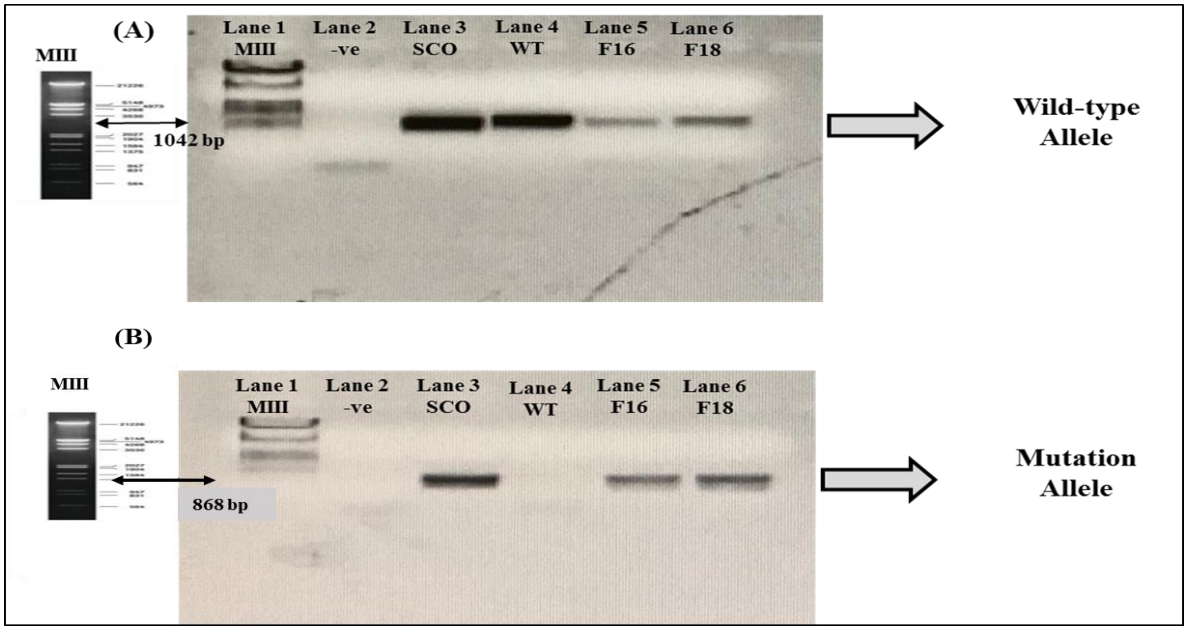

Figure 4.14: PCR confirmation of the *kdpDFC* mutation. The panel of samples at A and B represent PCR of wild-type and mutated alleles, respectively. The samples in lanes 1 - 6 represent molecular weight marker III, no DNA template, single-crossover, wild-type H_{37}Rv, F16 and F18, respectively.

4.4.3.2.2. Whole genome sequencing

Colonies 16 and 18, were sequenced for mutation of the *kdpFABC* operon by WGS, with the sequences of the WT H_{37}Rv and TK mutant strains used for alignment. The results are shown in Figure 4.15. Both colonies F16 and F18 showed absence of reads in the *kdpFABC* operon (shown by Red Cross) illustrating deletion of the *kdpFABC* genes, while the WT and the TK mutant strains showed the presence of reads.

As the TK double-knockout had inactivation of the *trk* (*ceoBC*) and *kdpDE* operons, mutations of these operons were further confirmed on the F16 and F18 colonies as shown in Figure 4.15F and G.

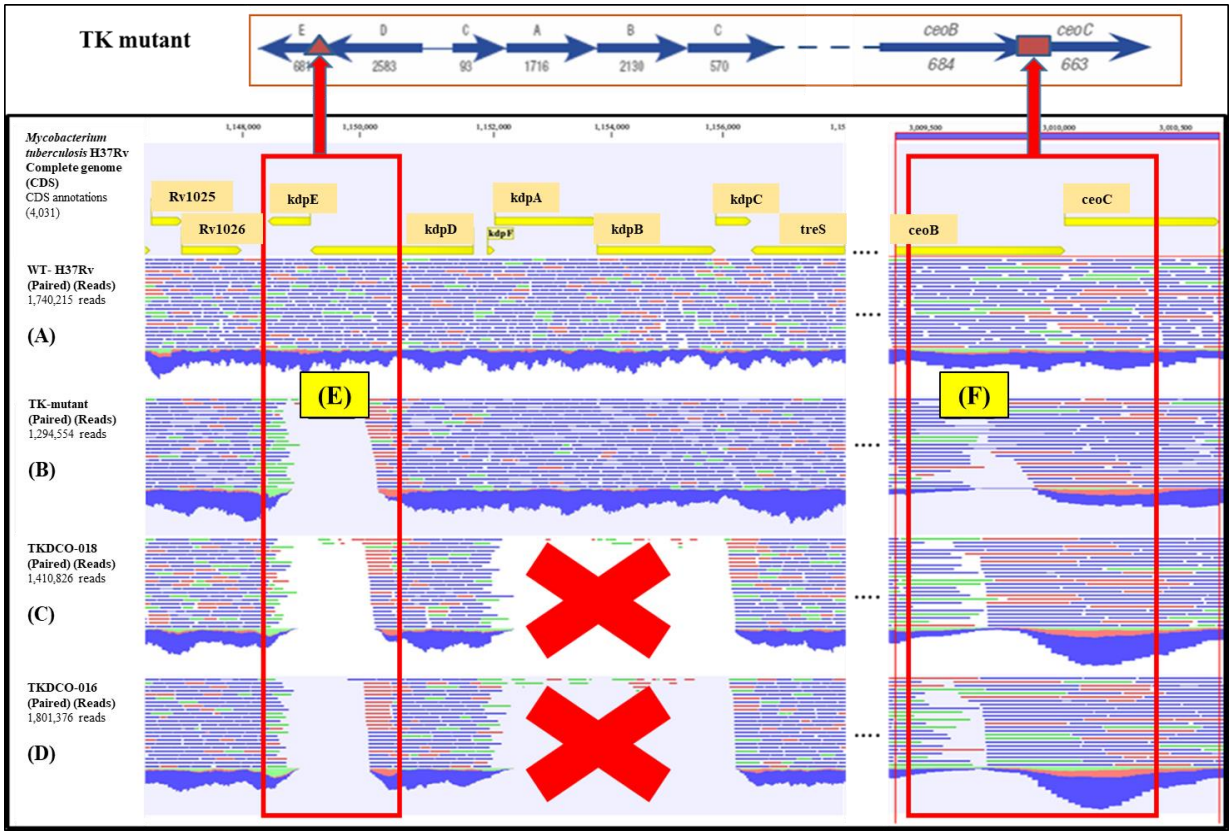

Figure 4.15: Whole genome sequencing of *Mycobacterium tuberculosis* strains, representing (A) wild-type $H_{37}Rv$; (B) TK mutant; (C) F18 and (D) F16. (E) and (F) indicate kdpDE and ceoBC muataions, respectively.

4.5. DISCUSSION

Homologous recombination (HR) methods using SDV resulting in AE via the development of SCO followed by DCO have been extensively applied for investigation of functions of genes in *Mtb*. Several mutants generated using p1NIL suicide plasmids as delivery vectors, have showed stability in their targeted mutation sites on the bacterial genome. These mutants also include the three K^+-uptake deletion mutants, viz. the Trk-, KdpDE and TK-deletion strains (Parish et al., 2003; Cholo et al., 2006).

In the current study, a new *Mtb* K^+-uptake mutant strain has been constructed by using a modified version of the p1NIL plasmid, the pNILRB5, as a delivery vector (Balhana et al., 2010). Using the pNILRB5 vector, construction of SDV was successful, resulting in isolation of specific clones as shown in the construction of the pRB5kdpDF` and pRB5kdpDFC` plasmids, yielding 100% of specific clones isolated. Despite the low number of colonies, two and four clones for construction of these two plasmids, respectively, only one clone from each plasmid construct was required for successful cloning purposes as these procedures are not quantitative but qualitative. Additionally, the LIC method, which depended on the creation of

H^+ bonds using T4 polymerase treatment, eliminated the use of the ligase enzyme, which requires optimum conditions for the enzyme activity necessary for annealing of fragments. Additionally, using the pNILRB5 vector, in this study, the number of restriction enzymes during cloning procedure was also reduced, being limited to three by involving only those that appear on the flanking sites of the phenotypic markers *lacZ* and *sacB* genes.

The application of HR using the SCO and DCO development has been used reliably in *Mtb* over several years. However, this step has also been associated with challenges and dependence on the efficiency of electroporation procedures. In the current study, these challenges in relation to electroporation were addressed by adjusting the temperature used for treatment of *Mtb* competent cells, increasing it from RT, as used in the past, to 30 °C during electroporation (Parish and Stoker, 2000). This resulted in an increase in the yield of the number of SCO. Additionally, this approach also led to successful electroporation of both UV-untreated and -treated SDV plasmids, resulting in comparable numbers of SCO following electroporation with both plasmids.

Other parameters that led to improvements in the mutagenesis procedure, in the current study, included the application of WGS. The use of WGS was beneficial in providing the information on the mutation target site of the genome. Additionally, due to sequencing of the entire genome of the bacteria, additional sequence information for other sites or genes of interest on the genome is accessible, requiring no repetition of experiments. In the current study, mutation analysis of additional sequences such as the *ceoBC* (for Trk) and *kdpDE* operons were provided using the same sequencing data.

The application of these mutagenesis procedures enabled successful construction of the *Mtb* TKkdpDFC mutant and will be applied for future construction of *Mtb* mutants. The TKkdpDFC mutant was further investigated phenotypically to characterise the possible involvement of the three targeted K^+-uptake-encoding operons in planktonic growth, biofilm formation and macrophage infection and intracellular survival as described in Chapter four.

4.6. CONCLUSION

The use of mutagenesis tools using the pNILRB5 suicide vector series for mutated allele delivery into the recipient *Mtb* bacteria for HR have been demonstrated to be valuable in the successful construction of mutants of this dangerous bacterial pathogen.

4.7. REFERENCES

Aslanidis C. and de Jong P.J. (1990). Ligation-independent cloning of PCR products (LIC-PCR). *Nucleic Acids Research*, 18(20), 6069-6074.

Balhana R., Stoker N.G., Sikder M.H., Chauviac F.X. and Kendall S.L. (2010). Rapid construction of mycobacterial mutagenesis vectors using ligation-independent cloning. *Journal of Microbiological Methods*, 83(1), 34-41.

Basu P., Sandhu N., Bhatt A., Singh A., Balhana R., Gobe I., Crowhurst N.A., et al. (2018). The anaplerotic node is essential for the intracellular survival of *Mycobacterium tuberculosis*. *The Journal of Biological Chemistry*, 293(15), 5695-5704.

Cholo M.C., Boshoff H.I., Steel H.C., Cockeran R., Matlola N.M., Downing K.J., et al. (2006). Effects of clofazimine on potassium uptake by a Trk-deletion mutant of *Mycobacterium tuberculosis*. *The Journal of Antimicrobial Chemotherapy*, 57(1), 79-84.

Haun R.S., Serventi I.M. and Moss J. (1992). Rapid, reliable ligation-independent cloning of PCR products using modified plasmid vectors. *Biotechniques*, 13(4), 515-518.

Jain P., Hsu T., Arai M., Biermann K., Thaler D.S., Nguyen A., et al. (2014). Specialized transduction designed for precise high-throughput unmarked deletions in *Mycobacterium tuberculosis*. *M Bio*, 5(3), e01245-14.

Parish T., Gordhan B.G., McAdam R.A., Duncan K., Mizrahi V. and Stoker, N.G. (1999). Production of mutants in amino acid biosynthesis genes of *Mycobacterium tuberculosis* by homologous recombination. *Microbiology*, 145, 3497-3503.

Parish T., Smith D.A., Kendall S., Casali N., Bancroft G.J. and Stoker N.G. (2003). Deletion of two-component regulatory systems increases the virulence of *Mycobacterium tuberculosis*. *Infection and Immunity*, 71(3), 1134-1140.

Parish, T. and Stoker N.G. (2000). Use of a flexible cassette method to generate a double unmarked *Mycobacterium tuberculosis tlyA plcABC* mutant by gene replacement. *Microbiology*, 146 (8), 1969-1975.

Pelicic V., Jackson M., Reyrat J.M., Jacobs W.R. Jr., Gicquel B. and Guilhot C. (1997). Efficient allelic exchange and transposon mutagenesis in *Mycobacterium tuberculosis*. *Proceedings of the National Academy of Sciences of the United States of America*, 94(20), 10955-10960.

Sander P., Meier, A., and Böttger E.C. (1995), rpsL+: a dominant selectable marker for gene replacement in mycobacteria. *Molecular Microbiology*, 16, 991-1000.

van Embden J.D., Cave M.D., Crawford J.T., Dale J.W., Eisenach K.D., Gicquel B., et al. (1993). Strain identification of *Mycobacterium tuberculosis* by DNA fingerprinting: recommendations for a standardized methodology. *Journal of Clinical Microbiology*, 31(2), 406-409.

Yang S., Becker F.F. and Chan J.Y. (1993). Biochemical characterization of a protein inhibitor for DNA ligase I from human cells. Regulation/replication/repair/recombination. *Biochemical and Biophysical Research Communications*, 191(3), 1004-1013.

CHAPTER FIVE: PHENOTYPIC CHARACTERIZATION

5.1. INTRODUCTION

Potassium (K^+) is an intracellular cation, found in high concentrations, ranging between 0.1-1 M. The high intracellular concentration of K^+ is used by bacteria for several cellular processes, including growth and survival. In *Mtb*, growth in K^+-deficient environments alters bacterial metabolism from aerobic to anaerobic respiration, leading to development of slow replicatingand non-replicating organisms (Salina et al., 2014).

Bacteria are able to maintain this high intracellular concentration in varying extracellular K^+ concentrations. In *E. coli*, bacteria use several active K^+-uptake transporters, which include the Trk, Kup (TrkD) and the Kdp, with the Trk systems functioning as K^+/H^+ symporters and the Kdp as an antiporter, for growth and survival in various K^+ concentrations and pH levels (Roe et al., 2000).

The *Mtb* bacteria infect macrophages as hosts and grow actively intracellularly in elevated K^+ and pH levels and aerated conditions. However, during stressful conditions such as those found in granuloma and biofilm environments, defined by low K^+ and pH levels and hypoxic conditions, the bacteria alter their metabolic state, changing from actively-replicating to slow replicating persistent/ non-replicating dormant organisms. In *Mtb* two active K^+-uptake systems, the Trk and Kdp, have been identified (Cole et al., 1998). However, only limited studies have described the roles of these systems during growth in these varying environments.

The Trk systems are encoded by the *ceoBC* operon and have been shown to have low affinity for the cation, playing a role during growth in high K^+ and pH levels. They are however, upregulated when pH levels decrease (Cholo et al., 2015). In macrophages, the Trk systems play a role during bacterial intracellular survival in murine monocyte-derived macrophages, while the CeoB protein is also required for biofilm development (Kerns et al., 2014; MacGilvary et al., 2019).

The Kdp systems are encoded by the TCS *kdpDE* and *kdpFABC* operons. The KdpDE is the response regulator with the KdpD sensing the stimulus and transferring it to the KdpE, leading to the induction of the *kdpFABC* operon (Steyn et al., 2003). The KdpE system has been implicated in bacterial growth (Sassetti and Rubin, 2003) and intracellular survival in macrophages (Haydel and Clark-Curtiss et al., 2004), while the KdpD is required for dormancy (Sassetti et al., 2003; Salina et al., 2014). Both *kdpD* and *kdpE* genes are upregulated at low K^+ concentrations (Steyn et al., 2003; Salina et al., 2014) and pH levels (Cholo et al., 2015), while

in vivo, both genes are used during bacterial growth for suppression of virulence genes, as demonstrated in a murine model of experimental infection (Parish et al., 2003).

The KdpFABC system is a high-affinity K^+ uptake transporter, which is induced and regulated by the KdpDE system (Steyn et al., 2003; Cholo et al., 2006; Freeman et al., 2013). The system is suppressed during bacterial growth at high K^+ and pH levels when the Trk is operating. However, it serves as a backup in its absence (Cholo et al., 2006). In macrophages, information on the roles of the *kdpFABC* of *Mtb* is limited. However, similar to the *kdpDE*, the *kdpFABC* operon is expressed at low K^+ concentrations (Steyn et al., 2003; Saline et al., 2014) and pH levels, playing a role in dormancy development (Cholo et al., 2015).

In the current study, the roles of the two K^+ transporters in bacterial growth were investigated by comparing the growth kinetics of the TKkdpDFC mutant, which has both K^+-uptake systems inactivated, and the WT strains. Bacterial growth was measured in aqueous (planktonic) and biofilm environments, as well as in infected macrophages. Based on similar genetypic characteristics between the F16 and F18 strains (TKkdpDFC mutants), the F16 strain was selected for phenotypic characterisation.

5.2. AIM AND OBJECTIVES

5.2.1. AIM

To characterise the roles of the active K^+-uptake systems, Trk and Kdp, of *Mtb* on growth and survival using extracellular and intracellular assays.

5.2.2. OBJECTIVES

To determine the roles of the K^+-uptake transporters on:

- *Mtb* bacterial K^+ uptake efficiencies using the rubidium ($^{86}Rb^+$) uptake method.
- Extracellular bacterial growth using planktonic assays.
- Bacterial survival in stressful growth conditions, extracellularly and intracellularly, using *in vitro* biofilm and macrophage assays, respectively.

5.3. MATERIALS AND METHODS

5.3.1. MATERIALS

5.3.1.1. Bacterial strains

The strains used included WT *Mtb* ($H_{37}Rv$) ATCC 26518 and the TKkdpDFC-deletion knockout, F16, constructed in Chapter Four. The mutant strain is characterised by inactivation of *ceoBC* encoding for the Trk, and the *kdpDE* and *kdpFABC* operons for the Kdp system of *Mtb*.

5.3.1.2. Growth media

Preparation of all growth media is described in Appendix A. The Middlebrook 7H9 broth and 7H10 agar media, prepared as described in Chapter four, were used for preparation of inoculum and planktonic cultures, and for the development of colonies, respectively. The Sauton broth medium, prepared as described previously (Ojha et al., 2008; Mothiba et al., 2015) was used for biofilm culture preparation, while the RPMI 1640 (BioWhittaker, Walkersville, MD, USA) supplemented with an antibiotic mixture (penicillin: streptomycin: amphotericin B, 0.1: 0.25: 0.1 µg/mL) and 5% autologous serum was used as a tissue culture medium for macrophage assays (NB: streptomycin does not penetrate macrophages and is only used during the pre-infection phase, thereafter antibiotic-free medium is used post-infection).

5.3.1.3. Reagents and chemicals

Rubidium (rubidium-86: $^{86}Rb^{+}$ isotope, 1mCi/mL) was purchased from PerkinElmer, Johannesburg, South Africa, and was used as a tracer for K^{+}. Unless otherwise stated, all other chemicals and reagents were purchased from Sigma-Aldrich, Johannesburg, South Africa, and Lasec, Johannesburg, South Africa.

5.3.2. METHODS

The WT and mutant strains of *Mtb* were characterized for their growth extracellularly in planktonic and biofilm and intracellularly in macrophage cultures.

5.3.2.1. Inoculum preparation

Inocula of the WT and the TKkdpDFC mutant strains were prepared in 7H9 broth medium. Approximately 10^5 colony-forming unit (cfu)/mL cells of each strain were inoculated into the 7H9 broth and the cultures were grown at 37 °C under stirring conditions until an OD of 0.6-1 at 540 nm was reached using Spectronic Helios UV-Vis spectrophotometer (Merck, USA). Each culture was centrifuged at 2850 × g for 10 min at RT. The supernatant was discarded and the pellet was washed once with 50 mL PBS (pH 7.4). Approximately 5 mL volumes of 3 millimetre (mm) glass beads were added to the pellets and vortexed to disperse the clumps, and the bacterial cells were resuspended in sterile PBS. The cell suspension density was adjusted to OD of 0.6 at 540 nm, using Spectronic Helios UV-Vis spectrophotometer (Merck, USA). The cell suspension was used as inoculum for both the extracellular and intracellular assays.

The numbers of bacteria for the inoculum for each strain were determined by colony-counting procedures as described by Mothiba et al., (2015). The inoculum suspensions were used to prepare 10× serial dilutions followed by plating a volume of 100 µL of each dilution onto 7H10 agar medium. The plate cultures were incubated for three weeks at 37 ºC for development of colonies. The numbers of colonies were counted and the numbers of bacteria as CFU were determined as follows:

'No of bacteria (cfu/mL) = number of colonies × 10 × dilution factor'

5.3.2.2 Planktonic culture

The planktonic cultures were prepared by growing approximately 1 - 4 × 10^5 cfu/mL of cells in 50 mL 7H9 medium under aerobic conditions. The cultures were used for $^{86}Rb^+$ uptake, rates of growth and extracellular pH determination assays.

5.3.2.2.1. Rubidium uptake

Rubidium ($^{86}Rb^+$) was used as a surrogate tracer for K^+ for determination of the K^+-uptake efficiencies of the bacterial strains. Bacterial cultures prepared as described in Section 5.3.2.2, were grown to mid-log phase (0.6 -1.0 OD) at 37 ºC for 14 days. The cells were harvested by centrifugation at 2850 × g for 15 min at 25 ºC, washed once and resuspended in K^+- and nitrogen-free buffer (KONO). Approximately 10^6 cfu/mL of cells were incubated at 37 ºC for 30 min to release the intracellular K^+. The suspension was centrifuged (2850 × g for 15 min) and the pellets were resuspended in 2 mL KONO buffer supplemented with 22 mM glucose and 2 mCi/L RbCl and incubated at 37 ºC for 90 min to allow for the uptake of $^{86}Rb^+$. The cells

were then washed twice with cold PBS (0.15 M, pH 7.4) and lysed with 0.4 mL pre-heated 5% trichloroacetic acid (TCA) to release intracellular $^{86}Rb^{+}$. The lysates were added to a liquid scintillation cocktail and the radioactivity determined in a liquid scintillation spectrometer. The net uptake of $^{86}Rb^{+}$ was taken as the difference in uptake of $^{86}Rb^{+}$ between the tubes incubated at 37 ºC and the controls kept on ice. The net uptake of $^{86}Rb^{+}$ for each strain was recorded as absolute counts per minute (cpm) representing efficiency of $^{86}Rb^{+}$ uptake of each strain. The $^{86}Rb^{+}$-uptake efficiency of the mutant strain was compared to that of the WT.

5.3.2.2.2. Growth rate measurements for WT and TKkdpDFC strains

Following inoculation into 7H9 broth, the WT and TKkdpDFC bacteria were incubated at 37 °C for 15 days under stirring conditions. The cultures were sampled every three days between day 0 (D0) and day 15 (D15), and the OD of these samples were measured at 540 nm using Spectronic Helios UV-Vis spectrophotometer (Merck, USA) (Section 5.3.2.1) and the recorded measurements were plotted for determination of growth rates for each strain. The rates of growth for each strain were determined by comparing the OD values at each time point to that of the Day 0 (D0). The rates of growth between the mutant and the WT strains at each time point were compared.

5.3.2.2.3. Measurement of extracellular pH

The planktonic cultures prepared as described (Section 5.3.2.2.1.2) were sampled every three days corresponding to growth rate determination, and the pH levels were measured directly using pH 4 and 7 as references in the Janeway pH meter 3510 (Lasec, Johannesburg). The results were recorded as absolute pH values.

5.3.2.3. Biofilm culture

The biofilm cultures were prepared by growing approximately 10^5 cfu/mL of cells in 2 mL Sauton broth medium, in 24-well tissue culture plates (Greiner Bio-One GmbH, Frickenhausen, Germany) under anaerobic conditions.

5.3.2.3.1. Biofilm growth rate determination

The biofilm culture plates were wrapped in parafilm and incubated at 37 °C in the presence of 5% CO_2 in the dark, as static cultures for five weeks. The contents of each well were sampled and plated on the initial day of the experiment, referred to as Week 0 (W0), followed by W1,

W3 and W5. Prior to plating, the wells were treated with 0.05% Tween 80 at 37 °C for six hours under shaking conditions to release the bacteria from the biofilm matrix into the growth medium. The bacterial suspensions were sampled, plated and the numbers of bacteria were determined as described in Section 5.3.2.1. The rates of biofilm bacterial growth for each strain were determined by comparing the number of bacteria at each time point to that of the W0. The rates of biofilm bacterial growth between the mutant and WT strains at each time point were compared.

5.3.2.3.2 Biofilm quantification

After five weeks of incubation at 37 °C in the presence of 5% CO_2 in the dark, the amounts of biofilm biomass in the static cultures were quantitated using a crystal violet-based staining procedure as previously described (Mothiba et al., 2015) with minor modifications. The supernatants, containing planktonic cells in the biofilm-forming cultures, were removed and the residual biomass in the wells was washed once with 1 mL dH_2O and air-dried. The residual matrix was stained with 1 mL of 1% crystal violet and incubated for 30 min at RT followed by three washes with 1 mL dH_2O to remove the unbound crystal violet dye, and air-dried. The biofilm-associated crystal violet was extracted with 1 mL of 70% ethanol, followed by 10-fold dilution and measurement of OD at 570 nm using a Spectronic Helios UV-Vis spectrophotometer (Merck, USA).

5.3.2.3.3 Measurement of extracellular pH

The supernatants from biofilm cultures were harvested and pH measurements were measured directly as described for planktonic cultures in Section 5.3.2.2.1.3.

5.3.2.4. Intracellular assay

5.3.2.4.1. Macrophage cultures

The macrophage cultures were prepared to $1 – 2 \times 10^5$ cells per well in RPMI in 48-well tissue culture plates to a final volume of 500 µL. Macrophages were prepared from human blood-derived monocytes isolated from venous blood as described below.

5.3.2.4.1.1. Preparation of macrophages

5.3.2.4.1.1.1. Venous blood

Venous blood was drawn from healthy, adult, human volunteers after permission was granted by the Main Research Ethics Committee of the Faculty of Health Sciences, University of Pretoria and acquisition of consent from participants (protocol number: 242/2011). All blood donors, following prior informed consent, underwent a blood pressure check and an overall health assessment (questionnaire) by a qualified nursing sister. The informed consent form was used only as a tool to screen the health of the donors and has no impact on the experimental design analysis and the outcome. On satisfactory completion of the informed consent/health assessment procedures, venous blood was collected into a sterile receptacle containing preservative-free heparin (5 units/mL blood). Copies of the approval letter obtained from the Ethics Committee and the informed consent form are shown in Appendices D and E, respectively

5.3.2.4.1.1.2. Isolation of mononuclear leucocytes from blood

The mononuclear leucocytes (MNL) were isolated from heparinised venous blood using a standard barrier centrifugation procedure. Briefly, blood was overlaid onto Histopaque-1077 to the ratio 1:3 blood: histopaque volumes, and was centrifuged at 750 × g for 25 min at 22 ºC to separate the various blood cells based on density. The MNL layer (found at the plasma-ficoll interphase), was harvested and washed with sterile PBS (0.15 M, pH 7.4). The cell suspension was centrifuged at 335 × g for 10 min at 4 ºC. The cell pellet, which consisted predominantly of MNL and contaminating erythrocytes and granulocytes, was resuspended in 20 mL of sterile, ice-cold, 0.83% ammonium chloride (NH_4CI) and held on ice for 10 min to remove the contaminating erythrocytes, followed by centrifugation at 335 × g for 10 min at 4 ºC. The cell pellet was resuspended in Hanks' balanced salt solution (HBSS), indicator-free, containing 1.25 mM calcium chloride ($CaCl_2$), pH 7.4, (Highveld Biological, Johannesburg).

The numbers of cells were enumerated microscopically using a light microscope and flow cytometrically using a FC500 Flow Cytometer (Beckman Coulter, USA) to distinguish between the various MNL sub-populations (monocytes, B cells, T cells, natural killer (NK) cells using the fluorochrome-labelled monoclonal antibodies: CD3 (FITC), CD14 (PE), CD15 (FITC) and CD19 (PE) for T cells, monocytes, granulocytes and B cells respectively.

5.3.2.4.1.1.3. Separation and maturation of monocytes

The monocytes were separated from other cells of the MNL population by a differential plastic adherence method. The MNL (30 mL of a 3×10^7 MNL/mL suspension in HBSS) were seeded into a sterile 75 cm^3 tissue culture flask and incubated for two hours at 37 ºC in 5% CO_2 to promote adherence of monocytes. The flask was gently rinsed twice with 25 mL volumes of PBS to remove the non-adherent cells. Thirty mL of tissue culture medium RPMI 1640 (BioWhittaker, Walkersville, MD, USA) supplemented with antibiotics and serum was added and the cell cultures were incubated for seven days at 37 ºC in 5% CO_2 for maturation of monocytes into macrophages.

5.3.2.4.1.1.4. Harvesting of macrophages

Follwing maturation of monocytes into macrophages, the tissue culture medium from each flask was discarded and the flask was rinsed once with 20 mL PBS, followed by addition of 10 mL Dulbecco's phosphate buffered saline (DPBS) without calcium (Ca^{2+}) or magnesium (Mg^{2+}) containing the Ca^{2+}-chelating agent ethylene glycol-bis (2-aminoethylene)-N,N,N,N-tetraceticacid (EGTA, 2 mM, final). All flasks were held on ice with gentle agitation every 10 min for at least 30 min, to promote detachment of the cells. Using a sterile 1.8 × 25 cm cell scraper (Adcock Ingram, Scientific Group), the surfaces of the flasks were scraped to dislodge the adherent cells to achieve a cell suspension, which was centrifuged at 335 × g for 10 min at 4 °C and the pellets resuspended in Ca^{2+}-free HBSS containing 2 mM EGTA.

The cell suspension was then analysed flow cytometrically using fluorochrome-labelled monoclonal antibodies CD14-PE and CD16-FITC to enumerate monocytes and macrophages, respectively.

5.3.2.4.1.1.5. Preparation of macrophages for infection

Approximately 1×10^5 of macrophages (Section 5.3.2.3.1) in 200 µL were plated in 48-well tissue culture plates and 10 mM $CaCl_2$ was added for macrophage adherence. The plate was incubated at 37 °C in the presence of 5% CO_2 for two hours. The $CaCl_2$ medium was removed and 500 µL of RPMI 1640 containing antibiotics and serum were added to the adherent cells followed by incubation at 37 °C/5% CO_2 for 24 hours.

5.3.2.4.2. Intracellular growth in macrophages

As described in section 5.3.2.1, the bacterial suspension was prepared in 200 µL antibiotic-free RPMI with 5% autologous serum and was added to cultured macrophages to achieve a multiple of infection (MOI) of 10:1, bacteria: macrophages. Prior to macrophage infection, growth medium was removed and the wells were washed once with 500 µL pre-warmed PBS followed by infection as described above. The infected macrophage cultures were incubated at 37 °C/5% CO_2 for one hour and 18 - 24 hours for uptake and intracellular survival, respectively. The supernatants were removed and the wells were washed once in PBS to remove the non-internalised bacteria. There was no step in this experiment to allow the removal of adherent bacterila cells. A 500 µL volume of RPMI supplemented with 5% autologous serum was added to infected macrophages and the cultures incubated for six days at 37 °C in the presence of 5% CO_2 for bacterial growth. The numbers of intracellular bacteria were determined by removing the supernatants, followed by washing once with PBS and lysing the macrophages with 100 µL of 0.2% SDS at 37 °C for 20 min. The lysis of macrophages was performed at one hour and D0, D3 and D6 following infection. The D0 time point was determined at 18 - 24 hours post infection. The content of each well was sampled and serial dilutions were plated on 7H10 agar medium for colony development. The number of bacteria was determined as described in Section 5.3.2.1. The rate of growth of each strain was determined by comparing the number of bacteria at each time point to that of D0. The rate of growth of the mutant strain at each time point was compared to that of the WT strain.

5.3.2.5. Statistical analysis and presentation of data

Data was analysed using Graph Pad statistical package and presented as means ± standard deviation. Statistical differences between the WT and mutant strains were determined by a p value < 0.05.

5.4. RESULTS

5.4.1. Inoculum

For both, the extracellular and intracellular assays, inocula of the WT and the TKkdpDFC mutant strains were prepared in 7H9 broth medium. Approximately 10^5 colony-forming unit (cfu)/mL cells of each strain were inoculated into the 7H9 broth and the cultures were grown at 37 °C under stirring conditions until an OD of 0.6-1 at 540 nm was reached using Spectronic Helios UV-Vis spectrophotometer (Merck, USA). The numbers of bacteria in the inocula were

$7.3 \times 10^6 \pm 2 \times 10^6$ and $2.6 \times 10^7 \pm 3.5 \times 10^6$ cfu/mL for the WT and mutant strain, respectively (Figure 5.1).

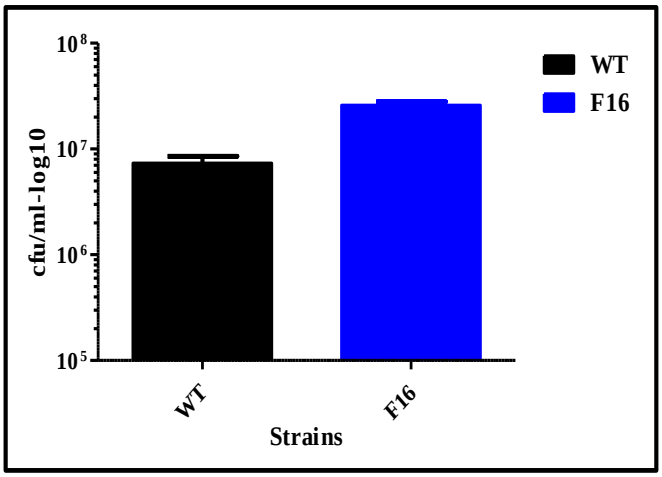

Figure 5.1: The inoculum sizes of the wild-type and mutant strain of *Mycobacterium tuberculosis*. Strains were grown at 37 °C under stirring conditions until an OD of 0.6-1 at 540 nm was reached. The results represent two biological replicates with three technical replicates each.

5.3.2. Extracellular assays

5.3.2.1. Planktonic cultures

5.3.2.1.1. Rubidium uptake

The uptake of $^{86}Rb^+$ by the TKkdpDFC mutant strain was significantly higher than that of the WT strain, achieving 40124 ± 12291 and 76233 ± 6921 cpm for the WT and the mutant strains, respectively, (*p* value = 0.0079) (Figure 5.2A).

5.3.2.1.2. Rates of growth

The growth rate of the TKkdpDFC mutant strain was significantly higher than those of the WT strain being evident between D6, D9 and D12 (p values = 0.0022 for the three time points during the exponential growth phase) while they were similar at D15 with both strains reaching an OD of 2.47 at stationary phase (Figure 5.2B).

5.3.2.1.3. Extracellular pH

The pH levels were comparable between the WT and the TKkdpDFC mutant strain at all time points, decreasing during bacterial growth. The pH levels were 6.729 ± 0.042 and 6.750 ± 0.071 at D0, which were similar to pH levels of the 7H9 growth medium, and decreased to 6.580 ± 0.017 and 6.581 ± 0.003 for WT and F16 strains respectively (5.2C).

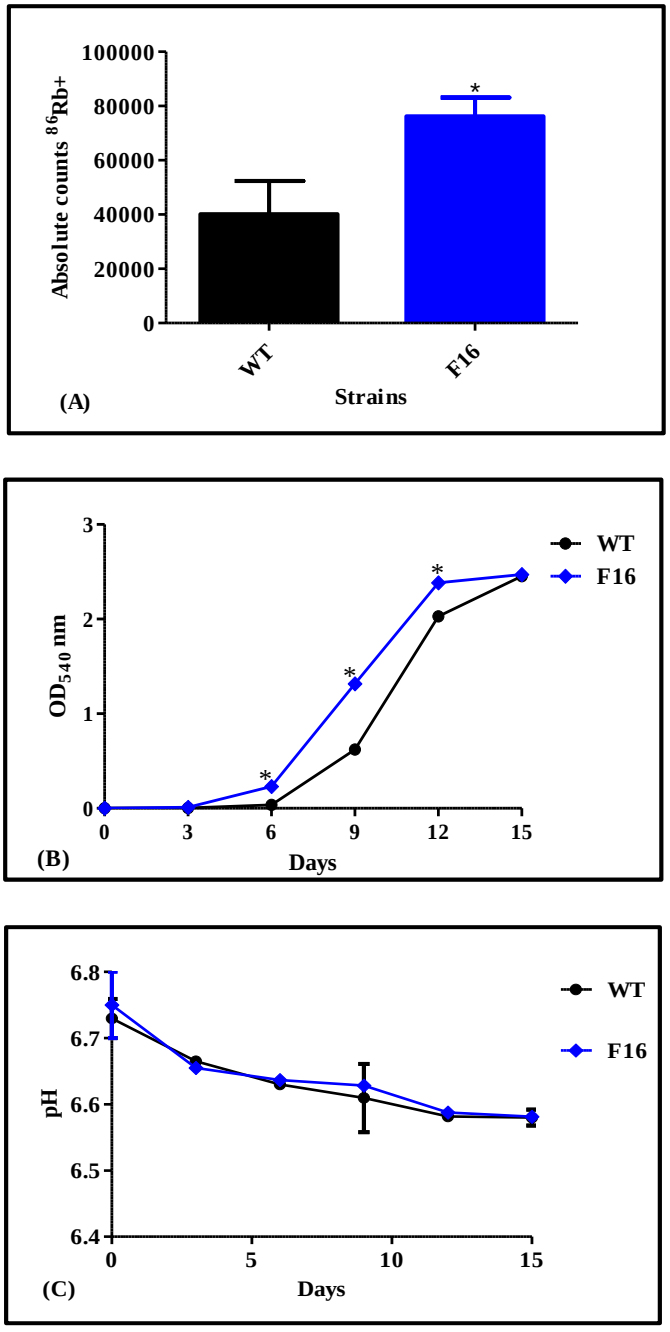

Figure 5.2: Planktonic cultures of the wild-type and TKkdpDFC mutant strains of *Mycobacterium tuberculosis* showing (A) rubidium uptake, (B) rates of growth, and (C) extracellular pH levels. Statistical significance is represented by (*) showing difference between WT and mutant strains. The results represent threebiological replicates with three technical replicates each.

5.3.2.2 Biofilm culture

5.3.2.2.1 Biofilm quantification

The WT and the mutant strains formed biofilm (Figure 5.3A). However, biofilm development was significantly attenuated in the mutant strain (p value = 0.0022) (Figure 5.3B).

5.3.2.2.2 Biofilm rates of growth

The growth rates of the WT and TKkdpDFC mutant strains were slow with the number of bacteria increasing from $7.3 \times 10^4 \pm 2 \times 10^4$ and $2.6 \times 10^5 \pm 3.5 \times 10^4$ cfu/mL to $1.5 \times 10^7 \pm 3.8 \times 10^5$ and $1.3 \times 10^7 \pm 1.4 \times 10^6$ cfu/mL at W5 for WT and mutant strains respectively (Figure 5.3C). However, the growth rates were similar between the WT and the mutant strains.

5.3.2.2.3 Extracellular pH

The pH levels were determined at W0 and W5 and the results are as shown in Figure 5.3D. The pH levels were 7.2 ± 0 at D0, which was the pH level of the Sauton growth medium, and the levels decreased to pH 5.1 ± 0.1 in the WT (p value = 0.0022), but increased to pH 7.915 ± 0.067 (p value = 0.0022) in the TKkdpDFC mutant strain at W5 as compared to the control.

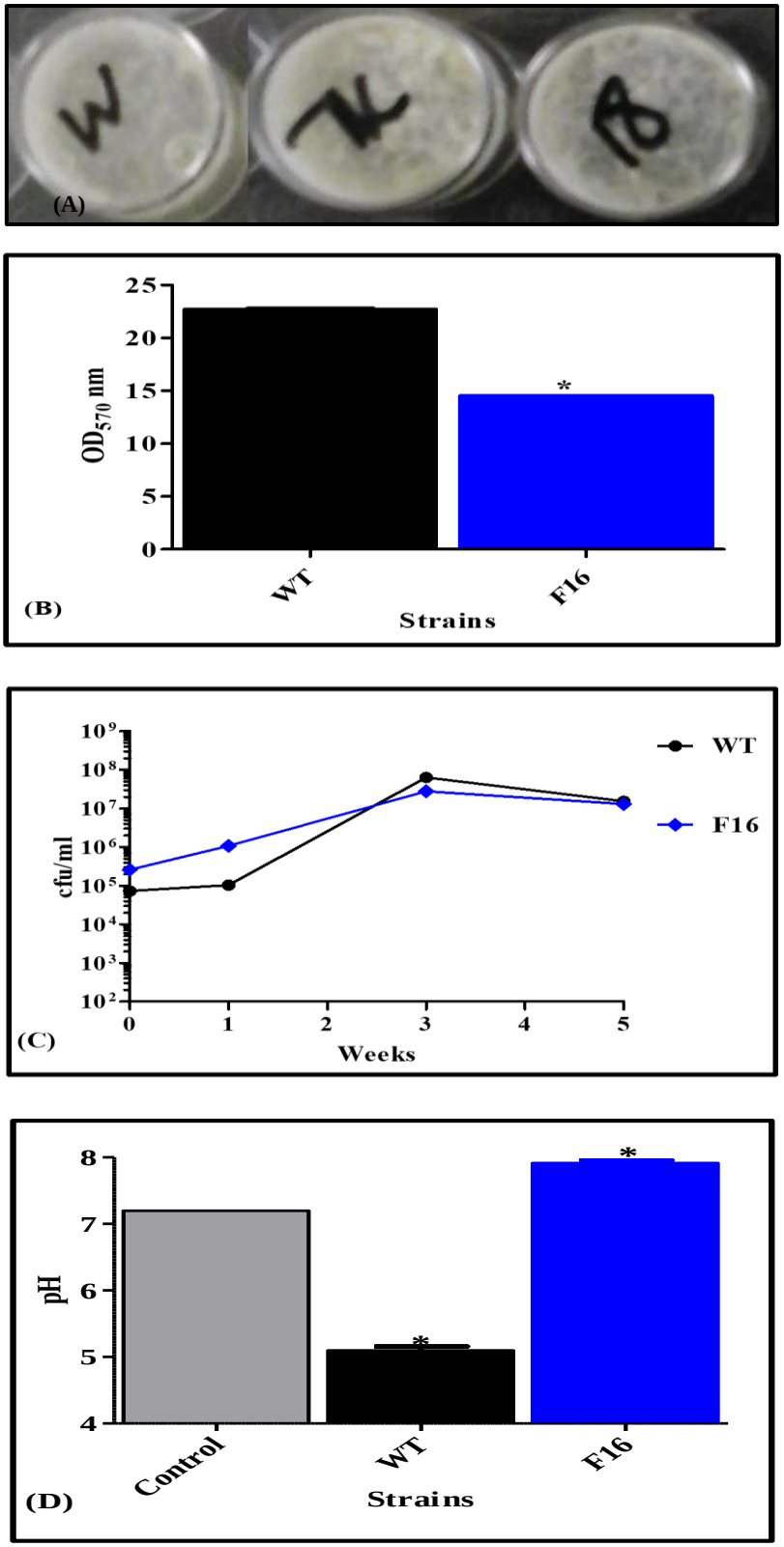

Figure 5.3: Biofilm cultures of the wild-type and the mutant strains of *Mycobacterium tuberculosis*. (A) Biofilm formation by visual examination, (B) biofilm quantification using the crystal violet procedure, (C) rates of growth by colony-counting method, and (D) the pH levels between the strains. Statistical significance is represented by (*) showing the difference between the WT and the mutant strains. The results are of two biological replicates with three technical replicates each

5.3.2.3 Macrophage cultures

5.3.2.3.1. Bacterial uptake by macrophages

After one hour, the numbers of mutant bacteria taken up by macrophages were higher than the WT strain and were $9.9 \times 10^3 \pm 1.1 \times 10^3$ and $4.7 \times 10^4 \pm 4 \times 10^3$ cfu/well for the WT and the mutant strains respectively, with p value < 0.0001 (Figure 5.4A).

5.3.2.3.2. Intracellular growth in macrophages

When comparing the number of mutant vs WT bacterial cells that were internalised by macrophages, at D0, $1.1 \times 10^4 \pm 3.8 \times 10^3$ and $9.2 \times 10^4 \pm 2.9 \times 10^3$ cfu/well were observed. However, bacterial growth rates were attenuated in the mutant, while they were increased in the WT during growth (p values = 0.0022 for the three time points) (Figure 5.4B). In contrast, after two days, the number of mutant bacterial cells decreased compared to the WT bacteria.

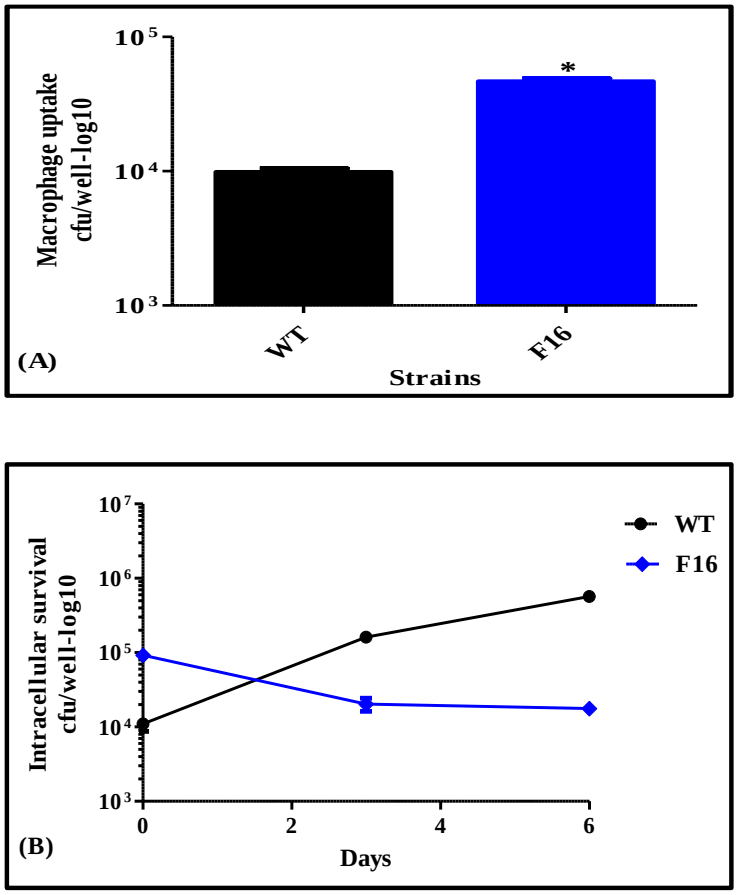

Figure 5.4: Macrophage cultures comparing the wild-type and mutant strains of *Mycobacterium tuberculosis*. (A) Bacterial uptake by macrophages at D0, and (B) intracellular growth in macrophages. Statistical significance is shown by (*) representing differences between the WT and mutant strains. The results represent two biological replicates with three technical replicates each

5.5. DISCUSSION

The Trk and Kdp K^+ transporters are used by most bacteria, such as *E. coli*, for bacterial growth, with utilisation of each transporter varying according to extracellular K^+ concentrations and extracellular pH. The Trk systems function as K^+/H^+ symporters, while the Kdp is an antiporter.

During planktonic growth, bacteria are exposed to nutrient- and K^+-enriched (15 mM) environments under mildly acidic pH (pH 6.8) conditions, growing as AR isolated cells (Cholo et al., 2015). In these conditions, bacteria utilise the Trk systems, which have a low affinity for the cation, and is associated with slow bacterial growth rates. In this setting, the Kdp system is suppressed, but is de-repressed in the absence of Trk. (Cholo et al., 2006; 2015).

However, in the current study, inactivation of both Trk and Kdp active K^+-uptake transporters, somewhat counter-intuitively, led to an increase in K^+-uptake efficiency in *Mtb*. Notwithstanding membrane potential-driven uptake of K^+, these findings appear to indicate the presence of an additional K^+-uptake system(s) operative in the bacteria. In *Mtb*, additional potential K^+ transporters include the L-lysine 6-monooxygenase, the putative transmembrane cation transporter Rv3200c and a conserved hypothetical protein Rv3237c (Cole et al., 1998). The Rv3200c protein is non-essential for bacterial growth, but has been associated with drug resistance development in some *Mtb* isolates (Sassetti et al., 2003; Faksri et al., 2016) while the Rv3237c, which is also non-essential for growth, is apparently required for biofilm formation (Kerns et al., 2014).

Encased in biofilm, bacteria encounter an environment which is hypoxic with a low K^+ concentration (4 mM) and mildly elevated pH (7.2), In this setting, the bacteria grow as aggregates producing EPS that intensify the biofilm matrix, protecting against external factors such as antibiotics and the host immune system. Attenuation of biofilm development in the absence of the Trk and Kdp K^+ transporters, as observed in the current study, may increase the susceptibility of the bacteria to these external factors, highlighting the potential of the K^+ transporters to serve as potential drug targets. The decrease in biofilm formation was associated with increase in pH to alkalinic levels.

In macrophages, in this study, bacterial uptake has been performed as a measurement of adherence and phagocytosis. During macrophage phagocytosis, bacteria encounter elevated K^+ concentrations (19 - 40 mM) and acidic pH levels (6.1 - 6.8) (Wagner et al., 2005; Vandal et al., 2008). An increase in uptake of the mutant strain during macrophage infection may indicate a role for the K^+-uptake transporters in slowing phagocytosis. Following phagocytosis, *Mtb* utilises K^+ transporters for intracellular growth, as shown by decreased intracellular

survival of the mutant strain. Previous studies have demonstrated the role of the Trk system in *Mtb* intracellular survival in macrophages while the *kdpE* gene is upregulated during mid-stage (48 hours post infection) of bacterial infection in macrophages (Haydel and Clark-Curtiss et al., 2004; MacGilvary et al., 2019).

5.6. CONCLUSION

The findings of the current study demonstrate that the major K^+ transporters of *Mtb* appear to harmonise in promoting the virulence of the pathogen, with their involvement being evident during the planktonic, biofilm and intracellular stages of bacterial growth, underscoring their potential as novel drug and vaccine targets. However, additional experiments are being conducted to confirm these phenotypic findings.

5.7. REFERENCES

Cholo M.C., Boshoff H.I., Steel H.C., Cockeran R., Matlola N.M., Downing K.J., et al. (2006). Effects of clofazimine on potassium uptake by a Trk-deletion mutant of *Mycobacterium tuberculosis*. *The Journal of Antimicrobial Chemistry*, 57(1), 79-84.

Cholo M.C., van Rensburg E.J., Osman A.G. and Anderson R. (2015). Expression of the genes encoding the Trk and Kdp potassium transport systems of *Mycobacterium tuberculosis* during growth *in vitro*. *BioMed Research International*, 608682.

Cole S.T., Brosch R., Parkhill J., Garnier T., Churcher C., Harris D., et al. (1998). Deciphering the biology of *Mycobacterium tuberculosis* from complete genome sequence. *Nature*, 393, 537-544.

Faksri K., Tan J.H., Disratthakit A., Xia E., Prammananan T., Suriyaphol P., et al. (2016). Whole-genome sequencing analysis of serially isolated multi-drug and extensively drug resistant *Mycobacterium tuberculosis* from Thai Patients. *PLoS One*, 11(8), e0160992.

Freeman Z.N., Dorus S. and Waterfield N.R. (2013). The KdpD/KdpE two-component system: integrating K^+ homeostasis and virulence. *PLoS Pathogens*, 9(3), e1003201.

Haydel S.E. and Clark-Curtiss J.E. (2004). Global expression analysis of two-component system regulator genes during *Mycobacterium tuberculosis* growth in human macrophages. *FEMS Microbiology Letters*, 236(2), 341-347.

Kerns P.W., Ackhart D.F., Basaraba R.J., Leid J.G. and Shirtliff M.E. (2014). *Mycobacterium tuberculosis* pellicles express unique proteins recognized by the host humoral response. *Pathogen Disease*, 70(3), 347-358.

MacGilvary N.J., Kevorkian Y.L. and Tan S. (2019). Potassium response and homeostasis in *Mycobacterium tuberculosis* modulates environmental adaptation and is important for host colonization. *PLoS Pathogens*, 15(2), e1007591.

Mothiba M.T., Anderson R., Fourie B., Germishuizen W.A., and Cholo M.C. (2015). Effects of clofazimine on planktonic and biofilm growth of *Mycobacterium tuberculosis* and *Mycobacterium smegmatis*. *Journal of Global Antimicrobial Resistance*, 3(1), 13-18.

Ojha A.K., Baughn A.D., Sambandan D. et al. (2008). Growth of *Mycobacterium tuberculosis* biofilms containing free mycolic acids and harbouring drug-tolerant bacteria. *Molecular Microbiology*, 69(1), 164-174.

Parish T., Smith D.A., Kendall S., Casali N., Bancroft G.J., and Stoker, N.G. (2003). Deletion of two-component regulatory systems increases the virulence of *Mycobacterium tuberculosis*. *Infection and Immunity*, 71(3), 1134-1140.

Roe A.J., McLaggan D., O'Byrne C.P. and Booth, I.R. (2000). Rapid inactivation of the *Escherichia coli* Kdp K^+ uptake system by high potassium concentrations. *Mol Microbiol*, 35(5), 1235-1243.

Salina E.G., Waddell S.J., Hoffmann N., Rosenkrands I., Butcher P.D. and Kaprelyants A.S. (2014). Potassium availability triggers *Mycobacterium tuberculosis* transition to, and resuscitation from, non-culturable (dormant) states. *Open Biology*, 4(10), pii: 140106.

Sassetti C.M., Boyd D.H. and Rubin E.J. (2003). Genes required for mycobacterial growth defined by high density mutagenesis. *Molecular Microbiology*, 48(1), 77-84.

Sassetti C.M. and Rubin E.J. (2003). Genetic requirements for mycobacterial survival during infection. *Proceedings of the National Academy of Sciences of the United States of America*, 100(22), 12989-12994.

Steyn A.J.C., Joseph J. and Bloom B.R. (2003). Interaction of the sensor module of *Mycobacterium tuberculosis* H_{37}Rv KdpD with members of the Lpr family. *Molecular Microbiology*, 47(4), 1075-1089.

Vandal O.H., Pierini L.M., Schnappinger D., Nathan C.F. and Ehrt S. (2008). A membrane protein preserves intrabacterial pH in intraphagosomal *Mycobacterium tuberculosis*. *Nature Medicine*, 14(8), 849-854.

Wagner D., Maser J., Barry L., Cai Z., Barry C.E.3rd, Bentrup H.K., et al. (2005). Elemental Analysis of *Mycobacterium avium*-, *Mycobacterium tuberculosis*-, and *Mycobacterium smegmatis*-containing phagosomes indicates pathogen-induced microenvironments within the host cell's endosomal system. *Journal of Immunology*, 174(3), 1491-1500.

CHAPTER SIX: GENERAL DISCUSSION AND CONCLUSION

Previous studies have demonstrated the importance of K^+ in mycobacterial growth (Salina et al., 2014). However, the roles of the major K^+ transporters of *Mtb*, specifically Trk and Kdp, in regulating uptake of the cation during the various stages of bacterial growth (planktonic, biofilm and intracellular) and their possible implications for disease pathogenesis are largely unexplored. In the current study, these issues were investigated by developing a triple gene-knockout strain of the pathogen in which both the Trk and Kdp systems were selectively deleted (F16 strain). This was successfully achieved and represented the major accomplishment of this research study. The triple gene-knockout mutant was then evaluated phenotypically to probe the requirement for the tandem presence of intact Trk and Kdp systems on bacterial growth by using *in vitro* models of planktonic, biofilm and intracellular (macrophages) growth, representing the various stages of mycobacterial growth in the host (Ojha et al., 2008; Mothiba et al., 2015).

Phenotypic analysis revealed that all three stages of bacterial growth were affected, albeit differentially, by dual knockout of the Trk and Kdp systems. In the case of planktonic growth, the triple gene-knockout mutant demonstrated significantly accelerated growth and uptake of $^{86}Rb^+$, seemingly consistent with a restraining effect of the Trk and Kdp systems on bacterial growth, possibly favouring persistence and resistance to antibiotics. Although the mechanism underpinning accelerated growth of the mutant remains to be identified, utilisation of alternative K^+ transporters is a possibility. In settings conducive to biofilm formation, albeit *in vitro*, dual inactivation of the Trk and Kdp systems resulted in decreased assembly of the biofilm matrix. Again the underlying mechanism remains to be identified. However, alterations in the acid/base balance of the exracellular milieu may play a role. Finally, dual inactivation of the Trk/Kdp systems was found to render the triple gene-knockout mutant more susceptible to phagocytosis and intracellular killing by isolated human blood monocyte/macrophages. Increased phagocytosis may simply reflect increased adherence of the pathogen due to alterations in the bacterial surface charge, while increased intracellular killing may result from increased acidification of the phagocytic vacuole.

These findings may not, however, accurately reflect the situation during host infection with *Mtb*, in which bacteria are found in macrophages and granuloma lesions, where they interact with the host immune system. Due to different growth conditions between the *in vitro* and *in vivo* environments, further investigation is required to evaluate the growth and survival of the triple gene-knockout of *Mtb* in natural environments in animal models of infection,

specifically the guinea pig model that leads to formation of granuloma lesions similar to those which develop in humans (Lenaerts et al., 2015).

Nevertheless, the outcomes of this study, seemingly demonstrate the essentiality of the Trk and Kdp K^+ transporters in bacterial growth and survival, as well as their genomic sequences, which are unique to the bacteria (Cole et al., 1998), underscoring the potential of these systems to serve as drug targets.

In addition, the findings of the current study using the dual Trk/Kdp gene-knockout mutant appear to implicate the existence of alternative K^+ uptake mechanisms utilised by *Mtb*. In this context, K^+-uptake membrane channels, have been described in *Mtb* and further research involving characterisation and possible involvement of these ion channels in bacterial growth may enable identification of additional drug targets.

STUDY LIMITATIONS AND FUTURE STUDIES

To completely characterise the roles of the K^+ transporters in *Mtb*, several future and ongoing studies have been identified. These include:

- Construction of additional mutant strains with different combination of inactivated K^+ transporters: These could include the KdpFABC-, Trk-KdpFABC- and Kdp-deletion mutants as well as mutants with K^+ membrane channels inactivated. Studying additional mutant strains will provide better understanding about the invlovment of each transporter and its genes in the extracellular and intracellular growth of *Mtb*.
- Evaluation of the K^+ transporters in animal models: The current study as well as few previous studies have only focussed on in-vitro evaluation of the K^+ transporters. Animals models would provide insights on the effect of the K^+ transporters in disease progression and response to standard therapy.
- Characterisation of the K^+ transporters as drug targets: the current mutant starin should be tested aginst the standard TB regimen as well as the newly discoverd anti-TB drugs. Additionally, these specific genes and proteins can be tested and explored as new treatment and vaccine targets.

REFERENCES

Cole S.T., Brosch R., Parkhill J., Garnier T., Churcher C., Harris D., et al. (1998). Deciphering the biology of *Mycobacterium tuberculosis* from complete genome sequence. *Nature,* 393, 537-544.

Lenaerts A., Barry C.E. and Dartois V. (2015). Heterogeneity in tuberculosis pathology, microenvironments and therapeutic responses. *Immunological Reviews,* 264(1), 288-307.

Mothiba M.T., Anderson R, Fourie B, Germishuizen W.A. and Cholo M.C. (2015). Effects of clofazimine on planktonic and biofilm growth of *Mycobacterium tuberculosis* and *Mycobacterium smegmatis*. *Journal of Global Antimicrobal Resistance,* 3(1), 13-18.

Ojha A.K., Baughn A.D., Sambandan D. et al. (2008). Growth of *Mycobacterium tuberculosis* biofilms containing free mycolic acids and harbouring drug-tolerant bacteria. *Molecular Microbiology*, 69(1), 164-174.

Salina E.G., Waddell S.J., Hoffmann N., Rosenkrands I., Butcher P.D. and Kaprelyants A.S. (2014). Potassium availability triggers *Mycobacterium tuberculosis* transition to, and resuscitation from, non-culturable (dormant) states. *Open Biology,* 4(10), pii: 140106.

APPENDICES

APPENDIX A: CULTURE MEDIA

1. **Luria-Bertani (LB) broth**

10 g tryptone, 5 g yeast extract, 10 g NaCl, 1 L dH_2O

2. **Luria-Bertani (LA) agar**

LB+15 g agar, 1 L H_2O

3. Middlebrook 7H9

4.7 g of the powder, 900 mL of dH_2O (containing 2 mL glycerol), 100 mL of Middlebrook OADC Enrichment

4. Middlebrook 7H10

19 g of the powder, 900 mL of dH_2O (containing 5 mL glycerol), 100 mL of Middlebrook OADC Enrichment.

5. Sauton's broth medium

0.5 g Potassium dihydrogen phosphate (KH_2PO_4), 0.5 g magnesium sulphate ($MgSO_4$), 2.0 g citric acid, 0.05 g ferric ammonium citrate, 60 mL glycerol, 4.0 g asparagine, dissolved in 1000 mL (dH_2O).

6. 2 X TY broth

16 g tryptone, 10 g yeast extract, 5 g NaCl, 1 L dH_2O

7. Middlebrook 7H9 supplemented with glycine

4.7 g of the powder, 900 mL of dH_2O (containing 2 mL glycerol), 100 mL of Middlebrook OADC Enrichment, glycine

8. RPMI 1640 supplemented with antibiotics

500 mL of RPMI 1640, 500 µL of antibiotic mixture:

- Penicillin: 10 000 units/mL
- Streptomycin: 10 000 µg/mL
- Amphotericin B: 25 µg/mL

To prepare 5% autologous serum, 2.5 mL of serum was added to an aliquot of 47.5 mL RPMI 1640 supplemented with antibiotics.

9. SOB broth

20 g tryptone, 5 g yeast extract, 0.5 g NaCl, 1 L dH_2O

APPENDIX B: SOLUTIONS AND BUFFERS

1. CTAB solution

4.1 g NaCl, 80 mL H_2O, while stirring add 10 g N-Ceyl-N, N, N-trimethyl ammonium bromide, if necessary, heat the solution to 65 °C, adjust volume to 100 mL, filter-sterilize when warm, store at RT.

2. NH_4Cl

16.6 g NH_4Cl, 2 g $NaHCO_3$, 0.148 g EDTA, 2L sH_2O, autoclave at 121 °C for 15-20 min.

3. Phosphate-buffered saline (PBS)

9.23 g haemoagglutinin powder, 1 L dH_2O, adjust pH to 7.4, autoclave at 121 °C for 15-20 min.

4. SOB

20 g Bacto-tryptone, 5 g yeast extract, 0.58 g NaCl, 0.19 g potassium chloride (KCl), 10 mL of 1M $MgCl_2$, 10 mL of 1 M $MgSO_4$, 1 L of dH_2O, adjust pH to 6.0-7.0 with NaOH, autoclave at 121 °C for 15-20 min.

5. SOC buffer

100 mL SOB, 1 mL of 2M glucose solution

6. TE buffer - 10×

15.759 g of Tris-Cl, 2.92 g of EDTA, 800 mL dH_2O, pH 8

7. Tris-acetate-EDTA (TAE) buffer - 50×

242 g of Tris-Cl dissolved in approximately 750 mL of dH_2O. Carefully add 57.1 mL of glacial acid and 100 mL of 0.5 M EDTA (pH 8.0).

APPENDIX C: MOLECULAR REACTIONS AND CONDITIONS

1. **Digestion conditions of the vector pNILRB5**

Component	**Volume (Final concentration)**
Plasmid DNA	7 µL (750 ng – 1000 ng)
Buffer (10×)	2 µL (1×)
Enzyme (*Bsa*I or *Bse*RI)	1 µL (*Bsa*I-10 units; or)
PCR Water	10 µL
Total volume	20 µL

2. **T4 treatment of the digested pNILRB5 with dGTP**

Component	**Volume (Final concentration)**
Cut plasmid	10 µL (500 ng – 750 ng)
T4 Buffer (10×)	2 µL (1×)
dGTP (25 mM)	2 µL (2.5 mM)
DTT (100 mM)	1 µL (5 mM)
BSA (1 mg/mL)	2 µL (0.1 mg/mL)
T4 DNA polymerase	1.5 µL (4.5 units)
PCR Water	1.5 µL
Total volume	20 µL

3. **PCR synthesis conditions**

Component	**Volume (Final) concentration)**
Amplification Buffer	5 µL (1×)
dNTP mixture	1 µL (0.8 mM)
DMSO	1 µL
F- Primer mix (10 µM)	1 µL (0.04 mM)
R- Primer mix (10 µM)	1 µL (0.04 mM)
Template DNA (10 pg -200 ng)	5 µL
DNA Polymerase	1 µL
PCR Water	35 µL
Total volume	50 µL

4. **T4 treatment of purified PCR products with dCTP**

Component	**Reaction**
DNA	10 µL (1000 ng - 2000 ng)
T4 Buffer (10×)	2 µL (1×)
dCTP (25 mM)	2 µL (2.5 mM)
DTT (100 mM)	1 µL (5 mM)
BSA (1 mg/mL)	2 µL (0.1 mg/mL)
T4 DNA polymerase	1.5 µL (4.5 units)
Water	1.5 µL
Total volume	20 µL

APPENDIX D: APPROVAL LETTER FROM THE MAIN RESEARCH ETHICS COMMITTEE OF THE FACULTY OF HEALTH SCIENCES, UNIVERSITY OF PRETORIA

UNIVERSITEIT VAN PRETORIA
UNIVERSITY OF PRETORIA
YUNIBESITHI YA PRETORIA

Faculty of Health Sciences

The Research Ethics Committee, Faculty Health Sciences, University of Pretoria complies with ICH-GCP guidelines and the US Federal wide Assurance

- FWA 00002567, Approved dd 22 May 2002 and Expires 03/20/2022.
- IRB 0000 2235 IORG0001762 Approved dd 22/04/2014 and Expires 03/14/2020.

21 January 2020

Approval Certificate
Annual Renewal

Ethics Reference No.: 242/2011
Title: The roles of the potassium-uptake systems, Trk and Kdp, in the extracellular and intracellular growth of Mycobacterium tuberculosis.

Dear Mr AGE Osman

The **Annual Renewal** as supported by documents received between 2019-12-10 and 2020-01-21 for your research, was approved by the Faculty of Health Sciences Research Ethics Committee on its quorate meeting of 2020-01-21.

Please note the following about your ethics approval:

- Renewal of ethics approval is valid for 1 year, subsequent annual renewal will become due on 2021-01-21.
- Please remember to use your protocol number (242/2011) on any documents or correspondence with the Research Ethics Committee regarding your research.
- Please note that the Research Ethics Committee may ask further questions, seek additional information, require further modification, monitor the conduct of your research, or suspend or withdraw ethics approval.

Ethics approval is subject to the following:

- The ethics approval is conditional on the research being conducted as stipulated by the details of all documents submitted to the Committee. In the event that a further need arises to change who the investigators are, the methods or any other aspect, such changes must be submitted as an Amendment for approval by the Committee.

We wish you the best with your research.

Yours sincerely

Dr R Sommers
MBChB MMed (Int) MPharmMed PhD
Deputy Chairperson of the Faculty of Health Sciences Research Ethics Committee, University of Pretoria

The Faculty of Health Sciences Research Ethics Committee complies with the SA National Act 61 of 2003 as it pertains to health research and the United States Code of Federal Regulations Title 46 and 46. This committee abides by the ethical norms and principles for research, established by the Declaration of Helsinki, the South African Medical Research Council Guidelines as well as the Guidelines for Ethical Research: Principles Structures and Processes, Second Edition 2016 (Department of Health)

Research Ethics Committee
Room 4-68, Level 4, Tswelopele Building
University of Pretoria, Private Bag x323
Gezina 0031, South Africa
Tel 427 (0)12 356 3084
Email: deepeka.behari@up.ac.za
www.up.ac.za

Fakulteit Gesondheidswetenskappe
Lefapha le Disaense tsa Maphelo

APPENDIX E: INFORMED CONSENT

AUTHORIZATION TO PARTICIPATE IN A RESEARCH PROJECT

TITLE: The roles of the potassium-uptake systems, Trk and Kdp, in the extracellular and intracellular growth of *Mycobacterium tuberculosis*.

1. Invitation to participant

Dear Mr/Mrs/Ms ..... Date ...../...../.....

You are invited to participate in the above-mentioned research study by donation a blood sample, which will be used for the preparation of cell cultures in the laboratory for experimental purposes. The outcome of the study will be published in such a way that your name is not revealed (i.e. anonymously). When you donate this blood you will not be asked to pay anything.

2. The Nature and purpose of this study:

2.1 Nature of the study

This is a lab-based study which will investigate the physiology of the bacteria that cause tuberculosis disease.

2.2 Purpose of the study

The purpose of the study is to isolate white blood cells from blood of healthy, adult volunteers and infect them with the bacteria that cause tuberculosis. The results will provide information that will lead to new treatment for tuberculosis disease.

3. Explanation of procedures to be followed:

You will be asked to complete a health questionnaire so that we can determine whether or not it is safe for you to donate a volume of blood. Following the questionnaire, a trained nursing sister will check your pulse, blood pressure and mucous membranes (tongue, lips) to make sure that you do not have anaemia or any abnormal pulse or blood pressure before the blood sample is taken. We request that, with your permission, a volume of blood (100-300 mL) be taken from your arm. This blood will be taken to the Immunology Department for further study. Your pulse and blood pressure will be checked again 15 minutes later, before you leave and should you experience any problems, our trained nursing sisters will take appropriate care of you.

4. Risk and discomfort involved

Any discomfort experienced may be due to insertion of the needle into a vein on your arm during taking of the blood sample. This discomfort is for a very short time only.

We will attempt to reduce any risk to yourself by checking your answers to the questionnaire that serves to screen for potential problems, and should you be found to have a too low or too high pulse or blood pressure or if you are pale (anaemic), no blood will be taken from you.

5. Possible benefits of this study:

The results of this study will be useful for the development of new drugs and vaccines against tuberculosis. However, as a volunteer, there are no direct benefits in any way from participating in the study.

6. Consent to participate in this study:

I have read or had read to me in a language that I understand the above information before signing this consent form. The content and meaning of this information have been explained to me. I have been given the opportunity to ask questions and am satisfied that they have been answered satisfactorily.

I understand that if I do not participate in this study, I will not be penalized in any way.

I have completed the questionnaire and I confirm that the Nursing Sister has checked my pulse, blood pressure and mucous membranes today.

I hereby volunteer to take part in this study.

I have received a signed copy of this informed consent agreement.

....

Patient / Guardian/ Participant signature Date

....

Witness (person obtaining informed Consent) Date

....

Witness Date

QUESTIONNAIRE TO ASSESS YOUR HEALTH

NOTE: All information will be strictly confidential

Only the nursing sister will have access to this information

PART I: PERSONAL INFORMATION (PLEASE PRINT)

PARTICIPANT NO : _____

DATE OF BIRTH : .....

ADDRESS : .....

.....

.....

TELEPHONE NUMBERS :

.....

PART II

		Yes	No
1.	Are you feeling in anyway unwell today?		
2.	Did you have breakfast this morning?		
3.	Have you donated blood during the past 3 months?		
4.	What is your occupation?		

.....

		Yes	No
5.	Will you be returning directly to work after donating a blood sample?		
6.	Are you suffering from any illnesses at present?		

Please list these:

.....

.....

7. Are you taking any regular medication? **Yes No**

Please list these:

.....

.....

.....

Yes No

8. Have you taken any medications this morning other than those listed above?

9. Have you suffered any serious injury, operation or illness in the previous 6 months?

10. Have you been to see your doctor in the last month?

If so, what treatment was given to you?

.....

11. Do have any diseases affecting any of the following organs? **Yes No**

- Heart
- Lungs
- Blood
- Kidneys
- Nervous system
- Stomach and digestive system

12. Have you ever been diagnosed with anaemia (lack of blood)?

13. Have you lost any significant amount of weight in the last 3 months?

14. Is there any reason not mentioned above that you feel may place you at any risk should you donate blood today?

15. Are you experiencing any of these symptoms? **Yes No**

- Cough that lasts for more than two weeks
- Night sweat
- Loss of appetite
- Tiredness

16. **Female donors:** **Yes No**

Are you currently pregnant or breastfeeding?

PART III: EXAMINATION BY NURSING SISTER

DATE: ..... **TIME:** .....

PULSE: ..... **/min**

BLOOD PRESSURE: ..... **mmHg**

COLOUR OF MUCOUS MEMBRANES: **Yes No**

PALE?

PART IV: DECISION OF NURSING SISTER

Yes No

a) Donor is FIT to donate blood without any obvious risks to his/her health.

....

NAME **SIGNATURE**